

**ADSORPTION PROPERTIES OF CROSPVIDONE AND USE OF
CROSPVIDONE IN DRUG-IN-ADHESIVE PATCHES**

Dissertation zur Erlangung des akademischen Grades des
Doktors der Naturwissenschaften (Dr. rer. nat.)

eingereicht im Fachbereich Biologie, Chemie, Pharmazie
der Freien Universität Berlin

vorgelegt von

MARTIN SCHULZ
aus Würzburg

März, 2009

1. Gutachter: Prof. Dr. Roland Bodmeier
2. Gutachter: Prof. Dr. Philippe Maincent

Tag der mündlichen Prüfung: 29.Mai 2009

To my family.

ACKNOWLEDGEMENTS

I am very thankful to Prof. Dr. Roland Bodmeier for providing this interesting and challenging research topic and for his support throughout the dissertation. Additionally, I am deeply grateful for his help in setting up my internship at Kos Pharmaceuticals/Abbott Laboratories in Hollywood, FL, USA.

I want to thank Prof. Dr. Philippe Maincent for co-evaluating this thesis and Prof. Dr. Ronald Gust, Prof. Dr. Philippe Maincent, Prof. Dr. Heinz Pertz and Dr. Wolfgang Mehnert for serving as members of my thesis advisory committee.

Special acknowledgements go to Dr. Bernd Fussnegger at BASF AG for the valuable discussions and to BASF AG for the financial support.

I am particularly thankful to Katrin Möbus, Julia Herrmann, Katrin Steiner, Zahra Ghalanbor, Burkhard Dickenhorst and Mirko Voigt for evaluating parts of this thesis. Special thanks also to Burkhard Dickenhorst for his help with complex software problems, Angelika Schwarz for her assistance with administrative issues and Stefan Walter for the prompt and diligent technical support.

I would like to thank all present workgroup members and alumni I had the pleasure of getting to know for the friendly atmosphere in our workgroup and in particular for the stimulating discussions and the enjoyable atmosphere during lunchtime.

I am very thankful to Dr. Pepe Rocca and all members of his group at Kos Pharmaceuticals/Abbott Laboratories, Hollywood, FL, USA. The chance to work in his research group was extremely valuable for me.

My deepest gratitude is dedicated to my family for their love and ongoing support.

TABLE OF CONTENTS

1	INTRODUCTION	1
1.1	BACKGROUND	1
1.2	SKIN	2
1.2.1	<i>Skin physiology and metabolism</i>	3
1.2.2	<i>Skin penetration</i>	5
1.3	TRANSDERMAL DRUG DELIVERY	8
1.3.1	<i>Advantages and limitations</i>	8
1.3.2	<i>Transdermal patch design</i>	9
1.3.3	<i>Physicochemical properties of compounds and skin permeation</i>	15
1.3.4	<i>The ideal transdermal drug delivery system</i>	17
1.4	APPROACHES TO INCREASE TRANSDERMAL ABSORPTION	17
1.4.1	<i>Physical methods</i>	18
1.4.2	<i>Electrically assisted methods</i>	21
1.4.3	<i>Chemical penetration enhancers</i>	25
1.4.4	<i>Modification of drug and formulation</i>	30
1.5	SUPERSATURATION AND RECRYSTALLIZATION INHIBITION	32
1.5.1	<i>Preparation of supersaturated formulations</i>	34
1.5.2	<i>Recrystallization in supersaturated formulations</i>	35
1.5.3	<i>Use of soluble additives to prevent drug recrystallization</i>	36
1.5.4	<i>Use of adsorbents to prevent drug recrystallization</i>	39
1.6	SKIN ADHESION	42
1.6.1	<i>Theories of pressure sensitive adhesion</i>	42
1.6.2	<i>Measurement of adhesive properties</i>	44
1.6.3	<i>Adhesives in transdermal drug delivery systems</i>	46
1.7	DRUG RELEASE AND PERMEATION STUDIES	49
1.7.1	<i>Drug release studies</i>	49
1.7.2	<i>Permeation studies</i>	49
1.8	RESEARCH OBJECTIVES	51
2	MATERIALS AND METHODS	52
2.1	MATERIALS	52
2.1.1	<i>Drugs</i>	52
2.1.2	<i>Adsorbents</i>	52
2.1.3	<i>Pressure sensitive adhesives</i>	52
2.1.4	<i>Solvents</i>	52

2.1.5	<i>Surfactant</i>	53
2.1.6	<i>Liners and membranes</i>	53
2.2	METHODS	53
2.2.1	<i>General data presentation in diagrams</i>	53
2.2.2	<i>Solubility determination</i>	53
2.2.3	<i>Specific surface area measurement</i>	54
2.2.4	<i>Particle size analysis</i>	54
2.2.5	<i>Solvent uptake and solvent binding studies of adsorbents</i>	55
2.2.6	<i>Adsorption studies</i>	56
2.2.7	<i>ATR-FTIR spectroscopy</i>	57
2.2.8	<i>Drug assay</i>	58
2.2.9	<i>Physical state of drug</i>	58
2.2.10	<i>Preparation of adsorbates and physical mixtures</i>	60
2.2.11	<i>Preparation of patches</i>	61
2.2.12	<i>Stability of transdermal patches</i>	63
2.2.13	<i>Drug release studies</i>	63
2.2.14	<i>Adhesion studies</i>	65
3	RESULTS AND DISCUSSION	66
3.1	ADSORPTION PROPERTIES OF CROSPROVIDONE	66
3.1.1	<i>Location of the drug in adsorbates</i>	66
3.1.2	<i>Adsorption isotherms</i>	68
3.1.3	<i>ATR-FTIR spectroscopy</i>	69
3.1.4	<i>Optimization of the drug-carrier ratio</i>	73
3.1.5	<i>Drug release</i>	80
3.1.6	<i>Conclusions</i>	81
3.2	METHOD DEVELOPMENT – TRANSDERMAL PATCHES	83
3.2.1	<i>Detection of drug crystals</i>	83
3.2.2	<i>Solubility considerations</i>	87
3.2.3	<i>Preparation of polyisobutene patches</i>	90
3.2.4	<i>Analytic of ethinyl estradiol and levonorgestrel</i>	91
3.2.5	<i>Development of the drug release study</i>	94
3.3	ADSORBATES IN TRANSDERMAL PATCHES	97
3.3.1	<i>Suitability screening of insoluble carriers</i>	97
3.3.2	<i>Patches containing adsorbates onto crospovidone</i>	106
3.3.3	<i>Conclusions</i>	114
3.4	INFLUENCE OF THE ADHESIVE	115
3.4.1	<i>Drug physical state</i>	115
3.4.2	<i>Drug release from patches based on polyisobutene</i>	117
3.4.3	<i>Drug release from patches based on acrylates</i>	120
3.4.4	<i>Drug release from acrylate patches containing adsorbates onto titanium dioxide</i>	124

3.4.5	<i>Comparison of the drug release from polyisobutene and acrylate patches</i>	126
3.4.6	<i>Conclusions</i>	126
3.5	ADHESIVE PROPERTIES	128
3.5.1	<i>Preparation of placebo patches</i>	128
3.5.2	<i>Development of probe tack method</i>	128
3.5.3	<i>In vitro adhesive properties of medium molecular weight polyisobutene</i>	131
3.5.4	<i>In vitro adhesive properties of different polyisobutene blends</i>	133
3.5.5	<i>In vitro adhesive properties of Durotak-87 202A</i>	135
3.5.6	<i>In vivo adhesion, matrix creep and skin irritation</i>	137
3.5.7	<i>Conclusions</i>	141
4	SUMMARY	142
5	ZUSAMMENFASSUNG	146
6	REFERENCES	150
7	PUBLICATIONS & PRESENTATIONS RESULTING FROM THIS WORK	163
8	CURRICULUM VITAE	164

1 INTRODUCTION

1.1 BACKGROUND

A multitude of drugs cannot simply be administered in the preferred oral way for different reasons. Short biological half-lives, small bioavailability and narrow therapeutic indices are common problems that necessitate more advanced ways of administration. The ideal drug profile in these cases, especially if a prolonged application of the drug is the goal, could be obtained by continuous intravenous infusion. Both first liver passage and spikes in the drug plasma levels would be avoided. But the drug administration by intravenous infusion has serious drawbacks, especially with regard to patient compliance. In general, it requires the patient's hospitalization, and it is, as all invasive therapies, burdensome for the patient (Payne et al. 1998). Furthermore, problems related to inflammations at the injection site, the possibility of germs entering the body and the mechanical stress caused to the veins during chronic therapy can occur.

One alternative to efficiently administer drugs in the above described scenario is transdermal drug delivery. By this means, drug plasma curves that have a similar shape as curves obtained after infusion can be achieved (Fig. 1).

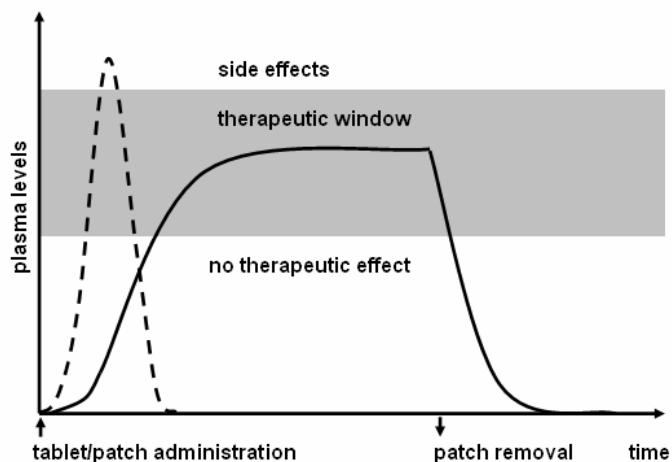


Fig. 1 Plasma profiles after tablet (- -) and patch (—) administration

After a lag time, in which the drug passes the barrier of the stratum corneum and arrives at the capillaries in the dermis, constant plasma levels, below the minimal toxic concentration and above the minimal effective concentration can be achieved.

After pioneering findings of Scheuplein with regard to the permeation of substances across the skin (Scheuplein 1965), it took until 1979 for the first transdermal patch (Scopoderm TTS®) to become commercially available (Prausnitz et al. 2004). Now the annual market for transdermal patches alone in the US is greater than \$ 3 billion (Prausnitz et al. 2004). Successful commercial products include patches for the treatment of motion sickness with scopolamin, patches for the treatment of chronic severe pain with fentanyl and patches with sex hormones for hormone replacement therapy and birth control. Patches have been shown bioequivalent (Fujimura et al. 1994; Mattsson et al. 1999; Lin and Chien 2006) to other routes of administration and several recent review studies showed their superiority with regard to safety, tolerability and patient compliance (Small and Dubois 2007; Zernikow et al. 2007; Robinson and Amsterdam 2008).

1.2 SKIN

The human skin is the body's largest organ (Menon 2002). It covers an area of approximately 1.5 to 2 m² and receives around one-third of all blood circulating through the body (Chien 1978; Pflugel and Dittgen 1987). It provides an effective barrier between our body and the external environment and controls the water loss and the ingress of foreign substances. Furthermore, it regulates the body temperature, participates in the adjustment of the blood pressure and prevents the penetration of ultraviolet rays. Lastly, the skin is an important sense organ that perceives stimuli like temperature, pressure and pain. These stimuli are transmitted to the nervous system and lead to physiological reactions.

The pH in the stratum corneum is approximately 5.5 and rises approximately 2 pH units in the viable dermis (Wagner et al. 2003). The skin temperature is influenced by various factors, like anatomic site, age or certain disease conditions. It was found that a male subject's skin temperature after 20 min at ambient conditions can vary from 24°C to 36°C, depending on the anatomic location (Sun 1997).

1.2.1 Skin physiology and metabolism

1.2.1.1 Skin physiology

Histologically, human skin consists of three different layers: The hypodermis, the dermis and the epidermis (from inside to outside, Fig. 2). The epidermis can be further divided into four different layers (Menon 2002): The stratum germinativum (also: stratum basale), the stratum spinosum, the stratum granulosum and the stratum corneum (from inside to outside). The inner three epidermal layers are living tissue and therefore called viable epidermis while the outermost layer of the epidermis, the stratum corneum, is build up by dead cells.

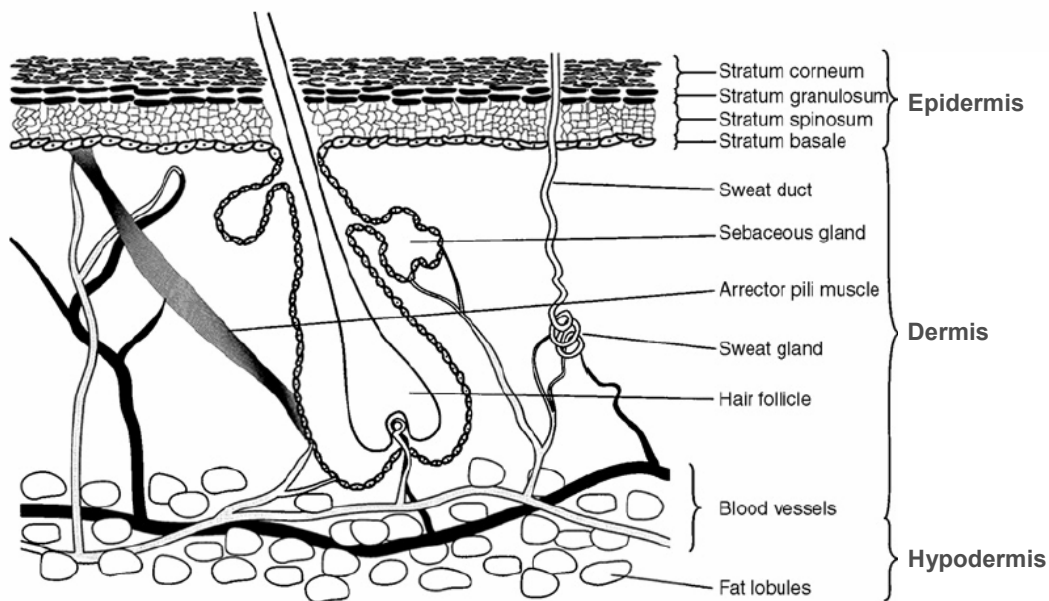


Fig. 2 Schematic of the skin from (modified from El Maghraby et al. 2008)

The stratum germinativum consists of epidermal stem cells and is mitotically active. It continuously produces keratinocytes, which migrate outward. On their way, they differentiate (the cells flatten, lose their nuclei and become more and more keratinized) until they form a protective layer of dead cells: The stratum corneum. The fully differentiated, dead keratinocytes are called corneocytes. A cell's journey from the stratum germinativum to the stratum corneum takes at least 14 days (Halprin 1972) and the residence time of a cell in the stratum corneum was shown to be 14 days with radio-active marked glycine (Rothberg et al. 1961). Hence the total residence time of a cell in the epidermis, from leaving the stratum germinativum until desquamation (i.e., the permanent process of shedding) is about 28 days.

The stratum spinosum contains lipid-enriched lamellar bodies, the so-called Odland bodies. These bodies contain lipid material, which is released at the border of the stratum granulosum and the stratum corneum.

The stratum corneum is best described by the mortar-and-brick model (Michaels et al. 1975; Elias et al. 1979). In this model, the corneocytes correspond to the bricks and the intercellular lipids released from the Odland bodies, as described in the last paragraph, to the mortar. The stratum corneum has, depending on the anatomic site, a thickness of approximately 10 to 15 μm (an exception is the stratum corneum on the sole of the feet), which corresponds to approximately 20 layers of cells and is for most drugs the actual penetration barrier (Scheuplein 1965). The corneocytes contain keratin, amino acids, sugars and sugar derivatives (Eckert 1989); their interior is therefore hydrophilic. The intercellular lipids, which essentially glue the corneocytes, are primarily comprised of ceramides, free fatty acids (and their esters), and cholesterol (and its sulfate) (Hadgraft 2001). Their phospholipid content is low compared to other biological membranes (Ghosh and Pfister 1997). The conformation of these lipids has been investigated by X-ray diffractometry, which showed that they exist in bilayers (White et al. 1988; Bouwstra et al. 1991).

Besides the keratinocytes, the viable epidermis contains various other cell types, e.g., the melanocytes, which are responsible for the pigmentation of the skin, the Langerhans cells, which play a role in the immune reaction of the skin and the Merkel cells, which are associated with the sense of touch.

The dermis is situated beneath the epidermis and represents the biggest part of the skin. It contains mainly connective tissue (collagen and elastin, which contribute to its elasticity) embedded in an amorphous glycosaminoglycan ground substance (Foldvari 2000). This layer is rich in blood vessels and nerve endings and contains hair follicles, sebaceous glands and sweat glands.

The lowermost layer of the skin, the hypodermis, is mainly used for fat storage in adipose cells. Apart from storing energy, this tissue serves as a mechanical cushion and protects the body from the cold.

1.2.1.2 Skin metabolism

Due to enzyme systems within the epidermis, the skin performs a wide range of active metabolic functions. It contains cytochrome P450 isoenzymes (Merk and Jugert 1993), phosphatases, proteases, nucleases, esterases and steroid sulfatases (Foldvari 2000). Compared to the liver, which is the central organ of xenobiotic metabolism, the extent of

metabolism is significantly lower. Remarkably, the skin does not just have less metabolic activity than the liver, it also favors different enzyme systems for the detoxification of foreign substances: e.g., transferase levels are approximately 10% of the hepatic values while the total activity of cytochrome P450 in the skin is about 1-5% of that in the liver (Merk and Jugert 1993). However the cutaneous first-pass effect can be significant for sensitive compounds. It was estimated to be 15-20% for nitroglycerin (Delago-Charro and Guy 2001). Ways to exploit skin metabolism by formulating pro-drugs with improved penetration characteristics have been developed and are described in chapter 1.4.3.1.

1.2.2 Skin penetration

1.2.2.1 Penetration pathways through the stratum corneum

Three penetration pathways by which topically applied substances can cross the stratum corneum are well accepted: The intercellular, the transcellular and the appendageal (through either sweat glands or hair follicles) route (Barry 2001; Hadgraft 2001; Patzelt et al. 2008) (Fig. 3).

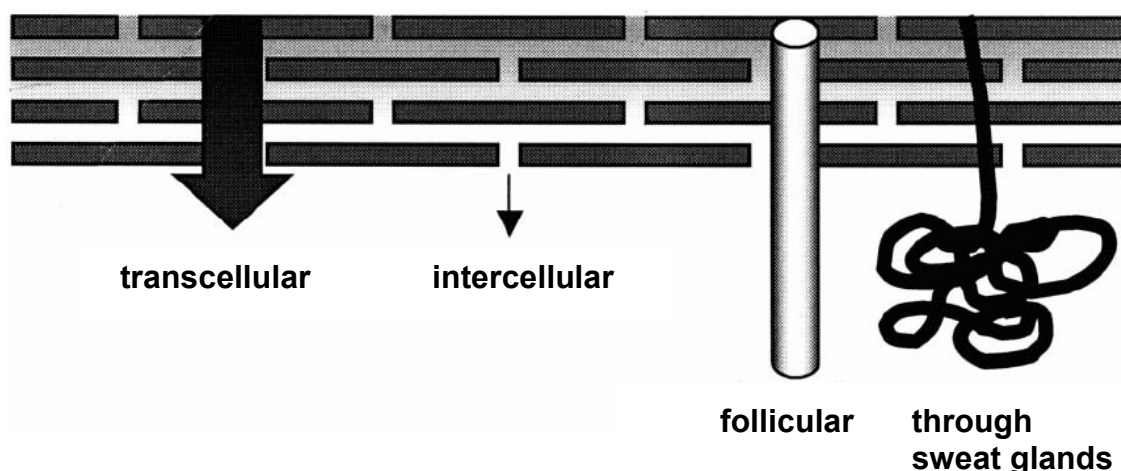


Fig. 3 Schematic of possible penetration routes through the stratum corneum (modified from Hadgraft 2001)

The intercellular penetration is regarded as the predominant pathway for most drugs (Barry 2001; Patzelt et al. 2008). It involves the diffusion of the substance through the intercellular lipids that glue the flat corneocytes. In some instances, a drug depot builds up in the stratum corneum, especially when the drug is only taken up slowly by the viable epidermis (i.e., if the drug is very lipophilic). The effective diffusion distance is much longer than the thickness of

the stratum corneum as a result of the tortuous diffusional pathway around the dead cells the molecules have to take (Shah et al. 1992; Bunge et al. 1999).

The transcellular route leads through the stratum corneum by alternately crossing the lipophilic matrix and the corneocytes. Therefore, the diffusion pathway is similar to the thickness of the stratum corneum. Yet, the general assumption is that the contribution of this route to the total diffusion is small for lipophilic compounds and might play a role for hydrophilic substances (Boddé et al. 1991; Bunge et al. 1999) and water (Patzelt et al. 2008). The fractional area of the skin occupied by hair follicles and sebaceous glands is only about 0.1%. For lipophilic, molecular-sized substances this pathway usually contributes negligibly to their permeation across the stratum corneum (Barry 2001; Patzelt et al. 2008). However, it seems to be of importance for the uptake of nanoparticles (average size: 320 nm) (Lademann et al. 2007) and hydrophilic substances (Otberg et al. 2008). Apparently, it becomes significant for substances or particles that struggle to cross the intact stratum corneum (Barry 2001).

1.2.2.2 Penetration of drugs through the viable epidermis and dermis

The viable epidermis is hydrophilic in nature. The molecules that have successfully crossed the stratum corneum are transported in its intercellular fluids. As described before the viable epidermis is metabolically active. It is only considered a barrier for very hydrophobic drugs due to their low solubility in this environment (Roy 1997; Hadgraft 1999).

The dermis is also hydrophilic in nature and might pose a barrier for very lipophilic compounds. It is pervaded by microcapillaries that readily absorb the drug (Roy 1997).

1.2.2.3 Pharmacokinetic concepts

The process of transdermal drug uptake is governed by passive diffusion of drug molecules through the skin and can be described by Fick's first law of diffusion (Delago-Charro and Guy 2001; Hadgraft 2001; Moser et al. 2001b):

$$J = D \cdot K \cdot \frac{c_{donor} - c_{acceptor}}{h} \quad \text{Equation 1}$$

J: flux per unit area

D: diffusion coefficient in the skin

K: stratum corneum-vehicle partition coefficient

c_{donor} : concentration in the formulation

c_{acceptor} : concentration in the blood

h : length of the diffusional pathway

1.2.2.4 Penetration from the inside to the outside

The systemic administration of drugs for skin diseases is common, especially in severe cases of scabies, fungal or bacterial infection and the treatment of tumors. It is assumed that the drugs find their way to the targeted skin site by the systemic circulation and “inverse penetration pathways”. However, little research has been carried out to investigate these pathways in detail. The results of articles reviewed by Patzelt (Patzelt et al. 2008) suggest that lipophilic substances predominantly reach the skin surface with the sebum while hydrophilic compounds are transported to the skin with the sweat.

1.2.2.5 Influence of body site

Dogma states that skin absorption varies widely for different body sites. As a matter of fact, there are some regions that are significantly more permeable for drugs (e.g., the scrotum, the axilla and the face). Some of these high-permeability sites have been exploited to enhance transdermal drug delivery: The first testosterone patch Testoderm® was worn on the shaved scrotum (the product was discontinued because of the inconvenience for the patients to shave the scrotum) or Scopoderm® TTS, which is worn behind the ear. However, the variability in transdermal absorption for the usually recommended body sites (back, chest, abdomen, upper arm) is mostly smaller than the inter-person variability (Gorsline et al. 1992; Sobue et al. 2005). The recommended site of application often serves psychological purposes (e.g., choosing a place near the heart for a nitroglycerin patch) or convenience (finding a discreet body site). Furthermore, a hairless area with minimal mechanical stress exposure is preferred to ensure optimal adhesion of the patch.

1.2.2.6 Influence of age

The skin undergoes certain changes during aging, e.g., the hydration decreases and the epidermis thickness decreases moderately (Gambichler et al. 2006). Still, the transdermal diffusion seems to stay constant for most compounds, except for relatively hydrophilic substances (Kaestli et al. 2008). Hence, the need for dose adaptation in elderly patients is not

related to changes in the barrier function of the skin, but a result of physiological changes, e.g., decreased hepatic clearance or decreased renal function.

1.3 TRANSDERMAL DRUG DELIVERY

In contrast to topical formulations, which have the goal to deliver a drug into the skin to treat dermal illnesses, transdermal drug delivery systems are designed to deliver the drug across the skin into the bloodstream to generate systemic effects (Shah et al. 1992).

Transdermal drug delivery is possible by applying a semisolid formulation (e.g., EstroGel®) onto the skin. To address the problem associated with dosing accuracy, metered-dose transdermal sprays have been developed (e.g., Evamist™, which was approved by the FDA in 2007). Another sophisticated approach is the formulation of the drugs into transdermal patches.

1.3.1 Advantages and limitations

1.3.1.1 Advantages of transdermal drug delivery

- Reduced presystemic metabolism: Avoidance of hepatic first-pass metabolism and degradation in the gastrointestinal tract and consequently the need for a lower daily dose
- More uniform plasma levels: Controlled zero-order absorption through the stratum corneum maintains drug plasma levels in the therapeutic window (i.e., below the levels where side effects become apparent and above the minimal effective concentration)
- Reduced inter- and inpatient variability: This is particularly true when the drug release from the dosage form is slower than the drug diffusion across the stratum corneum
- Improved patient compliance: Acceptability of the drug therapy due to reduced dosing frequency and reduced systemic side effects
- Interruptible action: Drug input can be terminated by patch removal

1.3.1.2 *Limitations of transdermal drug delivery*

The limitations of transdermal drug delivery are in principal a result of the skin's barrier function. In order to achieve a system with a reasonable size (smaller than 40 cm²) the following limitations need to be considered:

- Only possible for potent drugs with physico-chemical properties (see chapter 1.3.3) that allow percutaneous absorption: Normally drugs with daily doses exceeding 10 mg (which translates to plasma concentration is the low ng/ml range) cannot be delivered through the skin.
- Pharmacokinetic and pharmacodynamic criteria must be fulfilled: Drugs with short biological half-lives, large first-pass effect that necessitate inconvenient and frequent oral or parenteral administration are good candidates. Tolerance-inducing drugs are normally less eligible choices, unless a suitable “wash-out” period (e.g., nitroglycerin patches) is maintained.
- The drugs must not be locally sensitizing or irritating: Significant skin reactions during the application period of the patch will prevent the regulatory approval and decrease the patient compliance. This is called the “Achilles heel” of transdermal drug delivery (Brown et al. 2006) because the post-approval success of a transdermal drug delivery system that causes skin irritation will be greatly impaired (Toole et al. 2002).

1.3.2 **Transdermal patch design**

The categorization of different systems is not completely consistent in the literature (Peterson et al. 1997; Delago-Charro and Guy 2001; 3M 2008). Elements that all systems incorporate are: the backing liner (which covers the whole system and is the only visible element when the patch is worn), the adhesive, the release liner (which protects the patch and is removed and disposed before its application) and the drug.

Backing and release liners have to be inert to the formulation components and should have low permeabilities for them. Backing liners are comprised of polyester, polyurethane, polyethylene, terephthalate, polypropylene and polyvinyl chloride materials (Santoro and Rovati 2002). Release liners can in principle be made of the same materials and are typically coated with silicone or fluorocarbons to ensure their unproblematic removal from the patch surface. Some of the existing systems employ a semi-permeable membrane in order to control the drug release. Various materials, e.g., ethylene vinyl acetate copolymers, can be used for that purpose. The desired rate control is adjusted by varying the composition, the

pore size and the thickness of the membrane. Sometimes the pores of the membrane get impregnated with a diffusive medium (Kleiner and Gale 2002).

1.3.2.1 Membrane system (e.g., Duralgesic[®], Estraderm[®], Transderm-Nitro[®])

The membrane or reservoir system encloses a drug solution or suspension in a compartment separated by a semi-permeable membrane from the adhesive and the release liner (Fig. 4).

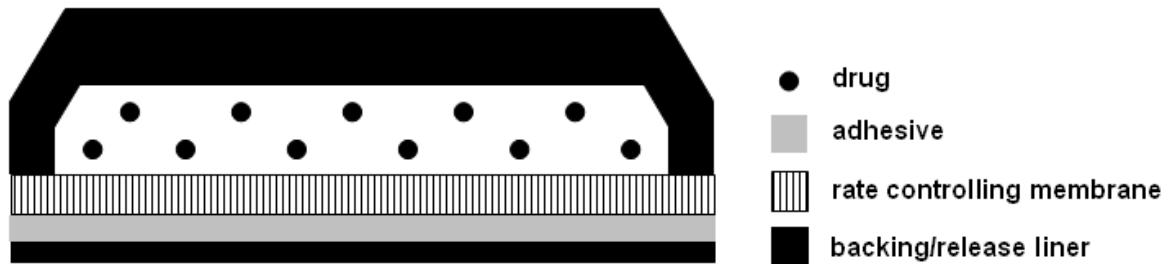


Fig. 4 Schematic of a membrane system

The adhesive can either exist in a circle around the membrane or cover the membrane completely. The latter configuration, wherein the adhesive is called “face adhesive”, is used by the vast majority of the modern reservoir-type systems because it maximizes the skin contact (Peterson et al. 1997).

The biggest advantage of membrane systems is that a properly designed system possesses zero-order release kinetics. The biggest drawback is the risk of a rate-controlling membrane rupture. A rupture could be caused by a material defect or unintentional puncture during application of the system and lead to dose-dumping, i.e., uncontrolled drug release from the formulation. Depending on the nature of the formulation and the drug this can lead to increased drug levels in the systemic circulation and serious side effects.

Release from membrane systems

The drug release from a membrane system is governed by the drug diffusion through the rate-controlling membrane and the adhesive layer. The total flux J can be described by the following equation:

$$\frac{1}{J} = \frac{1}{J_m} + \frac{1}{J_a} \quad \text{Equation 2}$$

J: drug release from the membrane controlled transdermal system

J_m : flux through the rate controlling membrane

J_a : flux through the adhesive layer

With Fick's first law of diffusion the following equation is obtained:

$$\frac{dm}{dt} = \frac{A \cdot K_{m/r} \cdot K_{a/m} \cdot D_m \cdot D_a \cdot c}{K_{m/r} \cdot D_m \cdot h_a + K_{a/m} \cdot D_a \cdot h_m} \quad \text{Equation 3}$$

$\frac{dm}{dt}$: drug release after time t

A: diffusion area

$K_{m/r}$: distribution coefficient membrane/reservoir

$K_{a/m}$: distribution coefficient adhesive layer/membrane

D_m : diffusion coefficient in the membrane

D_a : diffusion coefficient in the adhesive layer

c: drug concentration in the reservoir

h_a : thickness of the adhesive layer

h_m : thickness of the membrane

1.3.2.2 Matrix system (e.g., Habitrol[®], Nitrodisc[®], Prostep[®])

In this system, the drug is dissolved or suspended in a semi-solid matrix. The matrix is in direct contact with the release liner (and hence with the skin after application of the patch). The adhesive forms a ring around the matrix (Fig. 5).



Fig. 5 Schematic of a matrix system

The matrix, with drug and excipients, is separated from the adhesive, which avoids formulation complexities associated with drug/adhesive or excipient/adhesive interactions. Hence, this design may be superior in terms of excipient choice (Peterson et al. 1997).

On the other hand, this separation necessitates an increase in patch surface well over the actual delivery surface (Table 1). Furthermore, as the drug is delivered to the skin, the concentration in the formulation decreases and with it, according to Fick's law of diffusion, the driving force of the diffusion. Therefore, the release rate is not constant and decreases over time.

Release from matrix systems

The drug release from **solution type matrix systems** can be described by Higuchi:

$$Q = 2 \cdot c_0 \cdot \sqrt{\frac{D \cdot t}{\pi}} \quad \text{Equation 4}$$

Q: amount of drug released per area

c_0 : initial drug concentration in the adhesive

D: diffusion coefficient

t: time

This equation is only applicable if perfect sink conditions are maintained throughout the experiment and the released amount of drug does not exceed 30 to 60% of the formulation.

In **suspension type matrix patches** the initial drug concentration is higher than the solubility of the drug in the matrix.

The drug release can be described as follows:

$$Q = \sqrt{2 \cdot c_0 \cdot c_s \cdot D \cdot t} \quad \text{Equation 5}$$

c_s : drug solubility in the matrix

This equation is applicable if the diameter of the suspended drug particles is considerably smaller than the diffusion distance and the initial drug content of the matrix c_0 is substantially greater than the drug solubility in the matrix c_s .

For both solution and dispersion type matrix patches the drug release should be linear when plotted against the square root of time. The slope of the regression line represents the drug release rate k :

$$Q = k \cdot \sqrt{t} \quad \text{Equation 6}$$

k : release rate constant

1.3.2.3 Monolithic drug-in-adhesive (DIA) patch (e.g., Ortho-Evra[®], Climara[®])

In these systems the drug is directly included in the adhesive matrix (Fig. 6).

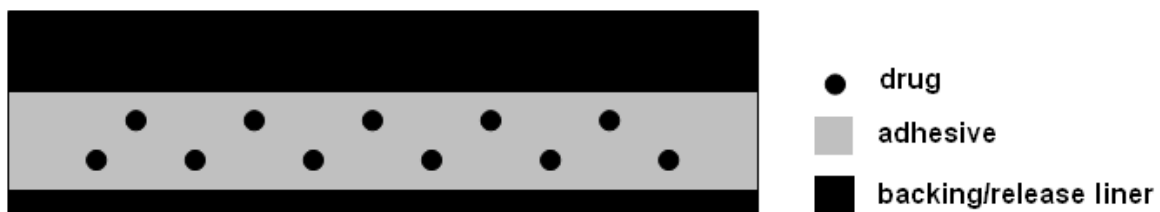


Fig. 6 Schematic of a monolithic drug-in-adhesive patch

Besides affixing the transdermal system to the skin, the adhesive matrix serves as the formulation foundation. This design possesses an additional degree of complexity because additives and drug can change the adhesive properties of the matrix (Dimas et al. 2000). Furthermore, since drug (and permeation enhancer) are released the mechanical and adhesive properties of the patch can change during the wearing period (Peterson et al. 1997).

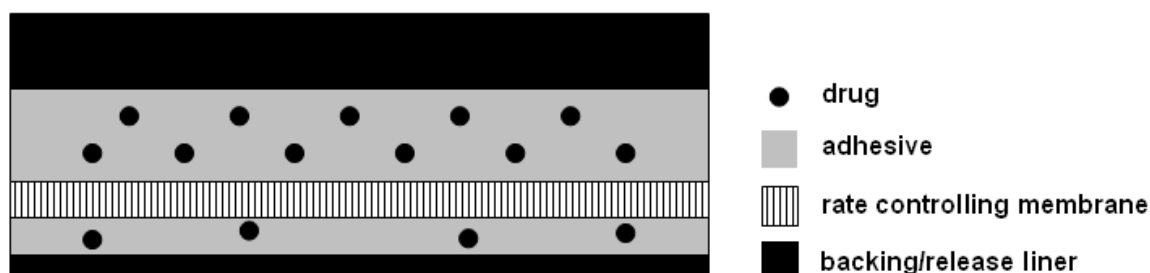
The advantages of this system are its small dimensions, both in thickness and surface area (the release surface area equals the patch size, Table. 1). Moreover, dose adjustment can be made by simply cutting the patch, e.g., for patients with impaired hepatic or renal functions. The drawback of DIA systems is that the drug release, as described earlier for matrix patches, decreases during the application period of the patch due to drug depletion.

Table 1 Influence of the patch design on the patch size: comparison of three nitroglycerin patches (modified from Peterson et al. 1997)

Patch design	Product	Delivery rate, mg/h	Delivery surface ¹ , cm ²	Patch size, cm ²
DIA	Minitran®	0.4	13.3	13.3
Matrix	Nitrodisc®	0.4	16	49
Reservoir	Transderm Nitro®	0.4	20	27

1: according to labeling*1.3.2.4 Multilaminate DIA patch (e.g., Nicoderm® , Catapres®-TSS)*

This system employs a rate controlling membrane between two distinct drug-in-adhesive layers or several drug-in-adhesive layers (Fig. 7).

**Fig. 7** Schematic of a multilaminar drug-in-adhesive patch

By this means the drug release can be customized, e.g., the bottom layer of the patch can contain drug for an initial burst, while the rate controlling membrane controls the release from the second drug-in-adhesive layer. This avoids the above mentioned problem of decreasing drug flux due to drug depletion.

1.3.2.5 Trends in the last years

Over the last years DIA patches became the preferred systems for passive transdermal drug delivery (Gordon and Peterson 2003). Besides their easy manufacture, this is probably a result of their high patient acceptance. Studies investigating several patient preference factors like comfort of wear, cosmetic appearance and adhesion found that patients preferred the DIA patch over the membrane system (Hougham et al. 1989; Lake and Pinnock 2000).

Patches containing highly drug-loaded acrylate particles dispersed in silicone matrix were invented by Noven Pharmaceuticals and are marketed as the Dot matrix™ technology. Since

silicone repels the acrylate particles, it stays uncompromised and can exert optimum skin adhesion as the drug-loaded acrylate particles release the drug (Brown et al. 2006). By this means Noven claims to produce patches with higher drug release and smaller size than patches prepared by conventional methods.

1.3.3 Physicochemical properties of compounds and skin permeation

The permeation behavior of a compound across the skin is to a large degree determined by its physicochemical properties (Prausnitz et al. 2004).

1.3.3.1 Octanol-water partition coefficient (logP)

The correlation between the logarithmic octanol-water partition coefficient (logP) and the permeation rate of a molecule through the skin is described by a parabolic curve (Roy 1997; Beetge et al. 2000; Delago-Charro and Guy 2001). Too polar and charged substances have a low affinity to the environment of the stratum corneum, which prevents their passive delivery. However, molecules that are excessively lipophilic have problems to reach the systemic circulation, too. The layers underneath the stratum corneum (the viable epidermis and the dermis) are aqueous and if the drug solubility herein is very poor, this “phase transfer” can become rate-limiting. Hence ideal drug candidates have good solubility in lipophilic and aqueous media. LogP values of drugs that have been successfully manufactured into commercial products range from 0.8 for clonidine to 4.2 for ethinyl estradiol. Nevertheless, newer entities that have been designed for transdermal use are often very lipophilic and insoluble (Hadgraft and Lane 2005). This leads to permeation problems that have to be overcome by formulation science, e.g., by the use of permeation enhancer combinations (Funke et al. 2002a; Funke et al. 2002b).

1.3.3.2 Solubility parameter

The correlation of the permeation coefficient and the solubility parameter shows a parabolic relationship. Drug molecules with solubility parameters of $10 \text{ (cal/cm}^3)^{1/2}$ exhibit the highest permeation. This result suggests that the human stratum corneum (or more precisely: the route that the drug molecules take in the stratum corneum) has a solubility parameter in that range (Roy 1997).

1.3.3.3 Molecular size/Molecular weight

A drug molecule's diffusivity in a medium depends on both the properties of the drug molecule and the properties of the medium. In more structured media (like the stratum corneum) diffusivities are more sensitive to the molecular weight of the drug than in liquids (Flynn and Yalkowsk.Sh 1972; Cantor 1999). Hence the molecular weight of a drug significantly influences its permeation properties. Drugs in commercially successful transdermal systems have molecular weight up to 337 Da (fentanyl) and the upper limit for a successful passive transdermal delivery was estimated to be between 500 and 1000 Da (Roy 1997). The maximum skin flux will decrease approximately by the factor 5 for an increase in 100 Da (Finnin and Morgan 1999).

1.3.3.4 Melting temperature

Drugs with a melting point below 200°C are believed to be best suited for transdermal drug delivery (Finnin and Morgan 1999). The rationale behind this requirement is that both solubility and melting point are a result of intermolecular forces. Hence, a high melting point (which is a very accessible drug property) indicates low intrinsic solubility of the drug in the stratum corneum and therefore a slow permeation. This relationship is also expressed by the following equation (Martin 1993b):

$$-\log X_2^i = \frac{\Delta H_f}{2.303R} \cdot \left(\frac{T_0 - T}{T \cdot T_0} \right) \quad \text{Equation 7}$$

X_2^i : ideal solubility of the solute expressed in mole fraction

ΔH_f : molar heat of fusion

R: gas constant

T_0 : melting point of the solute in absolute degrees

T: is the temperature of the solution

The maximum skin flux will decrease approximately by the factor 10 for an increase of 100°C in melting point (Finnin and Morgan 1999).

1.3.3.5 Influence of pH on the drug permeability

Since the lipophilic species normally has a higher affinity to the stratum corneum and therefore permeates the skin faster, the pH of the donor medium plays a role for acidic and

basic drugs. It was shown that a sigmoid relationship exists between the permeability coefficient and the donor solution pH with its turning point approximately at the pKs of the drug (Roy and Manoukian 1995).

1.3.4 The ideal transdermal drug delivery system

The properties of an ideal transdermal product can be summarized as follows:

- Adequate and reproducible biopharmaceutical performance
- Adequate stability (neither drug recrystallization nor chemical degradation during the shelf-life of the product)
- Adequate skin adhesion (no falloff during use, but easy removal of the patch after the wearing period)
- No unacceptable skin reactions (e.g., erythema, allergic reaction)
- Small patch size (normally less than 40 cm²)
- Cosmetically acceptable appearance

1.4 APPROACHES TO INCREASE TRANSDERMAL ABSORPTION

The transdermal route is not used more widely because it is difficult to get sufficient amounts of drug across the skin. To estimate the feasibility of a drug candidate to be transdermally delivered the following equation can be used (Delago-Charro and Guy 2001):

$$R = Cl \cdot C_{ss} \quad \text{Equation 8}$$

R: transdermal input rate

Cl: systemic clearance

C_{ss}: effective steady-state drug concentration

For zero-order input kinetic, R can also be expressed as:

$$R = A \cdot k_0 \quad \text{Equation 9}$$

A: release surface area of the patch, cm²

k_0 : steady-state delivery rate to the body

Substitution of equation 9 with equation 8 yields:

$$A = Cl \cdot C_{ss} \cdot k_0 \quad \text{Equation 10}$$

Assuming that a steady-state delivery rate of $25 \mu\text{gcm}^{-2}\text{h}^{-1}$ can be achieved (which is only the case for very rapid permeating drugs like nitroglycerin and nicotine) and knowing Cl and the required C_{ss} , the resulting patch size can be estimated (Table 2).

Table 2 Feasibility screening of drugs for transdermal delivery (modified from Delago-Charro and Guy 2001)

Drug	C_{ss} , $\mu\text{g/ml}$	Cl , l/h	A_{\min} , cm^2
Acetaminophen	15	23	13850
Cimetidine	1.0	49	1940
Isosorbide Dinatrate	0.001	175	7
Scopolamine	0.0002	43	0.35

As can be seen, the minimum patch size A_{\min} required to achieve target plasma levels can become very large for certain drugs. Therefore, much effort has been directed to increase the transdermal input rate by various methods:

1.4.1 Physical methods

1.4.1.1 Removal of the stratum corneum

One conceivable way to improve drug penetration across the skin is the (partial) removal of its predominant barrier, the stratum corneum. By this means, the molecules have to travel a shorter distance and they can reach the capillary system in the dermis faster. Several methods for stratum corneum removal have been described in the literature, including removal of the stratum corneum with motor-driven devices (Friedland and Buchel 2000) or laser (Dover et al. 2000). These methods are normally used by dermatologists for superficial skin removal in the treatment of hyperpigmentation or acne. Tape stripping, as the most simple method, is the removal of parts of the stratum corneum with corneocyte glue or adhesive tape.

Microdermabrasion-treated skin showed an increase in the skin flux and the skin deposition of vitamin C by approximately the factor 20 compared to intact skin (Lee et al. 2003).

Drawbacks of this straightforward method are obvious: The process of removal of cell layers can cause pain and inflammation. Hence patient compliance is small (Elias et al. 2002). Moreover, it is difficult to remove a defined amount of horny layer cells.

1.4.1.2 Skin puncture and perforation

Devices for skin puncture and perforation use blades or blade-like structures that create holes in the stratum corneum as a result of a defined movement (Brown et al. 2006). After the use of the device, the drug can be administered in a solution, cream or patch formulation.

1.4.1.3 Needleless injection

Needleless injection is a pain-free method to deliver drugs to the skin. It circumvents the pain, fear and safety concerns associated with the use of hypodermic needles. One example for a device able to transport particles in the skin is the PMED™ device. By forcing compressed helium with the drug formulation entrained in the gas through a special nozzle, the particles gain sufficient velocity for skin penetration (Burkoth et al. 1999). It is only used for solid particles that can be engineered to obtain tailored drug release.

Drawbacks of this application are the high development costs and the inability to adjust the drug delivery to intersubject variability in skin permeation (Brown et al. 2006).

1.4.1.4 Microneedle systems

A more sophisticated approach to physically overcome the stratum corneum's barrier is the use of microneedle systems (Prausnitz et al. 2002) (Fig. 8)

These devices are equipped with a multitude of microneedles that insert the drug underneath the stratum corneum. Either drug coated silicone needles or hollow metal needles (filled with drug solution) can be used for that purpose (McAllister et al. 2003). The needles penetrate the horny layer without destroying it and release the drug. Clinical studies report only minimal patient discomfort (Barry 2001)), low skin irritation and low erythema incidence (Kaushik et al. 2001).

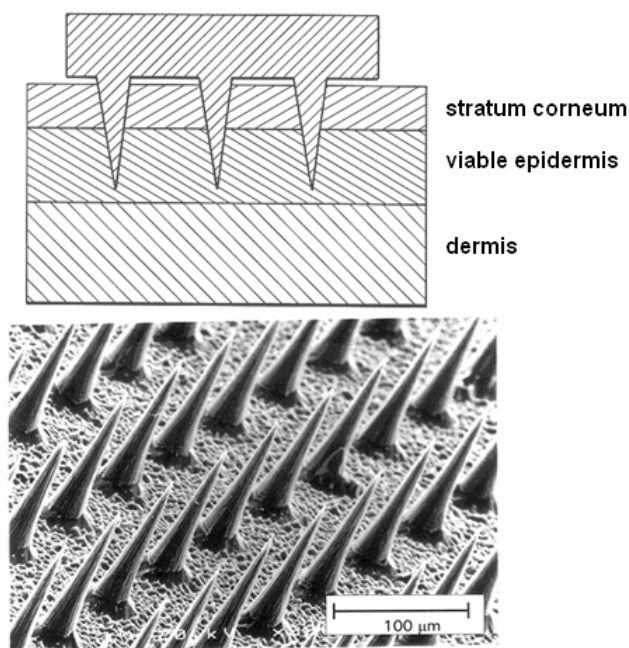


Fig. 8 Schematic of a microneedle system (modified from Prausnitz et al. 2002)

Recent commercializations of this technique are 3M's "Microstructured Transdermal System" (MTS) or Alza Corporation's Macroflux® (Brown et al. 2006).

This technology has the advantage that the delivery of drugs with extreme physicochemical properties (e.g., vaccines, large hydrophilic biopharmaceuticals) is possible. In mice the immunization with naked plasmid DNA using the microneedle technology induced stronger and less variable immune responses than with needle-based injections (Mikszta et al. 2002).

1.4.1.5 Thermophoresis

The average skin temperature is adjusted to 32°C by the homeostatic functions of the human body. In-vitro studies with three model drugs in saturated solution (to ensure similar thermodynamic activity of the drug) at different temperatures showed a 2-3 fold increase for every 7°C rise in skin surface temperature (Akomeah et al. 2004). The effects were attributed to an increase in drug diffusion in the solution and in the skin. In vivo the increased blood circulation in the targeted area might further increase the systemic drug absorption. A clinical study comparing fentanyl patches with and without attached heating device (42°C) showed that the patients' fentanyl blood plasma levels increased about 3 times with heat treatment. (Ashburn et al. 2003). The flux enhancement capacity of this method was limited by the heat tolerance of the patients, which was approximately 40-42°C (for a prolonged application).

Konno designed a self-heating transdermal patch (Fig. 9). After the removal of the seal, humidity from the air causes an exothermic reaction in the heating element. This provides heat to soften the wax and to facilitate the transdermal drug absorption.

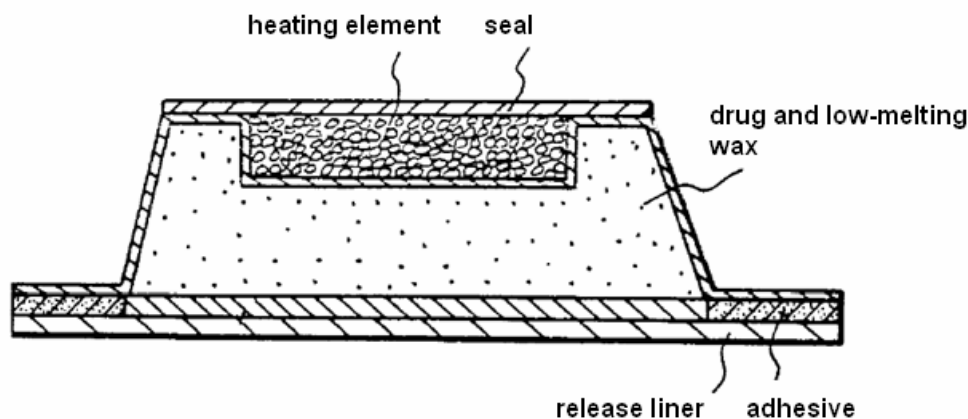


Fig. 9 Self-heating transdermal patch from US patent 4,685,911 (modified from Konno et al. 1985)

Another way of using temperature to increase the permeation of molecules through the skin is the approach used by ALTEA in their Passport™ patch. Here short bursts (30 ms) of focused thermal energy disrupt the structure of the stratum corneum. By this means, the delivery of macromolecules is possible. Currently, clinical studies with insulin are conducted.

1.4.2 Electrically assisted methods

1.4.2.1 Sonophoresis

Sonophoresis is the enhancement of drug penetration across the skin by ultrasound. It can be subdivided into simultaneous sonophoresis and pretreatment sonophoresis.

In the simultaneous approach, drugs are administered onto the skin and ultrasound is applied simultaneously. This method requires the patient to wear the ultrasound device during the treatment. The pretreatment approach uses ultrasound (e.g., the Sonoprep™ device) prior to the drug application. By this means, the skin is “permeabilized” and stays in a highly permeable state for several hours during which the drug is delivered through the skin. The latter method requires the determination of the degree of skin permeabilization prior to the drug application. For that purpose, correlations between the skin conductance and its permeability can be exploited (Mitragotri and Kost 2004). It was shown that low frequency ultrasound ($f < 100$ kHz) is more effective than higher frequencies (Mitragotri and Kost 2004).

The promotion of skin permeability by ultrasound is related to the disturbance of stratum corneum lipids (Mitragotri and Kost 2004; Ogura et al. 2008). This is a result of the collapse of gaseous cavities that appear predominantly in the coupling medium (i.e., the medium that is applied between the transducer device and the skin) under the oscillating pressure field of ultrasound. Lipid extraction might play an additional role in low-frequency sonophoresis (Alvarez-Roman et al. 2003), especially if the coupling medium contains surfactants. In simultaneous sonophoresis, the convection forces induced by the ultrasound additionally facilitate the penetration of the coupling medium into the stratum corneum, which increases its permeability (Ogura et al. 2008).

The immersion of hairless rats in a vessel filled with insulin in an ultrasound bath decreased their blood glucose levels by 50% in 240 min (Tachibana and Tachibana 1991). It was also shown that sonophoresis enabled the transport of insulin, γ -interferon and erythropoietin across human skin in vitro (Mitragotri et al. 1995). A double blinded clinical study using the Sonoprep™ device in combination with the local anesthetic EMLA was conducted. When patients were pricked with a hypodermic needle, they felt significantly less pain at spots pre-treated with ultrasound (Mitragotri and Kost 2004). The device was approved by the FDA for the use in dermal anesthesia in 2004. According to the manufacturer's website (<http://www.echotx.com>; visited on 18th of July 2008) successful feasibility studies in swines and rats were conducted with insulin and heparin. The Sonoprep™ device measures the skin impedance during the application and thereby controls the skin permeation. An example of a device employing simultaneous sonophoresis is Patch-Cap™. It delivers Insulin and is worn for 24-36 h. Up to date (19th July 2008) it has not gained market approval.

The selection of appropriate parameters for the ultrasound treatment is necessary to ensure the safety of the application. In general, low frequency ultrasound is better tolerated by patients than high frequency ultrasound. Continuous monitoring of skin permeability is proposed to avoid necrosis/pain and excessive penetration of compounds into the body (Ogura et al. 2008).

1.4.2.2 Iontophoresis

Iontophoresis is the increased delivery of an ionizable drug across the skin by an applied electrical potential (Delago-Charro and Guy 2001). An iontophoretic device comprises a current source and two electrode compartments that are usually equipped with Ag/AgCl electrodes (Fig. 10).

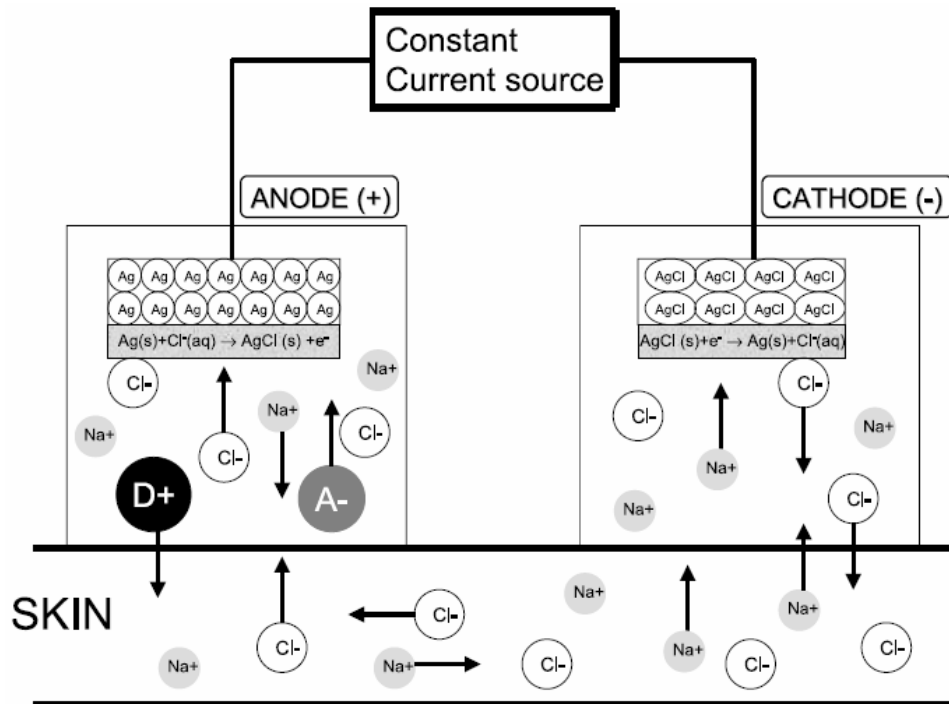
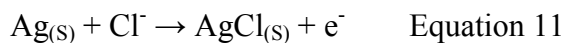


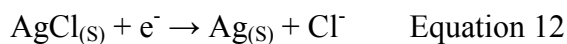
Fig. 10 Iontophoresis with an Ag/AgCl electrode system (modified from Kalia et al. 2004)

A weakly basic drug (D^+A^-) and NaCl are placed in the anodal compartment. After an electric current is applied, NaCl provides the chloride ions for the reaction at the anode, where insoluble AgCl is deposited on the electrode surface:



To maintain electroneutrality, a cation (Na^+ or D^+) migrates from the anodal compartment into the skin.

In the cathodal compartment, AgCl is reduced by the arriving electrons and elemental silver is deposited on the electrode surface:



Similar to the anodal electrode this is compensated for by the arrival of a cation from the skin or the loss of an anion.

Furthermore, iontophoresis induces a convective flow (“electro-osmosis”) in which both uncharged and charged compounds are transported.

The predominant pathway for charged molecules during iontophoretic drug delivery was found to be appendageal (e.g., through hair follicles) by confocal laser microscopy (Panchagnula et al. 2000; Alvarez-Román et al. 2004).

The drug flux through the skin depends on the drug concentration of the formulation and the pH because it effects the amount of ionized drug molecules (Kalia et al. 2004). The drug permeation is determined by the electrical current. If the current is doubled, the amount of drug permeating through the skin should also double. Analogously, if the current is turned off, the amount of drug permeating the skin should go back to the level of passive diffusion. Hence this method can control the drug delivery rate to a large degree and offers the possibility to individualize drug therapy (Delago-Charro and Guy 2001; Kalia et al. 2004).

Iontophoresis is able to deliver small molecules (e.g., opioids, NSAID) but also peptides and proteins. For example, luteinizing hormone-releasing hormone, human parathyroid hormone and insulin could be successfully delivered in animal models (Kalia et al. 2004).

Reverse iontophoresis, in which the molecule of interest does not travel into the skin but from the skin into the device, allowed for the development of Glucowatch® (Panchagnula et al. 2000). This device enables diabetes patients to monitor their glucose level non-invasively and was approved by the FDA in 2001.

1.4.2.3 Electroporation

Electroporation or electropermeabilization is the perturbation of the lipid bilayer membranes in the stratum corneum by applying high voltage pulses. The applied voltage is normally in the range of 100-1500 V and lasts for 10 μ s to 10 ms. The time between the pulses is usually in the range of seconds (Denet et al. 2004).

Electroporation creates new aqueous pathways in the lipid layers of the stratum corneum (Chizmadzhev et al. 1995). In combination with thermal effects that accompany this technique, it leads to an enhanced skin permeability for small drugs and macromolecules (Lombry et al. 2000).

The decrease in skin resistance and the increase of the transepidermal water loss after the application are only partly reversible and hence a safety concern (Denet et al. 2004). Furthermore, during the application the sensation of pain has been reported, which is probably a result of the main adverse effect: muscle contraction.

1.4.3 Chemical penetration enhancers

1.4.3.1 *Metabolic or biochemical enhancers*

Metabolic or biochemical enhancers interfere with metabolic or biochemical events in the skin and can potentially be used to alter its barrier function (Finnin and Morgan 1999).

As mentioned in section 1.2.1.1 the lipids in the stratum corneum are mainly comprised of ceramides, cholesterol and free fatty acids. A decrease in the content of either one of these main lipids leads to impaired barrier function (Man et al. 1995). Therefore, the application of lipid synthesis inhibitors (e.g., glycosylceramide synthase, HMG-CoA reductase, acetyl CoA carboxylase) results in increased transepidermal water loss and a decreased permeation barrier of the stratum corneum (Elias et al. 2002).

Other possible targets include the inhibition of the secretion of the Odland bodies (i.e., the lamellar bodies that release the lipids at the border of the stratum granulosum and the stratum corneum, see section 1.2.1.1) and inhibitors of enzymes that assemble the lipid bilayers in the stratum corneum.

The application of a metabolic permeation enhancer, in addition to a regular chemical permeation enhancer, results in a further increase of transdermal drug delivery (Tsai et al. 1996). However, questions with regards to the safety of their administration arise. Problematic issues include possible ingress of toxic substances and pathogenic microbes through the impaired skin. It was suggested that these problems might be overcome by “closing the window” in the stratum corneum after the application by applying physiologic lipids (Elias et al. 2002).

1.4.3.2 *Chemical enhancers*

At present the most widely used approach to increase transdermal penetration is the use of chemical penetration enhancers (Büyüktimkin et al. 1997). These compounds diffuse into the skin where they interact with structures of the stratum corneum and alter its barrier function. According to Barry’s Lipid-Protein-Partitioning theory (Barry 1991) penetration enhancers basically employ one or more of the following mechanisms:

- Disruption of the ordered intercellular lipids in the stratum corneum
- Interaction with the protein components inside the corneocytes
- Enhanced partitioning of the drug into the stratum corneum

The ideal properties of a permeation enhancer are (Büyüktimkin et al. 1997; Delago-Charro and Guy 2001; Williams and Barry 2004):

- Pharmacologically inert
- Non-toxic, non-irritant, non-allergenic
- Rapid onset of action; predictable and suitable duration of action
- After removal of the enhancer the skin should immediately and fully recover its barrier function
- Impairment of the skin's barrier function only unidirectional to prevent the efflux of endogenous material
- Compatible with all components of the drug delivery system
- Odorless, tasteless and colorless (cosmetically acceptable)
- Inexpensive

Water

The water content in the stratum corneum is under normal conditions approximately 15-20% (Williams and Barry 2004). One approach to increase transdermal delivery is to increase its water content. In a clinical setting this can be achieved by occlusion of the skin, e.g., with occlusive dressings (waterproof plaster), lipophilic ointments (paraffins, oils, fats) or transdermal patches (the degree of occlusion depends on the used adhesive and the backing) (Barry 2001). The transepidermal water loss, which is approximately 10 g/m²/h (Casiraghi et al. 2002), increases skin hydration. By this means, a weight gain of up to 400% of the hydrated skin compared to dry skin is possible (Williams and Barry 2004). Occlusion of the skin increases the permeation rates of most compounds (both lipophilic and hydrophilic).

The following mechanisms for the penetration enhancement of water are discussed in the literature: Free water in the tissue can change the solubility of a permeant in the stratum corneum and hence change its partition coefficient. According to freeze-fracture electron microscopic investigations (Van Hal et al. 1996) and results from transmission and cryo-scanning electron microscopy (Warner et al. 2003), fully hydrated stratum corneum contains pools of water in the intercellular lipid regions. The existence of these pools helps to explain the penetration enhancing effect of water for hydrophilic molecules. It was also suggested that the swollen corneocytes in the hydrated stratum corneum lead to a distortion in the stratum corneum's mortar-and-brick structure and consequently to new connections (Elias et al. 2002). These "pores" could be responsible for the faster permeation of molecules.

Sulfoxides and similar chemicals

Dimethylsulfoxide (DMSO), which is often used as the “universal solvent”, has excellent penetration enhancing effects on hydrophilic and lipophilic drugs (Horita and Weber 1964; Clancy et al. 1994; Santoyo et al. 1995). The onset of action is rapid (spillage of the solvent on the skin can be tasted in the mouth seconds later). Problems with DMSO arise from the fact that high concentrations are needed for an optimum penetration enhancement, which can cause erythema and protein denaturing. Kligman (1965) showed that healthy volunteers developed erythema, scaling, contact urticaria and stinging/burning sensations after being painted with DMSO twice daily for three weeks. A further problem is that a metabolite of DMSO produces a foul odor in the breath (Williams and Barry 2004). Since the use of DMSO is problematic for the above mentioned reasons, derivatives and chemically related materials have been investigated. These substances include dimethylformamide (DMF), dimethylacetamide (DMAC) and decylmethylsulfoxide (DCMS). DMF and DMAC are also strong accelerants, but the application of DMF results in irreversible membrane damage (Southwell and Barry 1983). DMAC possesses a stronger enhancing capacity for hydrophilic than for lipophilic drugs (Williams and Barry 2004).

The mechanism of penetration acceleration seems complex: Protein conformational changes of keratin in the corneocytes probably play a role (Oertel 1977). Furthermore, DMSO has been shown to interact with the intercellular lipids.

Azone

Azone, or 1-dodecylazacycloheptan-2-one, was the first substance actually designed as a skin permeation enhancer. It enhances the skin permeation of a multitude of hydrophilic and lipophilic drugs. It is typically used in low concentrations (1-3%) and is far less effective when used in higher concentrations (Williams and Barry 2004). Azone has a certain irritation potential (Hirvonen et al. 1993) and never received marketing approval in a commercial transdermal formulation.

Pyrrolidones

Certain pyrrolidones have showed skin penetration enhancing effect, predominantly for hydrophilic molecules. However, they can cause erythema and contact dermatitis (Jungbauer et al. 2001).

Fatty acids

A variety of fatty acids can enhance skin permeation. Oleic acid, the most popular, increases the salicylic acid flux 28-fold and the 5-fluorouracil flux 56-fold through human skin in vitro (Goodman and Barry 1989). Saturated fatty acids with an alkyl chain length of approximately 12 and unsaturated fatty acids with an alkyl chain length of 18 attached to a polar head group show optimum enhancement (Aungst et al. 1986; Williams and Barry 2004). These penetration enhancers interact with the lipid domains in the stratum corneum. They were also shown to increase the bilayer fluidity (Prausnitz et al. 2004).

Alcohols

Ethanol increases the flux of drugs across the stratum corneum (Pershing et al. 1990). It permeates the skin rapidly and can improve the drug solubility in the stratum corneum, which increases the partition coefficient between the vehicle and the membrane. Since ethanol can be released from formulations, where it is often used as a drug solvent, it might leave a metastable supersaturated system that releases faster due to increased thermodynamic activity (see section 1.5). Investigations of alcohols with different chain lengths found maximum enhancement for decanol (Williams and Barry 2004).

Surfactants

Most surfactants show penetration enhancement and are known to have low chronic toxicity. They solubilize the lipids in the stratum corneum and thereby increase the drug flux across the barrier. In general, it seems that anionic surfactants have a more pronounced penetration enhancement effect than non-ionic (Williams and Barry 2004).

Terpenes

Terpenes are non-aromatic compounds only comprised of carbon, hydrogen and oxygen. They consist of repeating (C₅H₈) units (Aqil et al. 2007). A variety of terpenes showed permeation enhancing effects for lipophilic and hydrophilic drugs (Büyüktimkin et al. 1997). They are a popular choice for formulators because the FDA classifies them as GRAS (generally regarded as safe), which facilitates their approval (Aqil et al. 2007). Terpenes disrupt the lipid layers and, as previously described for ethanol, might leave a supersaturated formulation after their release.

1.4.3.3 Synergistic effects and high throughput screening of chemical permeation enhancers

Penetration enhancer combinations can have synergistic effects (Funke et al. 2002a; Karande et al. 2004; Williams and Barry 2004; Karande et al. 2006) due to various reasons, e.g., permeation enhancer no. 1 could facilitate the partition of permeation enhancer no. 2 into the stratum corneum where permeation enhancer no. 2 exerts its action.

Finding synergistic combinations of permeation enhancers is a very time consuming procedure, especially when different ratios of enhancers are to be tested. Therefore the in-vitro skin impedance guided high-throughput (INSIGHT) method has been developed. This method uses changed of the skin impedance after application of a penetration enhancer combination as a surrogate marker for permeation enhancement. Leading formulations are then tested for skin irritation in in-vitro cultures of human keratinocytes (Epiderm). By this means, permeation enhancer combinations could be found that enabled the delivery of proteins through the skin (Karande et al. 2004).

1.4.3.4 Combinations of physical and chemical penetration enhancement

Various combinations of physical and chemical penetration enhancement have been tested (Mitragotri and Kost 2004). They might be beneficial with regard to safety issues because the strength of the individual enhancement technique can be decreased. Interestingly, some electrically assisted techniques need uncommon chemical enhancers for a maximum enhancement effect. Electroporation, for instance, which creates new aqueous pathways, benefits from enhancers that stabilize these channels more than from chemical enhancers that disrupt the lipid bilayers in the stratum corneum (Denet et al. 2004).

1.4.3.5 Regulatory issues

Hundreds of substances have been successfully investigated as penetration enhancers. Yet, only a small percentage of these compounds is used in pharmaceutical products, since the authorities treat new and unapproved chemical penetration enhancers like new chemical entities rather than simple excipients. Thus, safety issues have to be clarified in expensive preclinical and clinical studies (Büyüktimkin et al. 1997). Most of the penetration enhancers commercially used today can be found on the GRAS list, which contains substances that are “generally regarded as safe” by the FDA (Finnin and Morgan 1999).

1.4.4 Modification of drug and formulation

All the aforementioned methods to increase transdermal drug delivery have the goal to compromise the barrier function of the stratum corneum either by physical, electrical or chemical means. The inherent drawback of these methods is that these alterations are normally non-selective. Besides increasing the delivery of the drug, the ingress of foreign substances and microbes could also be facilitated. Alternative approaches to increase the amount of delivered drug by optimizing the formulation are described in the following section.

1.4.4.1 Use of prodrugs

A prodrug is an inactive pharmacological derivative of an active parent drug (Albert 1958). It undergoes a spontaneous or enzymatic transformation that results in the free drug. The prodrug approach aims at an alteration of the physico-chemical properties of a compound by covalently attaching a transport moiety that enables the molecule to reach its physiological target.

This approach is seldom described in the literature for transdermal drug delivery. Lipp et. al used esters of gestodene in transdermal patches, but primarily to enhance the drug solubility in the matrix. By this means, the drug loading of the system could be increased without drug recrystallization (Lipp et al. 1998). Hammell et. al increased the permeation of naltrexone through human skin by the factor 2 by using a gemini prodrug, which is a prodrug comprised of two molecules of the same drug (Hammell et al. 2004).

While the prodrug approach is successfully used in commercial dermal products (e.g., tazarotene for the treatment of acne vulgaris and psoriasis (Rautio et al. 2008)), it has not yet been successful on the transdermal level. The reason seems to be mostly financial; in order to get the regulatory approval, the prodrug must undergo the same safety assessment procedures as the parent compound (Delago-Charro and Guy 2001; Rautio et al. 2008).

1.4.4.2 Colloidal systems

Microemulsions

Microemulsions are clear, stable and isotropic mixtures of water, oil and surfactant. Their penetration enhancing effect is mostly due to their high content of oil and surfactant, which act as chemical permeation enhancers (Kogan and Garti 2006) (see section 1.4.3.2).

Liposomes

Liposomes are colloidal particles that typically consist of phospholipids and cholesterol. They form concentric bilayers that may entrap drugs for transdermal or dermal delivery. The possible penetration of liposomes across the stratum corneum is debated, but the general agreement is that they cannot pass the intact stratum corneum and act mostly locally (Barry 2001; El Maghraby et al. 2008). Transfersomes are liposomes with “edge activators”, such as a single-chain lipid or a surfactant. Claims have been made that they are ultradeformable and hence capable of crossing the stratum corneum (Cevc et al. 1996). They need non-occluded conditions because they follow a local hydration gradient through the skin (Barry 2001). It is also conceivable that contents of the abovementioned formulations (e.g., the phospholipids) interact with the lipids in the stratum corneum and thereby increase the drug penetration.

1.4.4.3 Reduction of drug particle size

Micronization is a simple and well-known method to enhance drug dissolution. It is widely used to increase the release of poorly water soluble drugs from different drug delivery systems. Reduction in particle size leads to an increase in surface area and hence to a faster dissolution. The Noyes-Whitney equation, which is derived from Fick’s law of diffusion, expresses the relationship between dissolution rate and the surface area of the drug particles:

$$\frac{dm}{dt} = \frac{D \cdot S \cdot (c_s - c_t)}{h} \quad \text{Equation 13}$$

dm/dt : mass of solute dissolved in time t

D : diffusion coefficient of the solute in solution

S : surface area of the exposed solid

h : thickness of the diffusion layer

c_s : solubility of the solid

c_t : concentration of solute in the bulk solution at time t

This approach has been used in the Menorest[®] patch, which contains a micronized suspension of estradiol in an acrylate adhesive matrix (Marty 1996). However, an increase in transdermal delivery is only possible if the dissolution of the drug in the therapeutic system is the rate-limiting step of the drug delivery to the body.

1.4.4.4 Ion pairs

Since charged molecules do not readily cross the stratum corneum, the technique of ion pairing has been investigated. The ion pair is believed to travel across the stratum corneum as a neutral species, and afterwards dissociate into its charged species. In general, only mild penetration enhancement (about 2-fold) can be achieved (Valenta et al. 2000).

1.4.4.5 Eutectic systems

As explained in section 1.3.3.3, the melting point of a compound influences its solubility in the stratum corneum according to the ideal solubility theory. The eutectic point is the lowest temperature at which a liquid phase exists in a 2-component system (Martin 1993c). Since the eutectic mixture of two components has a lower melting point than the two single components, the penetration behavior of eutectic mixtures has been investigated. An eutectic mixture of ibuprofen and thymol (ratio: 60:40, w/w) increased the flux through human epidermis 5.9 times, compared to a saturated aqueous ibuprofen solution. The skin samples were pre-treated for 12 h with a saturated thymol solution to correct thymol's penetration enhancing effect (Stott et al. 1998).

1.5 SUPERSATURATION AND RECRYSTALLIZATION INHIBITION

The steady state drug flux across a barrier can also be described using the thermodynamic activities (Higuchi 1960; Barry 2001):

$$\frac{dm}{dt} = \frac{aD}{\gamma h} \quad \text{Equation 14}$$

dm/dt : steady state drug flux

a : drug's thermodynamic activity in the vehicle

D : diffusion coefficient

γ : effective activity coefficient in the stratum corneum

h : thickness of the membrane

It is obvious from equation 14 that the permeation rate dm/dt increases when the drug's thermodynamic activity increases. In an equilibrated system, the drug's thermodynamic

activity is maximal when dissolved drug molecules are at equilibrium with undissolved, solid drug. Based on equation 14, it follows that in general all vehicles containing a drug suspension should produce the same steady state flux. This applies for ideal systems where no interaction between the vehicle and the stratum corneum takes place and dissolution of the drug is not rate limiting (which can be avoided by using finely ground drug substance). Twist and Zatz (1986) investigated the flux of paraben from saturated solutions in 11 solvent mixtures across a silicone membrane. They found that, although paraben concentrations in the solvent mixtures varied over 100-fold, the flux was similar. Lippold and Schneemann (1984) showed that the pharmacological response of a topical formulation was related to the drug's thermodynamic activity in the formulation and not to the drug concentration. In a double-blinded study, they assessed the pharmacological effect ("blanching response") of betamethasone-17-benzoate from three ointments. For a given ointment the response increased as long as the drug was in solution. Above the saturation concentration the pharmacological effect was constant. Although the drug solubility was different in the three ointments (2.8, 29 and 59 mg/100g), the blanching response was similar for all saturated formulations. These examples emphasize that the driving force for the drug penetration is the difference in the chemical potential between the formulation and the membrane, not its absolute concentration (Barry 2001; Hadgraft 2001; Moser et al. 2001b).

Increasing the drug concentration above its solubility results in non-equilibrated, supersaturated systems. The degree of supersaturation D is defined as (Megrab et al. 1995):

$$D = \frac{c_v}{c_{sat}} \quad \text{Equation 15}$$

c_v : drug concentration in the vehicle

c_{sat} : drug saturation solubility in the solution

By using supersaturated systems, an increased drug flux across membranes can be achieved. Iervolino et al. (2000) and Raghavan et al. (2001a) showed increased ibuprofen and hydrocortisone flux across a silicone membrane from supersaturated propylene glycol : water mixtures. It was also shown that the increased thermodynamic activity increased the permeation across the skin: Moser et al. (2001a) could linearly correlate the degree of supersaturation with the flux of a lipophilic model drug across pig ear skin. In their studies, the supersaturation had no influence on the diffusion coefficient and the partition coefficient.

They concluded that solely thermodynamic effects were responsible for the permeation enhancing effect. Pellet et al. (1997) could linearly correlate the piroxicam flux from supersaturated solutions across human skin with the degree of supersaturation.

1.5.1 Preparation of supersaturated formulations

Since the supersaturated state is metastable, one approach is to create the supersaturated system in-situ or shortly before application. By this means, issues with regard to long term stability are circumvented. Coldman et al. (1969) were the first to study the effect of supersaturated solutions on skin penetration. Their method of preparation was to use a nonvolatile-volatile solvent mixture to dissolve the drug. After the evaporation of the volatile solvent (i.e., isopropanol) a supersaturated drug solution remains. As mentioned in section 1.4.3.2, formulations containing drug solvents that penetrate the skin very fast can become supersaturated in-situ. This mechanism might contribute to the penetration enhancing effect of formulations with ethanol. In the mixed cosolvent method, a saturated drug solution in a good solvent is prepared. After diluting this solution with a non solvent, supersaturated solutions are generated (Fig. 11). The most commonly used system is the propylene glycol : water system (Moser et al. 2001b). A variation of this method relies on the water uptake of the formulation from the skin. Water-free micro-emulsion bases were saturated with drugs and applied to the skin of New Zealand albino rabbits under occluding conditions. The transepidermal water loss of the rabbits resulted in the formation of supersaturated microemulsions with increased penetration characteristics (Kemken et al. 1992).

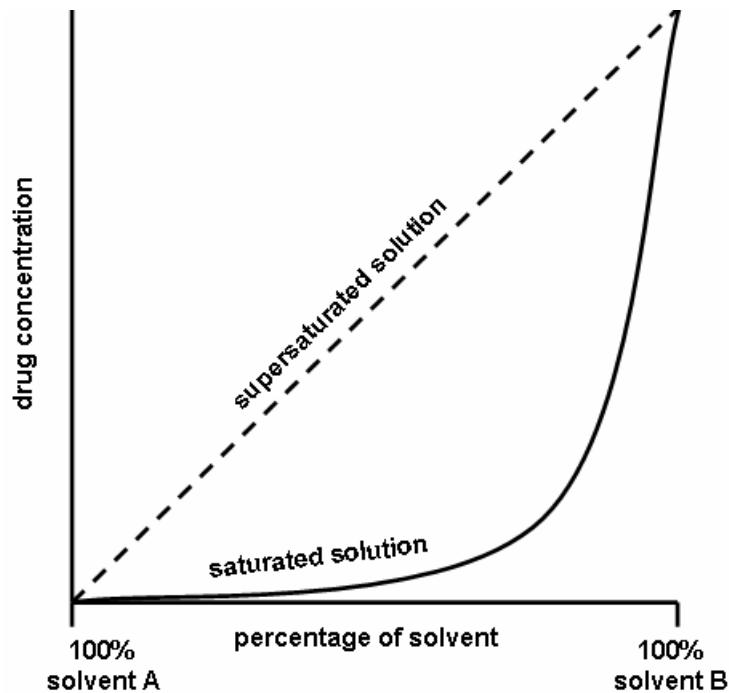


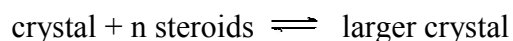
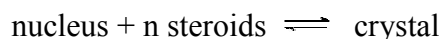
Fig. 11 Mixed co-solvent method for the preparation of supersaturated solutions. (—) represents the solubility of the drug in solvent mixtures of solvent A and solvent B, while (- -) represents the metastable supersaturated solution obtained by adding solvent A to a saturated drug solution in solvent B

1.5.2 Recrystallization in supersaturated formulations

Crystallization is in principle the result of two independent phenomena, nucleation and crystal growth. These two phenomena are temperature dependant; lower temperatures favor nucleation and higher temperatures favor crystal growth. The maximal crystallization rate of a compound is found at temperatures between its glass transition temperature (T_g) and melting point (T_m) (Yu 2001).

The crystallization process of supersaturated solutions includes several steps (Lipp 1998; Raghavan et al. 2001b): In the first step by collision of single molecules a so-called subnucleus or embryo is formed. Once this subnucleus attracts further molecules and exceeds its critical radius, it loses the ability to dissolve in the surrounding matrix. At that point, it accumulates further molecules and crystal formation takes place. Crystal growth in a matrix stops once the system is saturated. At that point, smaller crystals might redissolve in the matrix while larger crystals grow larger. This process is known as the Ostwald ripening. It is due to the fact that molecules at the surface of a crystal are energetically less stable than molecules in the interior of the crystal. Hence large crystals are favored because their surface : volume ratio is lower.

The following equilibria are of interest in patches containing steroid drugs (Lipp 1998):



Crystal-growth inhibitors commonly used in suspensions are effective within the equilibria 3 and 4, while effective crystallization inhibitors in transdermal matrix patches should affect the first two equilibria.

1.5.3 Use of soluble additives to prevent drug recrystallization

The supersaturated state is metastable by definition. For thermodynamic reasons, drug recrystallization will occur eventually. According to Fick's law of diffusion, only the amount of dissolved drug contributes to the drug flux. Hence drug recrystallization in transdermal patches can lead to reduced delivery across the skin and, consequently, to ineffective drug plasma levels. It is therefore a necessity to prevent drug recrystallization in these formulations for the duration of the shelf-life.

The main factors that prevent drug recrystallization in matrices are thought to be intermolecular interactions between the excipient and the drug (the excipient adsorbs onto the growing surface and "poisons" the crystallization) and the viscosity of the formulation (Doherty and York 1987; Taylor and Zografi 1997; Bhugra and Pikal 2008). Additionally, according to a model developed by Raghavan et al. (2001b), polymer-molecules that were rejected at the crystal surface can accumulate in the hydrodynamic layer which surrounds it and thereby increase the resistance for drug diffusion to the crystal (Fig. 12).

In general, the nucleation time of a drug in the supersaturated state increases with increasing concentration of the antinucleating agent and with decreasing degree of supersaturation (Raghavan et al. 2001b).

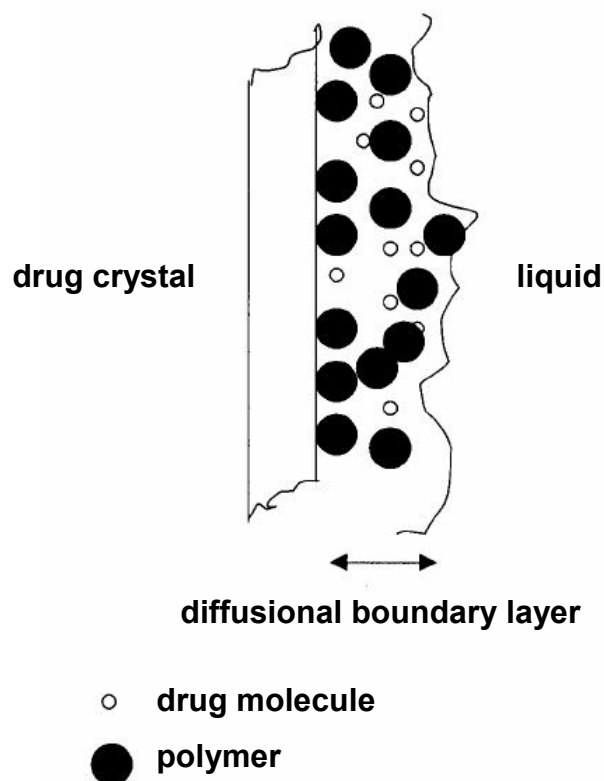


Fig. 12 Mechanism of crystal growth inhibition (modified from Raghavan et al. 2001b)

1.5.3.1 Polyvinylpyrrolidone and derivatives

Polyvinylpyrrolidone (PVP) has been used extensively to inhibit drug recrystallization in solid solutions. Over 60 different drugs have been dispersed in this polymer (Taylor and Zografi 1997), which is commonly used at molecular weights of 2500 - 50000 Da (K12 to K30) (Leuner and Dressman 2000).

Interactions between the polymer and the drug molecules seem to be the predominant reason for the stabilizing effect. PVP is able to form hydrogen bonds, electrostatic bonds and form complexes with different strengths. Hydrogen bonds are preferably formed by the C=O moiety of PVP for steric reasons (Doherty and York 1987; Sekizaki et al. 1995; Taylor and Zografi 1997).

In transdermal systems, PVP prevented the recrystallization of several hormones and ketoprofen (Megrab et al. 1995; Ma et al. 1996; Lipp 1998; Raghavan et al. 2001b; Kim and Choi 2002), with an optimal concentration of 10% (w/w) (Raghavan et al. 2001a). Higher polymer concentrations decreased the flux, which was attributed to an increase in drug solubility (and hence a lower degree of supersaturation) and an increase in microviscosity.

PVP derivatives, like PVP-vinyl acetate and PVP-hexadecene, also increased the nucleation time of a gestagen in an acrylate matrix, but they were found less effective than PVP (Ma et al. 1996).

1.5.3.2 Cellulose polymers

Substituted cellulose-polymers (e.g., HPMC, HPC, MC) have several potential binding sites for hydrogen bonds per unit. Hence, their optimum concentration as recrystallization inhibitors in transdermal patches is lower (0.5-1%, w/w) than for the PVP derivatives (Raghavan et al. 2001a). They were found suitable as antinucleating agents in several studies (Megrab et al. 1995; Lipp 1998; Raghavan et al. 2000; Raghavan et al. 2001b). A 4.8-times saturated hydrocortisone acetate solution stabilized with different amounts of different polymers yielded in the highest flux rates across silicone membranes when it was stabilized with HPC or HPMC in concentrations between 0.5% and 1% (Raghavan et al. 2001a).

1.5.3.3 Cyclodextrins

Hydroxypropyl- γ -cyclodextrin was able to stabilize supersaturated pancratistatin solutions for parenteral delivery for more than 4 h (Torreslabandeira et al. 1991). Hydroxypropyl- β -cyclodextrin inhibited the crystallization of isosorbide 5-mononitrate in a 1:1 powder formulation (Uekama et al. 1985) and also the recrystallization of ibuprofen from supersaturated propylene glycol-water cosolvent systems (Iervolino et al. 2000). It was concluded that the polymer prevents drug recrystallization mainly by increasing the drug solubility in the matrix.

1.5.3.4 Other additives

Other additives that were able to stabilize supersaturated transdermal matrices to a certain extent are: Eudragit® RL PO, Eudragit® E PO (Kotiyani and Vavia 2001), Eudragit® E and Eudragit® RL (Cilurzo et al. 2005), Tween 80 and Labrasol (Kim and Choi 2002). Para-acetoxy acetanilide, a tailor-made additive, has been found to reduce the growth of acetaminophen crystals (Chow et al. 1985).

1.5.3.5 Crystallization initiators

In contrast to crystallization inhibitors, some excipients (e.g., some surfactants, mannitol, glycerin) can act as crystallization initiators. They facilitate nucleation and crystal growth probably by decreasing the viscosity of the melt, by decreasing the interfacial energy at the

crystal-melt interface or by providing crystallization cores (Ma et al. 1996; Bhugra and Pikal 2008).

1.5.4 Use of adsorbents to prevent drug recrystallization

Another approach to inhibit drug recrystallization, which is mainly used for oral dosage forms, is the preparation of drug adsorbates onto insoluble carriers. The drug is adsorbed in a molecularly dispersed state onto the surface or absorbed into the bulk of the carrier material. By this means, the drug molecules are immobilized and thus prevented from aggregating and forming nuclei and crystals. Furthermore, the drug surface, a key parameter of the well-known Noyes-Whitney equation, is increased, which leads to enhanced drug dissolution. Predominantly, these adsorbates are prepared by the “solvent-deposition method”, a method in which the adsorbent is soaked with a concentrated drug-solution in a volatile solvent and subsequently dried.

1.5.4.1 Silica

Monkhouse and Lach (1972a) were the first to investigate the properties of drug adsorbates onto silica. They attributed the improved drug release behavior to the “minuscular form” in which the drugs were deposited onto the carriers’ surface. Subsequent studies (Rupprecht 1972; Bauer et al. 1975; Watanabe et al. 2001; Watanabe et al. 2002) suggested that specific drug interactions with the silanol groups immobilized the drug molecules which suppressed the drug crystal formation. Reports exist that $\text{Ca}(\text{OH})_2$ or other earth alkali hydroxides in combination with silica, provided more effective carrier systems. Probably stronger Brønsted acidic sites were formed on silica, which led to stronger drug-silica interactions (Watanabe et al. 1995; Watanabe et al. 1996). An alternative drug-loading procedure was performed with hydrophilic silica aerogels. To prevent the aerogel’s structure from collapsing, the organic solvent was exchanged for super-critical CO_2 (Smirnova et al. 2004).

1.5.4.2 Microcrystalline cellulose

The adsorption properties of cellulose derivatives have been studied in the paper and textile industry as well as in the pharmaceutical industry (Robert M. Franz 1982; Rivera and Ghodbane 1994). Cellulose has a large number of hydroxyl groups that can form hydrogen bonds with a variety of drugs. For example, cellulose was able to render ibuprofen partly amorphous in adsorbates prepared by the solvent deposition method (Williams et al. 2005).

Grinding of microcrystalline cellulose with benzoic acid rendered the drug amorphous. Dissolution studies of the co-ground mixtures in different organic solvents showed that solvents with primary hydroxyl groups enhanced the dissolution. It was concluded that the drug-polymer interactions were a result of hydrogen bonds (Oguchi et al. 1995).

1.5.4.3 Colloidal magnesium aluminum silicate

Adsorbates of several poorly water soluble drugs (griseofulvin, indomethacin, prednisone) onto colloidal magnesium aluminium silicate were prepared with the solvent deposition method using organic solvents (McGinity and Harris 1980). Increases in the dissolution profiles were attributed to improved wetting of the drugs and changes in their physical state.

1.5.4.4 Other adsorbents

Lactose and potato starch were investigated as carrier materials. They were not able to prevent the recrystallization of phenylbutazone in formulations with 10% drug loading. However, they showed increased dissolution rates which were mainly attributed to the better wettability of the drug (Johansen and Moller 1978).

1.5.4.5 Crospovidone

The use of crospovidone (CPVP) as adsorbent was studied in-depth within the scope of this PhD thesis. Therefore the carrier is discussed in more detail.

CPVP is prepared by popcorn polymerization (proliferous polymerization) of vinylpyrrolidone. Two ways to prepare CPVP are described in the literature: Heating of vinylpyrrolidone above 100°C in the presence of alkali metal hydroxide (Fig. 13), or warming of vinylpyrrolidone in the presence of approximately 2% (mol/mol) bifunctional monomer (e.g., 1-vinyl-3-ethylidenepyrrolidone). In the first process, the bifunctional monomer is formed in-situ (Haaf et al. 1985).

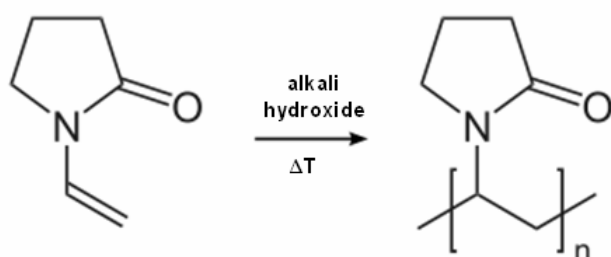


Fig. 13 Preparation of Crospovidone

The IR spectra of CPVP and linear polyvinylpyrrolidone are identical, which leads to the assumption that the number of chemical cross-links is small, and that crosslinking is mainly due to the physical entanglement of polymer chains.

Despite of its insolubility in all common solvents, CPVP is classified as a hydrophilic polymer (Bühler 1992). It has pronounced swelling and adsorption properties and is mainly used as:

Disintegrant. The disintegration of tablets and capsules is crucial for the drug release. Possible mechanisms of disintegration are swelling, repulsion of charged particles, wicking and deformation. In the case of CPVP, swelling seems to be the predominant factor (Bühler 1992). The required quantity of CPVP for that purpose depends on the formulation and the desired disintegration time and is approximately 1-5%.

Stabilizer of oral and topical suspensions. From a physical standpoint, suspensions are instable systems because the solid phase tends to sediment. This problem is addressed by adding excipients which prevent the “cake formation” of the sediment and thereby facilitate its redispersion prior to application. Micronized CPVP, in quantities of 5-10%, is used for this purpose (Bühler 1992).

Active agent for diarrhea and other gastrointestinal diseases. CPVP is used in some countries (e.g., France) for the treatment of gastrointestinal diseases. The mode of action is probably the formation of a protection layer on the intestinal mucosa and the adsorption of bacterial toxins (Queuille and Larde 1973 ; Bühler 1992).

Adsorbent. CPVP is used in the beverage industry to clear fruit juices and beer by adsorbing proanthocyanidins and catechins (Mitchell et al. 2005). This is possible because CPVP forms strong complexes with polyphenolic compounds like the abovementioned (Horn and Ditter 1982). CPVP can also be used as adsorbent material in chromatographic processes, e.g., for the isolation of indole-3-acetyl amino-acids (Percival 1986).

Crystallization inhibitor. CPVP has been used as carrier in the solvent deposition method (Carli et al. 1986; Friedrich et al. 2006), also in combination with methylcellulose (Hipasawa et al. 2004), and was able to prevent drug recrystallization. Solvents used to prepare the adsorbates included organic, volatile solvents (methanol, dimethylformamide) as well as non-

volatile solvents (PEG 400, 2-pyrrolidone). The drug release of these systems was increased more than 5-fold (Friedrich et al. 2006). Carli et al. (1986) showed a supersaturation pattern during the dissolution process of griseofulvin adsorbates onto CPVP, which was explained with the higher solubility of the drug in the amorphous state. Co-ground systems of poorly soluble drugs with CPVP (Martini et al. 1991) and a combination of CPVP and hydroxypropylmethylcellulose (Barzegar-Jalali et al. 2007) were investigated and reduced the crystallinity of the drugs. Solid solutions of CPVP and predominantly low melting drugs were prepared by heating physical drug-carrier mixtures in a high-speed elliptical-rotor type mixer (Fujii et al. 2005; Shibata et al. 2007). The resulting powder formulation could be formulated into tablets (Shibata et al. 2006) and the drugs showed enhanced solubility (e.g., indomethacin's solubility was increased by the factor 4).

1.6 SKIN ADHESION

The adhesive represents a mandatory structural element of transdermal drug delivery systems and is critical for their efficacy. A reduction in adhesion surface area leads to diminished drug delivery and hence improper dosing of the patient. Moreover, adhesion is a safety issue. Cases have been described in the literature whereby patches with insufficient adhesion characteristics were transferred from adults to children while hugging, which led to death or serious medical problems. Lastly, since lost patches have to be replaced, insufficient adhesion also leads to increased patient's cost (Wokovich et al. 2006). Adhesive failure is one of the major post-approval problems that occur for transdermal drug delivery systems (Brown et al. 2006). Hence, adequate adhesive properties are essential for the commercial success of a transdermal patch.

1.6.1 Theories of pressure sensitive adhesion

There are four main theories that explain the mechanisms of adsorption. However, there is no overall theory that explains every adhesive bond. It seems that all proposed mechanisms play a role in adsorption phenomena (Allen 1992d).

1.6.1.1 Surface energetic adsorption theory

The surface energetic adsorption theory essentially states that the adhesive has to wet the substrate in order to form a bond. Hence the following condition must be fulfilled:

$$\gamma_A \leq \gamma_S \quad \text{Equation 16}$$

γ_A : surface free energy of the adhesive

γ_S : surface free energy of the substrate

The surface free energy of the clean, dry human skin was measured to be 27 mN/m and increased for dirty or unwashed skin (Ginn et al. 1968). As a consequence, the first precondition that the adhesive has to fulfil in order to stick to human skin is to possess a surface free energy of at least 27 mN/m. According to this theory, the adherent will stick to the substrate because of interatomic and intermolecular forces. Common short range attractive forces include van der Waals interactions, hydrogen bonds and London dispersion forces. Since all these forces are of very short range, the adhesive has to meet kinetic requirements (i.e., adequate flow properties) as well in order to be able to establish close contact with the substrate.

1.6.1.2 Diffusion theory

The diffusion theory suggests that adhesive polymer segments or chain ends penetrate the substrate. This theory is useful to explain adhesion phenomena between structurally similar adhesives and substrates. However, it is not suitable to elucidate the adhesion of polymers on metal or the adhesion between dissimilar polymers (Allen 1992a).

1.6.1.3 Electrostatic theory

The electrostatic theory is based on the difference in electronegativities of adhesive and substrate. The formation of the bond is attributed to the transfer of electrons across the interface. By this means, opposite charges are created that attract one another. It has been demonstrated, for instance, that an attracting electrical double layer was formed between a metal and an adhering polymer (Allen 1992b).

1.6.1.4 Mechanical theory

The mechanical theory explains adhesion with the interlocking of the adhesive in the surface roughness of the substrate. This theory helps to explain the adhesion to fibrous materials, e.g., paper, but fails to explain adhesion to smooth surfaces (Allen 1992c).

1.6.2 Measurement of adhesive properties

1.6.2.1 Tack

Pressure sensitive tack is the adhesive property related to the instantaneous bond formation between the adhesive and the substrate after the application of low contact pressure (Minghetti et al. 2004). It is also called quick stick, initial adhesion or stickiness. Originally, it was developed to simulate the very subjective “thumb test” (i.e., touching the adhesive surface with the thumb and sensing the force that is required to break the bond) (Wokovich et al. 2006).

Older versions of tack tests include the rolling-ball test in which a stainless steel ball rolls down an inclined track onto the adhesive matrix previously fixed in the horizontal position with its adhesive side up. The distance the ball travels on the adhesive is taken as a measure of tack. The up-to-date version of this test is carried out with the texture analyzer in which a probe touches the adhesive surface with light pressure for defined a time period before it pulls back. The force required to break the bond is recorded. The resulting force-distance curve can be evaluated with regard to maximal force, area under the curve (AUC) and elongation at detachment. Zosel found that the AUC correlates best with the “thumb test” (Zosel 1998). Tack is greatly influenced by the experimental parameters (i.e., contact pressure, contact time, rate of separation) and is not simply a function of material properties (Wokovich et al. 2006). Hence, it is not solely a surface property but also depends on the bulk’s viscoelastic properties and the backing on which the adhesive is laminated (Venkatraman and Gale 1998).

1.6.2.2 Peel adhesion

Peel adhesion is defined as the resistance to peel. The measured variable is the force required to remove a pressure sensitive adhesive from a test panel. Commonly used peel angles are 90° and 180°. Test conditions (width, length and thickness of the sample, contact time, peel rate) have to be predefined and influence the result to a large degree. As the tack test, peel adhesion measurements are influenced by the backing and the viscoelastic properties of the adhesive (Venkatraman and Gale 1998; Minghetti et al. 2004).

1.6.2.3 Creep resistance

Creep resistance (also called shear adhesion and shear strength) provides an indicator for the matrix cohesion. If the matrix does not exhibit elastic cohesiveness and resistance to flow

under stress, the adhesive can ooze out and leave residues on the skin. These residues collect dirt and become unsightly. Furthermore, low creep resistance causes the patch to stick to clothing and move during stress. During storage, low creep resistance can lead to problems because the oozed out adhesive can stick to the inner side of the pouch (making it difficult to remove the patch without destroying it). Increasing creep resistance (which essentially is a viscoelastic property) normally decreases tack and peel adhesion. Therefore, a compromise between cohesive and adhesive properties of the adhesive has to be found, which can be achieved by using mixtures of different molecular weight polymers or by adjusting the degree of cross-linking (Venkatraman and Gale 1998; Minghetti et al. 2004). Creep resistance is determined by applying the test specimen to a test panel in an angle 2° from the vertical and the application of a vertical shearing force. The time needed to detach the TDDS sample from the test panel is reported.

1.6.2.4 In-vivo measurement

The in-vivo performance of transdermal patches is evaluated by subjective observations. The adhesion of patches in a clinical setting is commonly ranked according to a scoring system from 0 to 4 with 0 being “patch adheres at least 90%” and 4 being “patch fell off” (Wokovich et al. 2006). In these studies, the local tolerability (pruritus and skin irritation) can also be evaluated (Erienne and Winter 1997).

1.6.2.5 Modes of adhesive/cohesive failure

The failure of adhesives (Fig. 14) can be subdivided into adhesive failure case 1 (which is the preferred failure when removing the patch after the wearing period), adhesive failure case 2 (in which the backing liner peels off) and cohesive failure case 3 (in which the adhesive matrix lacks coherence).

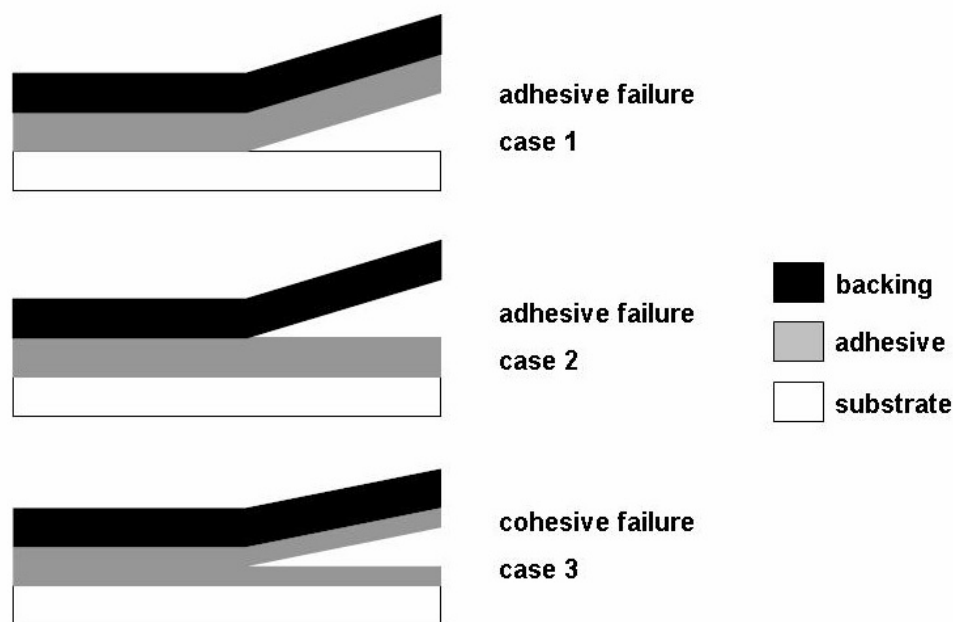


Fig. 14 Modes of adhesive/cohesive failure

1.6.3 Adhesives in transdermal drug delivery systems

Adhesives used in transdermal delivery systems fall in the category of “pressure sensitive adhesives” which means that they are able to form a bond to surfaces after the application of light pressure (Minghetti et al. 2004).

1.6.3.1 Polyisobutene-based adhesives

Polyisobutenes (PIB) are homopolymers of isobutylene (Fig. 15), polymerized by Lewis acid catalysts like AlCl_3 .

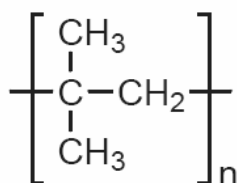


Fig. 15 Chemical structure of polyisobutene adhesives

Due to their hydrocarbon nature, PIBs are very stable and relatively resistant to heat and chemicals. They dissolve in typical hydrocarbon solvents, like hexane and chloroform, but

not in oxygenated solvents. Their low air moisture and gas permeability is attributed to their close molecular packing.

PIBs are manufactured over a wide range of molecular weights. High molecular weight PIBs are tough, rubber-like solids while low molecular weight PIBs are soft and tacky semi-solids. Their low glass transition temperature of approximately $-60\text{ }^{\circ}\text{C}$ results in a high internal mobility, which leads to flexibility and permanent tack (Tan and Pfister 1999).

PIBs adhere weakly to many surfaces due to their low polarity. To overcome this problem, tackifiers (like rosin ester resins) can be added to PIB adhesives. These substances introduce some polarity to the adhesive formulation and enable the bond formation with polar moieties of the substrate.

Since PIBs are not supplied as ready-to-use mixtures from the manufacturers, formulators prepare their own PIB pressure sensitive adhesive. In general, there are two ways to produce a PIB adhesive with the desired adhesive properties: The first one is to mix low and high or low, medium and high molecular weight polyisobutenes to obtain a balance of tack and cohesive strength. The second possibility is to incorporate plasticizers, fillers, tackifiers, waxes or oils into the formulation to adjust its adhesive properties.

Their stability and inertness, in addition to a broad acceptability of regulatory authorities (Transderm Scop[®], the first FDA approved transdermal patch used a PIB adhesive), renders PIBs good candidates for adhesives in transdermal delivery systems (Higgins et al. 1989).

1.6.3.2 Acrylate adhesives

Acrylate pressure sensitive adhesives (Fig. 16) are often copolymers (Table 3) of one or two monomers with high glass transition temperature (T_g) (“hard monomer/s”) and a monomer with low T_g (“soft monomer”) (Venkatraman and Gale 1998).

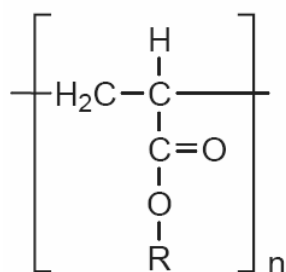


Fig. 16 Chemical structure of acrylate adhesives

By this means, the resulting polymer exhibits the necessary tack and cohesive strength properties. Functional monomers (e.g., acrylic acid) can be used to improve adhesion and increase moisture permeability. By the addition of modifying monomers (e.g., vinyl pyrrolidone, 2-ethoxyl acrylate) the polarity of the adhesive and hence the solubility of drug therein can be modified (Tan and Pfister 1999).

Table 3 Example for the monomer composition of an acrylate pressure sensitive adhesive (Tan and Pfister 1999)

Component	Function	Amount, %
2-ethylhexylacrylate	Backbone monomer	50
Butyl acrylate	Backbone monomer	45
Acrylic acid	Functional monomer	5

1.6.3.3 Silicone-based adhesives

Silicone pressure sensitive adhesives are condensation products of a polysiloxane (silicone) polymer and a silicate resin (Fig. 17).

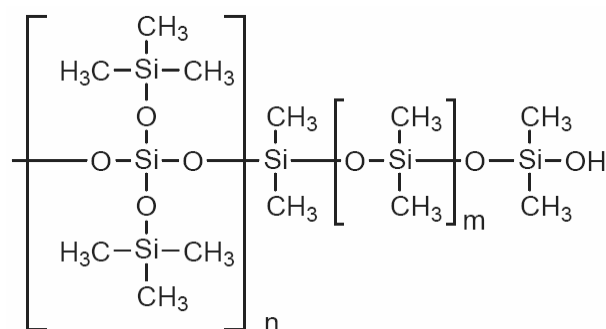


Fig. 17 Chemical structure of silicone adhesives

The final product is a one-component system consisting of a network of crosslinked polymer chains. The semi-organic structure of silicone (-O-Si-O-backbone with pendant CH₃-groups) results in a high flexibility and a high void volume. The high void volume explains the adhesive's high permeability to vapor, gases and a variety of therapeutic molecules (Tan and Pfister 1999).

Two types of silicone pressure sensitive adhesives are sold in preformulated products: Firstly, the regular type with residual silanol and secondly, the amine compatible type with end-capped silanol groups.

1.7 DRUG RELEASE AND PERMEATION STUDIES

1.7.1 Drug release studies

European and United States Pharmacopoeia require drug release studies to ensure the quality of the drug delivery systems (Pharm.Eur.4 2003; USP26 2003). They describe three types of apparatuses for this purpose:

In the “paddle over disk assembly”, the transdermal system is applied with the release side facing upwards to a stainless steel disk in a way that assures that the release surface is as flat as possible. This assembly is placed on the bottom of the release vessel with the release side of the patch facing upwards at a distance of 25 mm between the paddle blade and the patch. In the “cylinder assembly”, the transdermal system is attached to a stainless steel cylinder that replaces the basket in the vessel assembly for the testing of oral dosage forms. The “reciprocating holder assembly” consists of vertically reciprocating solution containers in a waterbath. The transdermal system is attached to a sample holder and immersed in the dissolution medium within the solution containers.

1.7.2 Permeation studies

1.7.2.1 Franz diffusion cells

Permeation studies are commonly conducted with Franz diffusion cells (Fig. 18).

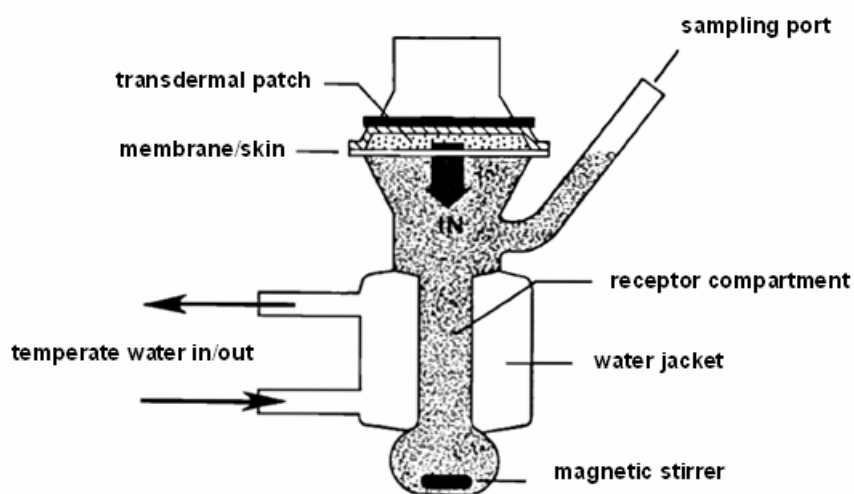


Fig. 18 Schematic of a Franz cell (modified from Chien 1978)

These cells consist of a donor and an acceptor compartment. In the case of transdermal patch testing, the acceptor medium normally is an aqueous (buffer) solution in which the drug is soluble enough to ensure “perfect sink” conditions. The donor compartment is separated from the acceptor compartment by a model membrane (skin or polymer) on top of which the transdermal system is applied. During the permeation study, drug molecules are released from the transdermal system and diffuse across the membrane into the acceptor medium. Samples of the acceptor medium are taken after predetermined intervals and analyzed for their drug content.

1.7.2.2 Model membranes

Model membranes used in Franz diffusion cell studies are either human skin, animal skin or polymer membranes (Spencer 1997). Differences in skin permeability of different animals and humans were compared by Bartek (1972). The skin permeability decreased in the order of rabbit > rat > miniature swine > man and varied widely for different drugs (e.g., caffeine permeates human and rabbit skin with nearly the same rate while haloprogin permeates human skin 10 times slower than rabbit skin). Furthermore, the effect of penetration enhancers can differ greatly between human and animal skin (Bond and Barry 1988). It is therefore risky to base the decision of which skin penetration enhancer system to use in formulation development solely on studies with animal skin. However, to rank the permeation kinetics of different formulations, animal skin is a suitable membrane.

Artificial polymer membranes cannot be used to indicate a penetration enhancing effect caused by chemical penetration enhancers. Nevertheless, they are very useful to compare delivery kinetics of different systems (Spencer 1997).

1.8 RESEARCH OBJECTIVES

The major objective of this work was to investigate the use of drug adsorbates onto insoluble carriers in transdermal drug-in-adhesive patches. Particular goals were:

- a) to investigate and explain the adsorption mechanism of the model drug carbamazepine onto the carrier crospovidone and to optimize the drug-carrier ratio;
- b) to establish a drug release method for drug-in-adhesive patches containing adsorbates including the simultaneous quantification of ethinyl estradiol and levonorgestrel at concentrations below 0.4 $\mu\text{g/ml}$;
- c) to investigate the effect of various process and formulation parameters on the physical state of the drug and the drug release from drug-in-adhesive patches containing adsorbates;
- d) to optimize the adhesive properties of drug-in-adhesive patches containing adsorbates.

2 MATERIALS AND METHODS

2.1 MATERIALS

2.1.1 Drugs

Micronized ethinyl estradiol (EE) (Pfannenschmidt, Hamburg, Germany), levonorgestrel (LNG) (Cayman Chemical, Hamburg, Germany), micronized carbamazepine (Sigma-Aldrich Laborchemikalien GmbH, Seelze, Germany).

2.1.2 Adsorbents

Micronized crosslinked polyvinylpyrrolidone (CPVP) (Kollidon[®] CL-M), crosslinked polyvinylpyrrolidone (Kollidon[®] CL) (BASF AG, Ludwigshafen, Germany), microcrystalline cellulose (MCC) (Avicel[®] PH 200) (FMC Biopolymer, Cork, Ireland), titanium dioxide (Caesar & Loretz GmbH, Hilden, Germany), hydrophilic fumed silica (Aerosil) (Aerosil[®] 200) (Degussa AG, Düsseldorf, Germany).

2.1.3 Pressure sensitive adhesives

Low molecular weight polyisobutene (LM-PIB) (Glissopal[®] V 1500), medium molecular weight polyisobutene (MM-PIB) (Oppanol[®] B 12 SFN), high molecular weight polyisobutene (HM-PIB) (Oppanol[®] B 100) (BASF AG, Ludwigshafen, Germany), acrylate adhesives (Durotak[®] 87-202A, Durotak[®] 87-2074, Durotak[®] 87-2677) (National Starch and Chemical B.V., Zutphen, The Netherlands).

2.1.4 Solvents

Ethanol, isopropanol, ethyl acetate, acetone, methylene chloride, hexane, chloroform, acetonitrile (HPLC grade) (Carl Roth GmbH & Co. KG, Karlsruhe, Germany), methanol (HPLC grade) (Merck KGaA, Darmstadt, Germany).

2.1.5 Surfactant

Sodium dodecyl sulfate (Texapon[®]) (Henkel KGaA, Düsseldorf, Germany).

2.1.6 Liners and membranes

Release liner (Scotchpak[™] 1020), backing liner (CoTran[™] 9720) (3M Medica, Borken, Germany), microporous polyethylene membranes (Solupor[®] 7P03A, Solupor[®] E-9H01A, Solupor[®] 10P05A) (DSM Solutech, Heerlen, The Netherlands).

2.2 METHODS

2.2.1 General data presentation in diagrams

The data points (symbols) in the diagrams represent the average value. The bars represent the standard deviation of n repetitions of the experiment.

2.2.2 Solubility determination

2.2.2.1 Drug solubility in solvents

Excess amounts of carbamazepine, ethinyl estradiol or levonorgestrel were added to 5 ml solvent (water, 2% aqueous SDS solution, methanol, ethanol, isopropanol, ethyl acetate, acetone, methylene chloride, chloroform, hexane) in glass vials (n=3). The samples were shaken for at least 5 days at 25±2 °C. 2 ml samples were taken from the saturated solutions and filtered through a 0.5 µm filter (Sartorius AG, Göttingen, Germany) or centrifuged at 13000 rpm for 30 min (Heraeus Biofuge 13 Haemo, Heraeus Instruments, Osterode, Germany). The drug concentrations were detected after appropriate dilution as described in section 2.2.6.

The ethinyl estradiol solubility in ethanol, ethyl acetate and chloroform was estimated by adding increments of 50 mg ethinyl estradiol to 1.0 ml solvent until the drug did not completely dissolve or a concentration of 200 mg/ml was reached.

2.2.2.2 Drug solubility in MM-PIB adhesive

The adhesive solution was prepared by adding small pieces of MM-PIB to chloroform (22.5% w/w) in a glass jar. The solution was magnetically stirred for 48 h until the PIB pieces were completely dissolved. Its solid content was confirmed by evaporating the solvent from a

small sample of known weight. Chloroformic ethinyl estradiol or levonorgestrel solution was added to a certain amount of MM-PIB solution in a 20 ml glass jar to yield matrices with a drug content of 0.1, 0.2, 0.5, 1 and 2 % w/w ethinyl estradiol or levonorgestrel, respectively. The vessels were closed tightly and the mixtures were magnetically stirred for 4 h. One drop of each casting mixture was applied onto a microscopic slide and the absence of drug crystals was confirmed by polarized light microscopy (Axiotrop, Carl Zeiss Jena GmbH, Jena, Germany). The casting mixtures were degassed for 30 min in a sonication bath (Retsch GmbH & Co KG, Haan, Germany) and cast onto microscopic slides (theoretical film thickness of 1000 μm , surface area of approximately 5 cm^2) using a casting knife setup (ZUA 200, MTV Messtechnik, Köln, Germany). The matrices were dried in the hood for 48 h at 25 ± 2 °C and subsequently for 1 h at 60 °C (UT 6060, Heraeus Instruments, Hanau, Germany). After 48 h at ambient conditions the matrices were investigated with polarized light microscopy as described in section 2.2.7.1.

2.2.2.3 Drug solubility in acrylate adhesives

The solubility of ethinyl estradiol and levonorgestrel in Durotak 87-202A, 87-2074 and 87-2677 was estimated using the software DURO-TAK[®] Drug-in-Polymer Solubility Calculator (available on www.nationalstarch.com). The estimation is based on the correlation of the drugs' $\log P_{\text{octanol/water}}$ and $\log P_{\text{polymer/water}}$ and input parameters were the aqueous solubility of the drugs and their $\log P_{\text{octanol/water}}$ values (Myatt et al. 2008).

2.2.3 Specific surface area measurement

The specific surface area of CPVP was measured with the BET gas adsorption method. The powder was prepared under vacuum for 1 h at 100 °C and then analyzed using a Gemini 2365 BET surface area analyzer (Micromeritics, Norcross, USA). Calculation of the specific surface area was done by the BET multipoint method. All measurements were conducted in triplicate.

2.2.4 Particle size analysis

Laser diffraction (LD, Coulter LS 230, Beckman Coulter, Krefeld, Germany) in water was employed to determine the particle size. Measurements were repeated three times and the results were calculated as volume distribution using the Fraunhofer theory.

2.2.5 Solvent uptake and solvent binding studies of adsorbents

2.2.5.1 Water uptake

Approximately 200 mg dried (80 °C to constant weight) titanium dioxide, MCC and CPVP were accurately weighed into 2.0 ml Eppendorf cups and 1.0 ml water was added (n=3). The suspensions were vortexed and shaken for 1 h at 25±2 °C using a horizontal shaker (HS 501 Digital, IKA-Labortechnik, Staufen, Germany). After centrifugation at 5000 rpm for 3 min (Heraeus Biofuge 13 Haemo, Heraeus Instruments, Osterode, Germany), the excess solvent was decanted / removed with a filter paper. The experiment was repeated with different centrifugation conditions (15 min at 13000 rpm) and subsequent incubation at 25±2 °C for 12 h. The water uptake U_w was defined as follows:

$$U_w = \frac{(m_{eq} - m_0)}{m_0 \cdot \rho} \quad \text{Equation 16}$$

where U_w : water uptake, ml/g; m_{eq} : mass of adsorbent after equilibration with water, g; m_0 : initial mass of the dried adsorbate, g; ρ : density of water at 25 °C, g/ml (=0.997 g/ml)

2.2.5.2 Solvent uptake and solvent binding capacity

The solvent uptake of CPVP was determined for water, ethyl acetate, ethanol and methanol employing the method described in section 2.2.3.1.

The binding capacity of CPVP for the above mentioned solvents was determined by mixing 1.0 g of thoroughly dried (80 °C to constant weight) CPVP with increasing amounts of water, ethyl acetate, ethanol or methanol (in increments of 100 mg) in a mortar with a pestle at ambient conditions (n=3). The solvent addition was stopped when CPVP was no longer capable of binding the entire solvent and changed into a paste. The solvent binding capacity (ml/g) was calculated according to the following equation:

$$\text{Solvent binding capacity} = \frac{m}{m_0 \cdot \rho} \quad \text{Equation 17}$$

where m : amount of solvent added, g; m_0 : initial mass of the dried powder; ρ : density of the solvent, g/ml.

2.2.5.3 *Dynamic vapor sorption (DVS)*

Dynamic vapor sorption experiments were conducted using a DVS-1/1000 (Surface Measurement Systems Limited, Alpertton, Middlesex, UK) automated moisture sorption instrument. The data was analyzed with DVSWin analysis suite, version 3.3 standard (Surface Measurement Systems Limited, Alpertton, Middlesex, UK).

Approximately 0.33 cm² of a dried (60 °C for 2 h, UT 6060, Heraeus Instruments, Hanau, Germany) patch without the release liner was inserted (release side up) into the sample chamber. The DVS method started with a drying step (0% RH for 360 min) followed by 90% RH until equilibration or 4000 min were reached. The recorded weight was corrected for the weight of the backing liner (which showed no significant water uptake) to determine the water uptake of the matrix. The water uptake, % was plotted against the time.

2.2.6 **Adsorption studies**

2.2.6.1 *Carbamazepine adsorption onto CPVP with different surface areas*

The conventional Brunauer, Emmet and Teller (BET) procedure was applied to evaluate the specific surface areas of outgassed (1 h at 100 °C) CPVP samples employing a Gemini 2365 sorption instrument (Micromeritics Instrument Corp., Atlanta, Georgia, USA).

10, 50, 100 or 200 mg of CPVP with different surface areas were added to 10.0 ml carbamazepine solution with a concentration of approximately 25 µg/ml. The vials were vortexed and shaken at 25±2 °C for 3 h. The carbamazepine concentration in the filtrate was analyzed UV-spectrophotometrically at λ=285 nm (UV-2101 PC, Shimadzu Scientific Instrument, Columbia, MD, USA) after filtration through a 0.22 µm filter (Acryl/Copolymer/Nylon, Sartorius AG, Göttingen, Germany).

2.2.6.2 *Adsorption isotherms*

The classical batch method (Seidel-Morgenstern 2004) was used to determine adsorption isotherms of carbamazepine onto CPVP in ethyl acetate and ethanol. Accurately weighed amounts of CPVP (approximately 50 mg) were added to 1.0 ml carbamazepine solution in 2.0 ml Eppendorf cups (n=3). The carbamazepine concentrations ranged from approx. 5 to 90% of the carbamazepine solubility in the respective solvent. The cups were vortexed and shaken at 25±2 °C for 3 h. After centrifugation (Heraeus Biofuge 13 Haemo, Heraeus Instruments, Osterode, Germany) at 13000 rpm for 30 min, the carbamazepine equilibrium concentration (c_{eq}) in the supernatant was analyzed UV-spectrophotometrically at λ=285 nm

(UV-2101 PC, Shimadzu Scientific Instrument, Columbia, MD, USA). The adsorbed amount of carbamazepine onto CPVP was calculated using the following equation:

$$x/m = \frac{(c_0 - c_{eq}) \cdot v}{m} \quad \text{Equation 18}$$

where: x: amount of carbamazepine, mg; m: amount of CPVP, g; c_0 : initial carbamazepine concentration, mg/ml; c_{eq} : concentration after equilibration with CPVP, mg/ml; v: volume carbamazepine solution, ml.

To obtain adsorption isotherms x/m was plotted against c_{eq} .

2.2.7 ATR-FTIR spectroscopy

2.2.7.1 Equilibration at different relative humidities

10 ml pure water or saturated salt solutions ($MgCl_2$, K_2CO_3 , NaCl, KNO_3) plus excess salt were filled into 100 ml plastic containers equipped with a mesh in the head space. Approximately 500 mg CPVP was accurately weighed into tared aluminum pans and placed on the mesh. The plastic containers were closed tightly and equilibrated at 25 ± 2 °C for at least 48 h to constant weight (Mettler AT 261 Delta Range, Greifensee, Switzerland). Dry CPVP and dried carbamazepine adsorbates onto CPVP were prepared by heating the polymer at 80 °C (UT 6060, Heraeus Instruments, Hanau, Germany) to constant weight.

2.2.7.2 Preparation of CPVP-solvent pastes

200 mg dried (80 °C to constant weight) CPVP and 500 μ l water, ethanol, ethyl acetate or chloroform were mixed in a 5 ml glass vessel with a spatula for 10 s until a homogeneous mass was formed. The vessels were closed and incubated for 10 min before the measurement took place.

2.2.7.3 ATR-FTIR spectroscopy

FTIR-spectra were generated with an Excalibur 3100 FTIR spectrophotometer (Varian Inc., Palo Alto, USA). The spectra were collected using a horizontal ATR accessory with a single reflection diamond crystal (Pike MIRacle, Pike Technologies, Madison, USA). 16 scans at 4 cm^{-1} resolution were averaged using Varian software (Resolution Pro 4.0).

Measurements were performed within 5 s after opening the containers to minimize the influence of the ambient humidity.

2.2.8 Drug assay

2.2.8.1 Carbamazepine

Carbamazepine was quantified UV-spectrophotometrically (UV 2101 PC, Shimadzu Scientific Instruments, Inc., Columbia, MD, USA) at $\lambda=285$ nm after appropriate dilution.

2.2.8.2 Ethinyl estradiol and levonorgestrel

The hormones were quantified by HPLC using a Shimadzu system consisting of a SCL-10AVP system controller, a LC-10 ADVP pump, a M10 AVP diode array detector, a SIL-10A autosampler and a DGU-14A degasser. A reversed phase C18 column (Spherimage-80 ODS2, 5 μm , 125 mm \times 4.6 mm, Knauer, Berlin, Germany) was used and the mobile phase consisted of water/methanol/acetonitrile (37/21/42 v/v). The temperature was adjusted to 30 $^{\circ}\text{C}$ and the flowrate to 0.8 ml/min. 25 μl (ethinyl estradiol concentration > 0.4 $\mu\text{g/ml}$) or 75 μl (ethinyl estradiol concentration < 0.4 $\mu\text{g/ml}$) samples were injected. UV-spectrometric detection was performed at 200 nm (ethinyl estradiol concentration < 0.4 $\mu\text{g/ml}$), 280 nm (ethinyl estradiol concentration > 0.4 $\mu\text{g/ml}$) and at 243 nm (levonorgestrel).

Quantification of ethinyl estradiol and levonorgestrel (retention times approximately 7.5 and 10.7 min, respectively) was achieved by using the external standard method and the peak area as quantification criteria.

The limit of quantification was determined using the signal-to-noise approach. A signal-to-noise ratio of 10:1 was considered sufficient for the reliable detection of the analyte. The key parameters to describe the HPLC method were calculated according to Neugebauer (1992).

2.2.9 Physical state of drug

2.2.9.1 Polarized light microscopy

The adsorbates, the casting mixtures and the freshly manufactured patches were investigated with regard to the existence of drug crystals using a polarized light microscope (Axiotrop, Carl Zeiss Jena GmbH, Jena, Germany) connected to a digital camera. The whole surface was scanned with transdermal patches. The images were evaluated using the Easy Measure Software (version 1.0.15; INTEQ Informationstechnik GmbH, Berlin, Germany).

Cross-sections of patches were prepared by cutting off a wedge-shaped piece with a sharp pair of scissors. After placing it on a microscopic slide, pictures of the specimen's thin side were taken.

All microscopic experiments were conducted at ambient temperature.

2.2.9.2 Differential scanning calorimetry (DSC)

DSC studies were performed using a Mettler DSC 821e (Mettler Toledo, Giessen, Germany). Approximately 5 mg samples were weighed into 40 μ l aluminum crucibles with three pinholes in their lid. DSC scans were recorded at a heating rate of 15 $^{\circ}$ C/min from 25-250 $^{\circ}$ C for ethinyl estradiol and levonorgestrel and at a heating rate of 20 $^{\circ}$ C/min from 25-110 $^{\circ}$ C and 5 $^{\circ}$ C/min from 110-240 $^{\circ}$ C for carbamazepine. All experiments were conducted under a nitrogen atmosphere. The melting transitions (T_m) were derived from the computed extrapolated peak maximum and the enthalpy values (ΔH) were calculated from the area under the transition peaks using the Star[®] Software version 8.10 (Mettler Toledo, Giessen, Germany). The crystallinity of the drug, x% in the formulation was calculated as follows:

$$x\% = \frac{HTm_f}{HTm_c} \cdot \frac{10000}{P} \quad \text{Equation 19}$$

where HTm_c : area under the curve of the crystalline drug; HTm_f : area under the curve of the drug in the formulation; P: drug loading of the formulation, %.

Drug precipitates of ethinyl estradiol and levonorgestrel from chloroform were prepared by placing drug solutions in open vessels under the hood until the solvent was evaporated.

2.2.9.3 X-ray diffraction (XRD)

Wide angle X-ray scattering measurements were performed on a Philips PW 1830 X-ray generator with a copper anode (Cu $K\alpha$ radiation, $\lambda=0.15418$ nm, 40 kV) and a Philips PW 1710 diffraction control unit (Philips Industrial and Electro-acoustic Systems Division, Almelo, The Netherlands). The scattered radiation was measured with a vertical goniometer (Philips PW 1820, Philips Industrial and Electro-acoustic Systems Division, Almelo, The Netherlands). Patterns were obtained using a step width of 0.02 $^{\circ}$ with a detector resolution in 2θ between 4 and 40 $^{\circ}$ at ambient temperature.

Freshly prepared physical mixtures of carbamazepine form III and CPVP (drug content: 4.8, 9.1, 13.0, 23.1, and 33.3%) were investigated and their crystallinity was plotted against the sum of the AUCs of carbamazepine form III's 3 main peaks (at 13.0, 15.2, and 27.2 $^{\circ}$). This correlation was used to calculate the crystallinity of the adsorbates.

2.2.9.4 Scanning electron microscopy (SEM)

For SEM analysis (Philips SEM, PW 6703, Philips Industrial Electronics, Kassel, Germany), the specimens were coated with gold-palladium prior to observation. The experiments were conducted at ambient temperature.

2.2.10 Preparation of adsorbates and physical mixtures

2.2.10.1 Carbamazepine adsorbates

Adsorbates of carbamazepine onto CPVP (drug loading: 4.8, 9.1, 13.0, 23.1, and 33.3%, w/w, based on the total weight) were prepared by the solvent deposition method. 1000 μ l methanolic carbamazepine-solution (50 mg/ml) were added to 1000 mg CPVP in a mortar and immediately mixed with a pestle. Methanol was evaporated at 65 °C for 10 min (UT 6060, Heraeus Instruments, Hanau, Germany) and the procedure was repeated for adsorbates with higher drug loadings.

2.2.10.2 Ethinyl estradiol and levonorgestrel adsorbates

Adsorbates of ethinyl estradiol and levonorgestrel onto CPVP, Aerosil, MCC and titanium dioxide were prepared by the solvent deposition method. In general, 450 mg carrier was soaked with 589 μ l chloroformic drug solution (containing 4.5 mg ethinyl estradiol and 22.5 mg levonorgestrel) in a mortar followed by immediate mixing with a pestle. The adsorbates were dried at 60 °C for 30 min (UT 6060, Heraeus Instruments, Hanau, Germany).

By varying the ethinyl estradiol and the levonorgestrel concentration in the chloroformic drug solution, adsorbates for patches with different drug contents were prepared. By varying the amount of CPVP, adsorbates for patches with different CPVP contents were prepared.

CPVP fractions with different particle sizes were obtained by classifying Kollidon[®] CL using sieves. Grinding the polymer (Amplitude: 100, 30 min, without cooling) using a ballmill (MM2000, F. Kurt Retsch GmbH and Co. KG, Haan, Germany) and subsequent separation with a gravity classifier (Multiplex[®] Zigzag Classifier MZR, Hosokawa Alpine AG, Augsburg, Germany) resulted in the finest fraction with CPVP particles in the lower micrometer range. The particle size distributions were analyzed in aqueous dispersions by laser diffraction (Coulter LS 230, Beckmann-Coulter, Krefeld, Germany) using the Fraunhofer theory.

2.2.10.3 Physical mixtures

Physical mixtures of ethinyl estradiol with titanium dioxide and carbamazepine with CPVP were prepared by adding the carrier by degrees to the drug in a mortar followed by careful mixing with the pestle and a plastic card between each addition.

2.2.11 Preparation of patches

2.2.11.1 Medium molecular weight polyisobutene patches containing adsorbents

The adhesive solution was prepared by adding small pieces of MM-PIB to chloroform (22.5% w/w) in a glass jar. The mixture was magnetically stirred for 48 h until the PIB pieces were completely dissolved. Its solid content was confirmed by driving off the solvent from a small sample of known weight. 450 mg freshly prepared adsorbate or 589 μ l chloroformic drug solution (for patches without adsorbents) were added to a certain amount of MM-PIB solution in a 20 ml glass vessel to yield matrices with 0.2% ethinyl estradiol, 1.0% levonorgestrel, 20% adsorbent and 78.8% MM-PIB after drying. In patches with less than 20% adsorbent, the amount of PIB solution was varied to keep the drug content constant. The vessels were closed tightly and the mixtures were magnetically stirred for 4 h until they were homogeneous. One drop of each casting mixture was applied onto a microscopic slide and the absence of drug crystals was confirmed by polarized light microscopy. The casting mixtures were degassed for 30 min in a sonication bath (Retsch GmbH & Co KG, Haan, Germany) and cast onto the fluorocoated side of the release liner (theoretical film thickness: 500-1500 μ m) with a casting knife setup (ZUA 200, MTV Messtechnik, Köln, Germany). The matrices were dried under a hood for 12 h at 25 ± 2 °C and subsequently for 1 h at 60 °C (UT 6060, Heraeus Instruments, Hanau, Germany). After cooling to room temperature, the matrices were laminated with the backing liner using a rubber roller. Circular patches (diameter 1.3 cm) for the drug release studies were manually die-cut using a punch.

2.2.11.2 Patches based on acrylates and blends of polyisobutenes containing adsorbates

PIB solutions with ratios of high:medium:low molecular weight PIB (HM:MM:LM PIB) = 1:5:0, 1:5:2, 1:5:4 were prepared by adding various amounts of Glissopal[®] V 1500, Oppanol[®] B 12 SFN and Oppanol[®] B 100 to chloroform in a glass jar. The total PIB concentrations ranged from 15% - 25% (w/w) depending on the amount of LM-PIB in the mixture. The mixtures were magnetically stirred for 48 h until the PIB pieces were completely dissolved. The ready-to-use acrylate solutions (Durotak[®] 87-202A, Durotak[®] 87-2074, Durotak[®] 87-

2677) were stirred for 30 min. The solid content of all adhesive mixtures was confirmed by driving off the solvent from a small sample of known weight. Subsequent manufacturing steps were similar to section 2.2.9.1.

2.2.11.3 *Placebo patches*

MM-PIB solutions and PIB solutions with ratios of high:medium:low molecular weight (HM:MM:LM) PIB = 1:5:0, 1:5:2 and 1:5:4 were prepared in hexane. The solutions were magnetically stirred for 24 h until the PIB pieces were completely dissolved. The ready-to-use acrylate solutions (Durotak[®] 87-202A, Durotak[®] 87-2074, Durotak[®] 87-2677) were stirred for 30 min. The solid content of all adhesive mixtures was confirmed by evaporating the solvent from a small sample of known weight. Casting mixtures were prepared by adding CPVP (0, (5), 10, 20, 30, 40 and 50% based on the dry matrix weight) to portions of the different adhesive solutions in 50 ml glass vessels. If necessary, the viscosity of casting mixtures with high CPVP contents were decreased by adding hexane (for PIB) or ethyl acetate (for acrylates). The vessels were closed tightly and the mixtures were magnetically stirred for 24 h until they were homogeneous. The casting mixtures were degassed for 30 min in a sonication bath (Retsch GmbH & Co KG, Haan, Germany) and cast (ZUA 200, MTV Messtechnik, Köln, Germany) onto rigid polyester films (theoretical film thickness: 1600-2400 μm) to yield specimens for the in-vitro study. For the in-vivo study, the casting mixtures based on different HM:MM:LM PIB were cast onto the fluorocoated release liner (theoretical film thickness: 500-1500 μm). The specimens were dried under a hood for 12 h at 25 ± 2 °C and subsequently for 1 h at 60 °C (UT 6060, Heraeus Instruments, Hanau, Germany). Specimens for the in-vitro study were obtained by cutting the matrices with a razor blade. Patches for the in-vivo study were obtained by laminating the matrix with the backing liner and die-cutting (circular patches: diameter 1.3 cm). The matrix thickness was determined with a thickness gauge (Minitest 600, Erichsen, Hemer, Germany) and the specimens were stored in a desiccator above orange gel.

2.2.11.4 *PIB matrices with suspended ethinyl estradiol and levonorgestrel*

The adhesive solution was prepared by adding small pieces of MM-PIB to hexane (50%, w/w) in a glass jar. It was magnetically stirred for 24 h until the PIB pieces were completely dissolved. Its solid content was confirmed by evaporating the solvent from a small sample of known weight. Ethinyl estradiol or levonorgestrel was added to a certain amount of PIB-solution in a 10 ml glass vessel to yield matrices with 0.2, 2 and 5% drug content. The vessels

were closed tightly and the mixtures were magnetically stirred for 30 min. The casting mixtures were cast onto the fluorocoated side of the release liner (theoretical film thickness: 1500 μm) with a casting knife setup (ZUA 200, MTV Messtechnik, Köln, Germany). The matrices were dried under a hood for 12 h at 25 ± 2 °C and subsequently for 1 h at 60 °C (UT 6060, Heraeus Instruments, Hanau, Germany) and analyzed by DSC, XRD and polarized light microscopy as described in section 2.2.7.

2.2.12 Stability of transdermal patches

The patches were stored in open containers in climatic chambers at 25 °C/ 60 RH (Weiss Umwelttechnik Typ 125SB/410IU, Lindenstruth, Germany) and 40 °C/ 75 RH (Thermotec Weilburg GmbH & CoKG, Wellburg, Germany). Immediately after preparation and after 1 and 3 months, the patches were investigated using a polarized light microscope (Axiotrop, Carl Zeiss Jena GmbH, Jena, Germany) connected to a digital camera. The patches were attached to microscopic slides. The investigation took place through the microscopic slide which facilitated the focusing on the transdermal matrix. The whole surface area of 3 transdermal patches per formulation was scanned per time point and the images were evaluated using the Easy Measure Software (version 1.0.15; INTEQ Informationstechnik GmbH, Berlin, Germany).

2.2.13 Drug release studies

2.2.13.1 Drug adsorbates onto CPVP

Tablets for dissolution testing were prepared using a hydraulic press (Specac 25.011, Specac limited, Orpington, UK) at 1.0 t for 20 s. The tablets consisted of either 300 mg freshly prepared adsorbate with 9.1% carbamazepine or the corresponding freshly prepared physical mixture.

A dissolution test (release medium: 250 ml water, 100 rpm, 37 °C, non-sink conditions) with the tablets and pure micronized carbamazepine was performed (PTW 2, Pharma Test Apparatebau GmbH, Hainburg, Germany) (n=3). Samples were taken after 5, 15, 30, 45 and 60 min and filtered through a 0.22 μm filter (Acryl/Copolymer/Nylon, Sartorius AG, Göttingen, Germany). The drug concentration was determined UV-spectrophotometrically (UV 2101 PC, Shimadzu Scientific Instruments, Inc., Columbia, MD, USA) at $\lambda=285$ nm.

2.2.13.2 Patches

Drug release studies were performed (n=3) with freshly prepared patches in static Franz cells with a receptor volume of 8.0 ml and a diffusion area of 1.0 cm². The receptor compartment contained 2.0% (w/w) aqueous sodium dodecyl sulfate solution at 37 °C (corresponding to 32 °C at the release interface) and was stirred at 400 rpm with a magnetic stirrer. Circular patches (diameter: 1.3 cm, film thickness: approximately 170 µm) were centrally attached to circular pieces of hydrophilic, microporous polyethylene membrane (Solupor E-9H01A) with a diameter of 1.6 cm. The membranes with the attached patches were mounted between the donor and the receptor compartment of Franz cells employing some vaseline to prevent leaking. 500 µl samples were taken after 1, 2, 4, 8, 24, 30 and 48 h and analyzed for their drug content as described in the section 2.2.6. After each sampling, the Franz cells were refilled with 500 µl pre-warmed medium and turned upside down to let potentially formed air bubbles escape through the sampling port.

2.2.13.3 Saturated drug solutions across different membranes

Saturated solutions of both hormones were prepared by adding 20 mg ethinyl estradiol and 10 mg levonorgestrel to 10 ml 2% SDS solution in a glass vial followed by magnetic stirring (48 h at 25±2 °C) and filtration through a 0.5 µm filter (Sartorius AG, Göttingen, Germany). Drug release studies were performed in static Franz cells with a receptor volume of 8.0 ml and a diffusion area of 1.0 cm². The receptor compartment contained 2.0% (w/w) aqueous SDS solution at 37 °C and was stirred at 400 rpm with a magnetic stirrer. Circular pieces (diameter 1.6 cm) of Solupor[®] 7P03A, Solupor[®] 9H01A, or Solupor[®] 10P05A (n=3) were mounted between the donor and the receptor compartment of Franz cells employing some vaseline to prevent leaking. The donor compartment contained 0.5 ml of the saturated ethinyl estradiol and levonorgestrel solution and was covered with Parafilm[®] to prevent evaporation. 500 µl samples were taken after different time points and analyzed for their drug content as described in the section 2.2.6. After each sampling the Franz cells were refilled with 500 µl prewarmed medium and turned upside down to let potentially formed air bubbles escape through the sampling port. The ethinyl estradiol or levonorgestrel concentration of the equilibrated system was employed as 100% value.

2.2.14 Adhesion studies

2.2.14.1 In vitro probe tack

Tack measurements were performed (n=6) using a texture analyzer (TAXT2i, Winopal Forschungsbedarf GmbH, Ahnsbeck, Germany) at 22 ± 1 °C. The specimens (film thickness: approximately 400 μm) were restricted from moving by sandwiching them between two stainless steel plates (the top plate had an orifice for the probe). A cylindrical stainless steel probe (diameter: 6 mm) was brought into contact with the specimen (contact time: 60 s, contact force: 50 g) and subsequently removed with a rate of 5 mm/s while the force was recorded. Force-distance diagrams were recorded and evaluated with regard to maximal force, AUC and elongation at detachment using Exponent Software Update Version 4.0.8.0.

2.2.14.2 In vivo skin adhesion

18 patches (3 different adhesive bases: HM:MM:LM-PIB 1:5:0, 1:5:2 and 1:5:4 with 0, 10, 20, 30, 40 and 50% CPVP each) with matrix thicknesses of approximately 170 μm were applied (10 seconds pressure with finger) to the exterior of the right upper arm of 6 healthy Caucasian study subjects (male: 2, female: 4). Skin adhesion of each patch was evaluated after a wearing period of 7 d. To assess the matrix creep, the removed patches were scanned with a white background using a Canon DR-2080 c. Histograms of the digital grey-scale images with 255 unit intervals were obtained using the BDsoft DeskMaster software. Dividing the sum of pixels with grey scale values from 0 to 50 by the total number of pixels for one patch yielded the value matrix creep (%).

2.2.14.3 Skin irritation

Directly after removal of the patches and 48 h later, the application sites were visually evaluated for their irritation degree by the same investigator using a modified method of Draize et al. (1944). Erythema scores were given from 0 to 4 depending on the degree of erythema as follows: no erythema 0, slight erythema (barely perceptible light pink) 1, moderate erythema (dark pink) 2, moderate to severe erythema (light red) 3, severe erythema (extreme redness) 4.

3 RESULTS AND DISCUSSION

3.1 ADSORPTION PROPERTIES OF CROSPVIDONE

Crospovidone (CPVP) is a synthetic insoluble polymer derived from the monomer vinylpyrrolidone by popcorn polymerization (Haaf et al. 1985). It has pronounced swelling properties and is mainly used as a disintegrant in tablets and capsules. Furthermore, it is known for its adsorption properties; CPVP is used to clear fruit juices and beer (Mitchell et al. 2005) and as an adsorbent material in chromatography (Percival 1986). It is also suitable as a polymeric carrier that prevents the recrystallization of drugs (Friedrich et al. 2006). The loading of CPVP with drugs is normally achieved by the solvent deposition method in which the polymer is soaked with a concentrated organic drug solution. After evaporation of the solvent, the drug is adsorbed onto the carrier, which prevents its crystallization and facilitates its dissolution. The studies described in this chapter investigate the adsorption process of the model drug carbamazepine onto CPVP.

3.1.1 Location of the drug in adsorbates

There are two possible locations for the drug in carbamazepine adsorbates onto CPVP: Either the drug is bound to the surface of the CPVP particle or loaded throughout its bulk. For other adsorbent systems, e.g., acetaminophen onto activated charcoal (Hoegberg et al. 2002) or alkaloids onto clay (Martin 1993a), the extent of drug adsorption is linearly correlated to the surface area of the adsorbent, indicating that the drug is bound to the adsorbent's surface. Adsorption studies of carbamazepine onto CPVP with different specific surface areas (Table 4) showed that the adsorption onto CPVP was independent of the specific surface area of the carrier (which differed by a factor of 3.8), but correlated linearly with the amount of CPVP (Fig. 19). Since the adsorption depended exclusively on the total amount of CPVP's binding sites, this result indicated that the carbamazepine adsorption took place throughout the bulk of the CPVP particles. For the sake of readability and because this study was not conducted for all investigated carriers the term "adsorption" is used throughout the dissertation for all sorption processes of molecules onto carrier materials.

Table 4 Particle size distribution determined by laser diffraction analysis in water and specific surface area of the CPVP batches determined by nitrogen adsorption (BET)

Batch	Particle size distribution			Specific surface area, m ² /g
	d 0.9, μm	d 0.5, μm	d 0.1, μm	
1	12.4	6.6	1.7	2.3
2	9.3	5.0	2.0	3.2
3	n.d.	n.d.	n.d.	1.0
4	11.3	5.3	1.5	3.8
5	11.1	5.8	1.6	3.3

This study is in good agreement with X-ray photoelectron spectroscopic data of a CPVP-griseofulvin system, which demonstrated drug diffusion inside the polymer particles during the loading procedure (Carli and Garbassi 1985).

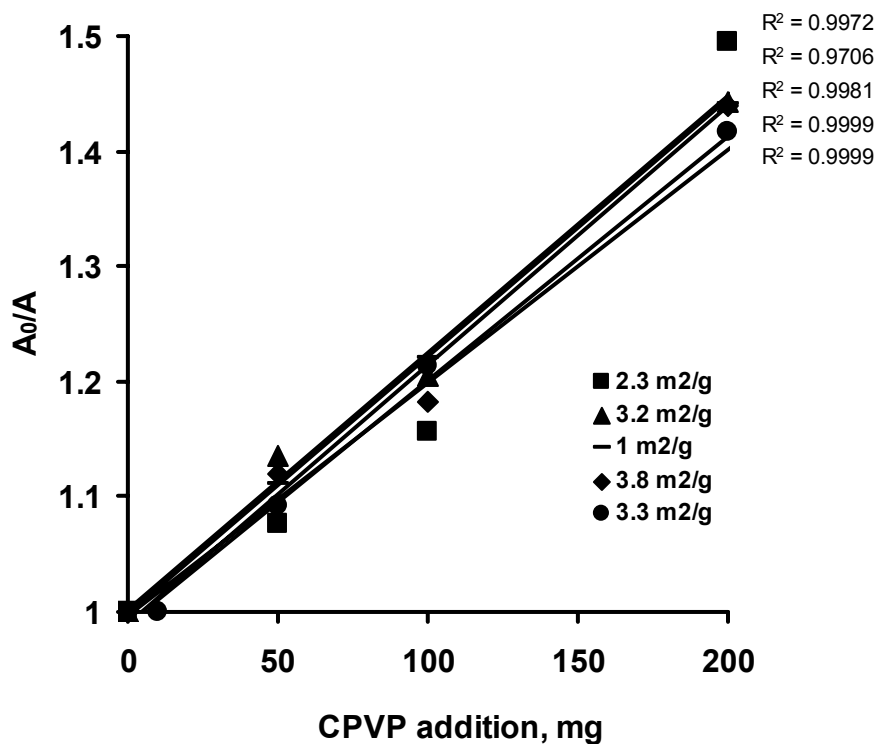


Fig. 19 Effect of CPVP's specific surface area on the carbamazepine adsorption (A_0/A = initial UV absorption/UV absorption after equilibration) from aqueous solution (drug concentration: 25 μg/ml).

3.1.2 Adsorption isotherms

The equilibrium drug concentration of a three component system with solvent, drug and carrier depends on the amount of adsorbent, the drug concentration and the volume of the drug solution.

To determine adsorption isotherms, CPVP was added to carbamazepine solutions of varying drug concentrations. The resulting equilibrium drug concentration was measured and correlated with the amount of drug that was bound to the adsorbent. Ethanol and ethyl acetate were investigated as solvents because they possess different hydrogen bonding abilities. The solubility of CPZ in different solvents is given in Table 5.

Table 5 Solubility of carbamazepine in different solvents

Solvent	Solubility, mg/ml
Methanol	160.4 ± 4.2
Ethanol	23.4 ± 0.9
Ethyl acetate	10.1 ± 0.5
Water	0.1 ± 0.1

The amount of carbamazepine bound to CPVP (x/m) at a certain equilibrium carbamazepine concentration was significantly smaller in ethanolic solution than in ethyl acetate (Fig. 20).

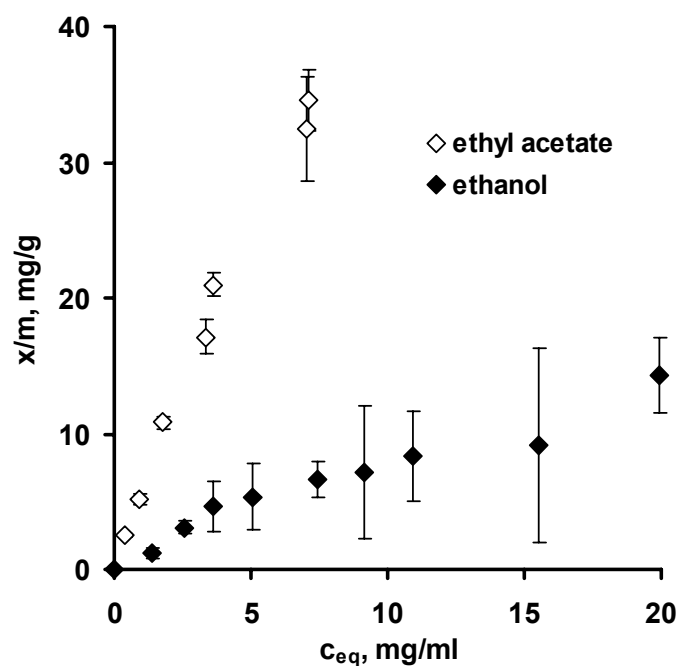


Fig. 20 Adsorption isotherms of carbamazepine onto CPVP in ethyl acetate and ethanol

Physical adsorption phenomena are often the result of specific interactions, primarily hydrogen bonds, between the drug and the adsorbate. Since CPVP's only functional group is the cyclic amide (Fig. 21), the polymer can only be the hydrogen acceptor in such a bond. The drug-polymer interaction could occur with carbamazepine's NH_2 group as hydrogen donor site. Ethyl acetate is also only able to act as a hydrogen acceptor and thus cannot interact with CPVP in this way. This could be the reason why carbamazepine molecules adsorb onto CPVP to a greater degree when ethyl acetate is used as a solvent. Ethanol, on the other hand, participates in hydrogen bonds as both hydrogen acceptor and donor. The lower binding of carbamazepine onto CPVP in ethanolic solution could be related to ethanol competing with carbamazepine for binding sites on CPVP.

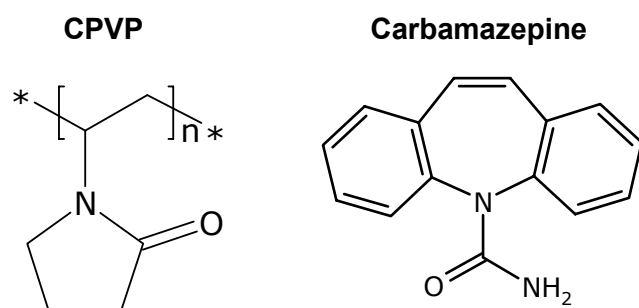


Fig. 21 Chemical structures of CPVP and carbamazepine

3.1.3 ATR-FTIR spectroscopy

Attenuated total reflection Fourier-transformation infrared (ATR-FTIR) spectroscopy is the method of choice to investigate the nature and extent of interactions between two compounds. If molecules interact, the oscillating dipoles of the involved moieties change and, as a consequence, their frequency and bandwidth in the IR spectrum (Silverstein, Bassler et al. 1991). Changes in the spectrum of CPVP were investigated (Fig. 22) to explain interactions of CPVP with solvents and carbamazepine.

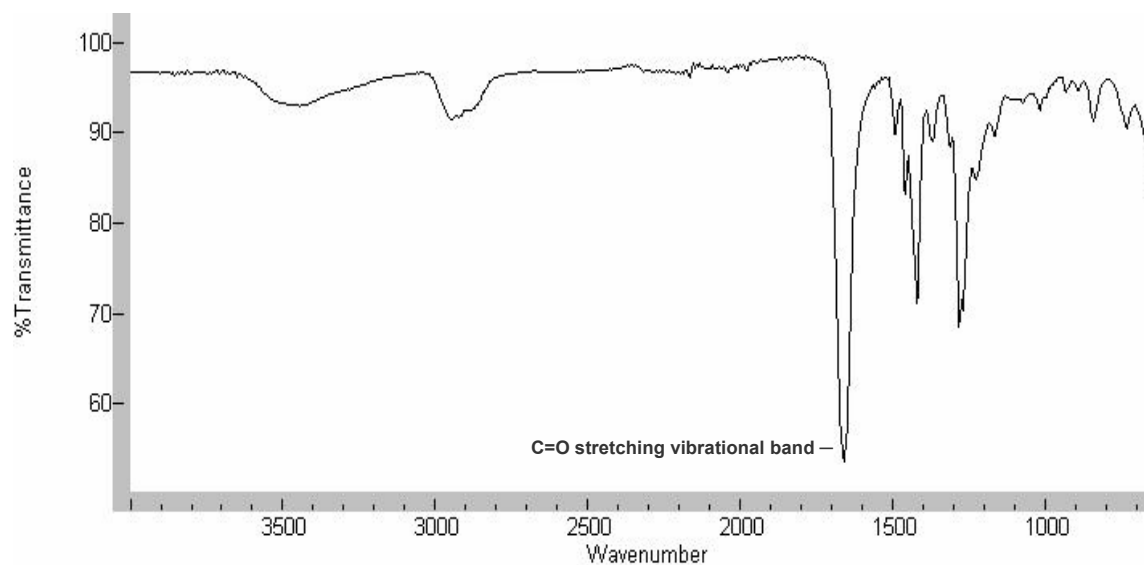


Fig. 22 FT-IR spectra of CPVP at ambient conditions

Since CPVP is a highly hygroscopic substance (Bühler 1992), the influence of CPVP's water content on its IR spectrum was investigated. CPVP samples were dried at 80 °C to constant weight and stored above orange gel or equilibrated at different relative humidities (Table 6).

Table 6 Relative humidities above saturated salt solutions in closed containers at 25 °C according to Wexler and Hasegawa (1954)

Aqueous saturated salt solutions	Relative humidity, %
MgCl ₂	33
K ₂ CO ₃	43
NaCl	75
KNO ₃	92
Water	100

The spectra showed shifts of the carbonyl stretching vibrational band of from 1671.5 cm⁻¹ for thoroughly dried CPVP to 1638.5 cm⁻¹ for CPVP equilibrated at 100% relative humidity (Fig. 23).

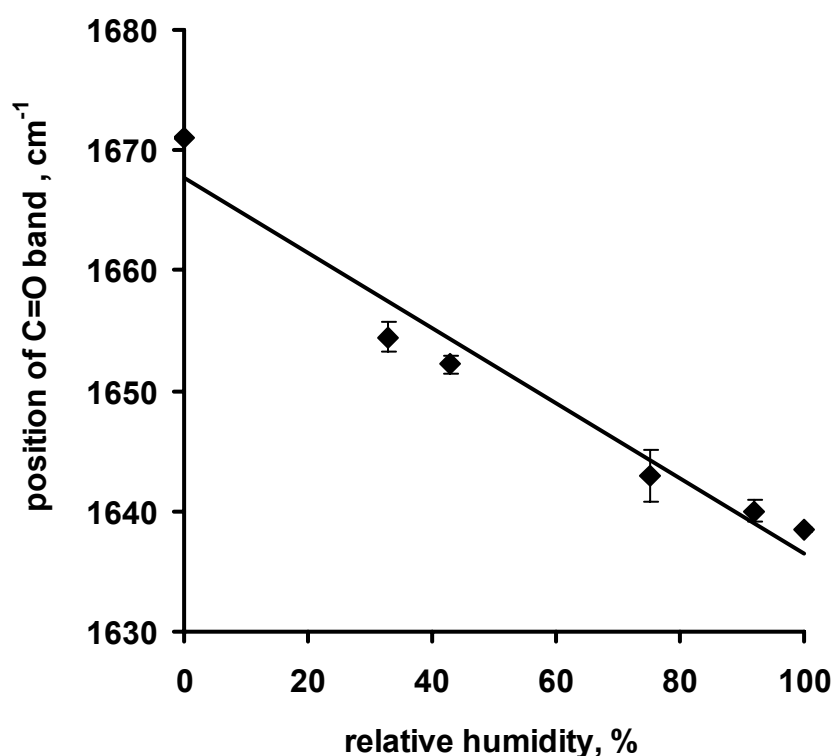


Fig. 23 Influence of relative humidity on the position of the C=O stretching vibrational band of CPVP

This result indicated a hydrogen bond formation between CPVP and water. CPVP possesses two hydrogen acceptor sites: The nitrogen and the oxygen atom of the cyclic amide. Since only the frequency of the carbonyl band shifted, the oxygen atom was apparently preferred. That seems reasonable, since steric constraints of the molecule might favor molecular interactions of this moiety and is similar to interactions between linear polyvinylpyrrolidone and ibuprofen (Sekizaki et al. 1995).

The ambient humidity influenced the water content of CPVP and had a tremendous influence on the frequency of the carbonyl group in the IR spectrum. Thus humidity effects had to be excluded when interactions between CPVP and other substances were investigated. This was achieved by using thoroughly dried CPVP in subsequent studies.

To investigate interactions of CPVP with solvents, the ATR-FTIR spectra of thoroughly dried CPVP and CPVP wetted with various solvents were compared. The extent of the carbonyl band shift was correlated to the strength of the formed hydrogen bond (Fig. 24).

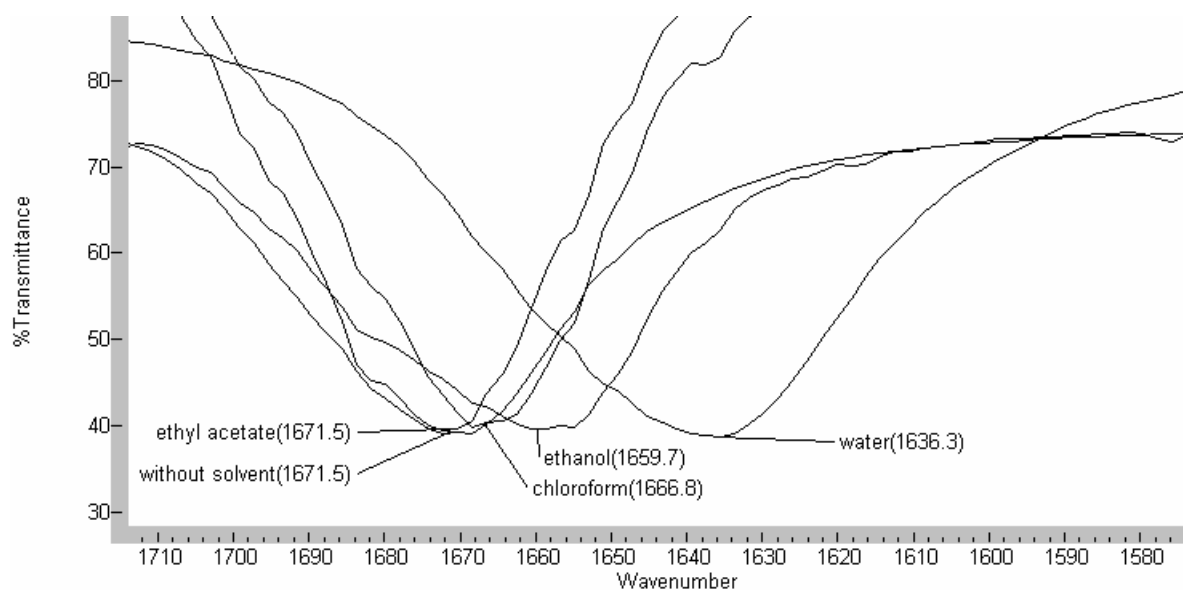


Fig. 24 FT-IR spectra of thoroughly dried CPVP and pastes of CPVP with ethyl acetate, ethanol, chloroform and water

Dry CPVP and ethyl acetate-CPVP pastes both showed the carbonyl band at 1671.5 cm^{-1} . Ethyl acetate's only functional group is an ester group which cannot provide a hydrogen atom for a hydrogen bond. Chloroform can act as a hydrogen donor because the electronegative chloride atoms attract and decentralize the electron cloud from the hydrogen nucleus and thereby leave the atom with a positive partial charge. As a consequence, the carbonyl band of CPVP shifted by 4.7 cm^{-1} in the ATR-FTIR spectrum of the chloroform-CPVP paste. Ethanol and water are well-known hydrogen donors due to their OH-moiety. This property led to a shift of CPVP's carbonyl band by 11.8 and 35.2 cm^{-1} in ethanol-CPVP and water-CPVP pastes, respectively.

To investigate the solid-state adsorption onto CPVP, a thoroughly dried carbamazepine adsorbate onto CPVP with 9.1% drug loading was investigated by ATR-FTIR spectroscopy (Fig. 25). CPVP's carbonyl band shifted by 3.2 cm^{-1} , indicating a hydrogen bond formation between carbamazepine and CPVP. Carbamazepine's only group able to act as hydrogen donor is the NH_2 -group of the urea function (Fig. 21). Interactions like this can immobilize drug molecules (Bhugra and Pikal 2008) and prevent them from forming nuclei, which are a precondition for crystal formation (Lipp 1998). The small extent of the $\text{C}=\text{O}$ shift of the carbamazepine adsorbate onto CPVP indicated a relatively weak bond formation between carbamazepine and CPVP. This is favorable, since a strong bond could impede the drug release from the adsorbate.

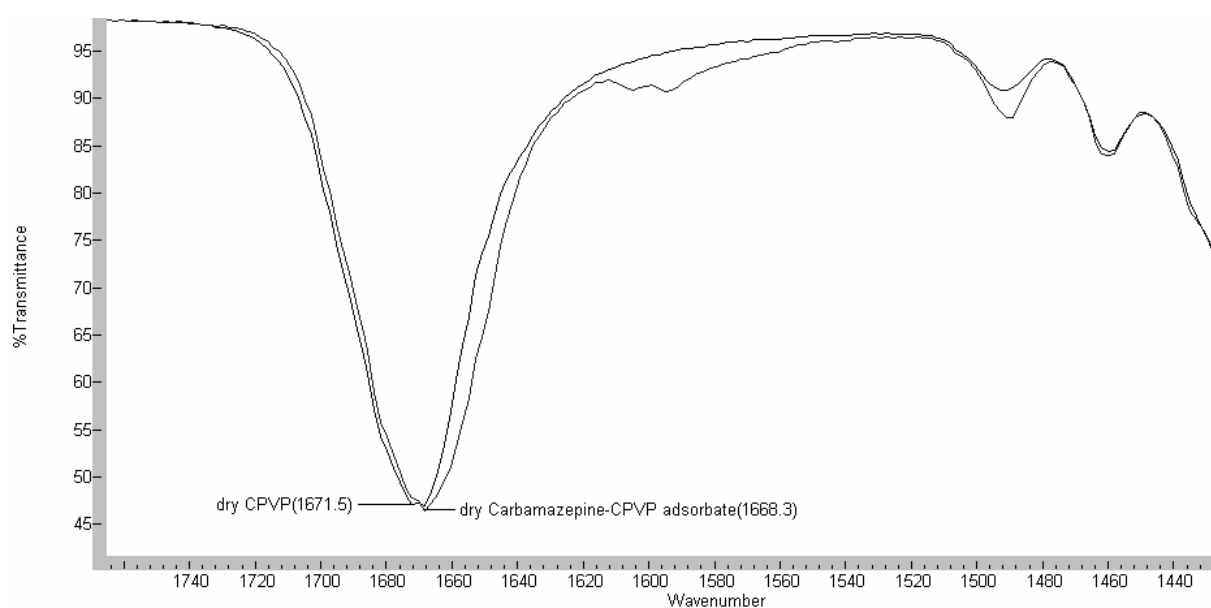


Fig. 25 Comparison of the FT-IR spectra of dry CPVP and dry carbamazepine adsorbate onto CPVP

3.1.4 Optimization of the drug-carrier ratio

CPVP is capable of preventing drugs from recrystallization and increasing drug dissolution (Friedrich et al. 2006). To find the optimum drug-CPVP ratio, adsorbates with different drug loadings were prepared by the solvent deposition method and analyzed for drug crystals by differential scanning calorimetry (DSC), X-ray diffraction (XRD), scanning electron microscopy (SEM) and polarized light microscopy.

The solvent uptake and binding capacity of CPVP for different solvents was determined by centrifuging CPVP suspensions in different solvents (Fig. 26). Solvents capable of acting as hydrogen donors (ethanol, methanol and water) caused CPVP to take up more solvent than ethyl acetate. The significant ethyl acetate uptake of CPVP determined with this method is probably the result of the mild centrifugation conditions and hence the presence of ethyl acetate in spaces between the carrier particles.

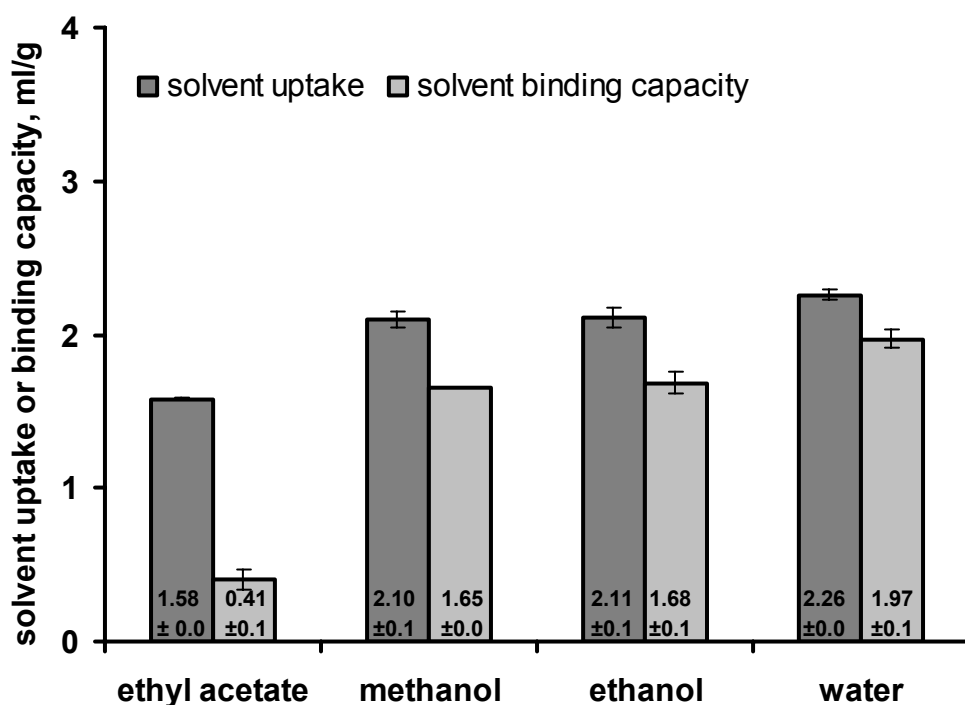


Fig. 26 Solvent uptake determined with the centrifuge method and solvent binding capacity determined with mortar/pestle and of CPVP in various solvents

The solvent binding capacity of CPVP is a measure of how much solvent the carrier can absorb before it becomes paste-like. The solvent binding capacity showed the same trends as the solvent uptake. However, the effects were more pronounced because only the amount of solvent that was taken up by the particles was measured. Interactions between methanol, ethanol and water and CPVP resulted in swelling of the polymer and thereby increased its binding capacity. Methanol was used for the preparation of the carbamazepine adsorbates onto CPVP for solubility reasons (Tab. 5) as well as CPVP's good binding capacity for this solvent. These properties are beneficial for the loading procedure of the carrier because a higher drug amount can be loaded onto the polymer in one step. Concentrated drug solutions could be problematic when they are not completely taken up by the adsorbent; the evaporation of the volatile solvent may lead to recrystallization of the drug that does not have intimate contact with the polymer.

The thermograms of carbamazepine-CPVP physical mixtures showed the characteristics of carbamazepine's P-monoclinic form III (Fig. 27), which melted at 176.1 °C. Form III is the most stable polymorph of carbamazepine based on DSC analysis and the density rule (Grzesiak et al. 2003). This event was immediately followed by an exothermic peak which

corresponded to the crystallization to form I. The last peak coincided with the melting of form I (191.3 °C). Due to insufficient sensitivity of the DSC method, the latter two events could not be detected in physical mixtures with low drug loading. The thermograms of carbamazepine-CPVP adsorbates with 33.3, 23.1 and 13.0% drug loading showed a melting point depression of 15-25 °C compared to the melting of form III in the physical mixtures. The melting point depression increased in the order of 33.3 < 23.1 < 13.0% drug loading. Furthermore, the thermal event was much broader than in the corresponding physical mixtures (Fig. 27B). Melting point depression and broadening of melting peaks have been described in the literature for drug adsorbates onto silanol (Monkhouse and Lach 1972a) and were attributed to interactions of the drug with the polymer and the minuscular form of the drug crystals. These factors facilitate the melting of the drug. Higher melting point depressions are thought to indicate increased drug-polymer interactions. The melting point depressions were more pronounced for adsorbates with lower carbamazepine loadings because the drug was more finely distributed in these formulations compared to adsorbates with higher drug loadings. Adsorbates with 9.1 and 4.8% drug loading did not show thermal events that indicated the melting of crystalline carbamazepine.

The adsorbates and the physical mixtures were investigated by XRD (Fig. 28). If the spectra showed crystallinity, they always exhibited the characteristic main peaks of carbamazepine form III at 13.0, 15.2, and 27.2° (Grzesiak et al. 2003).

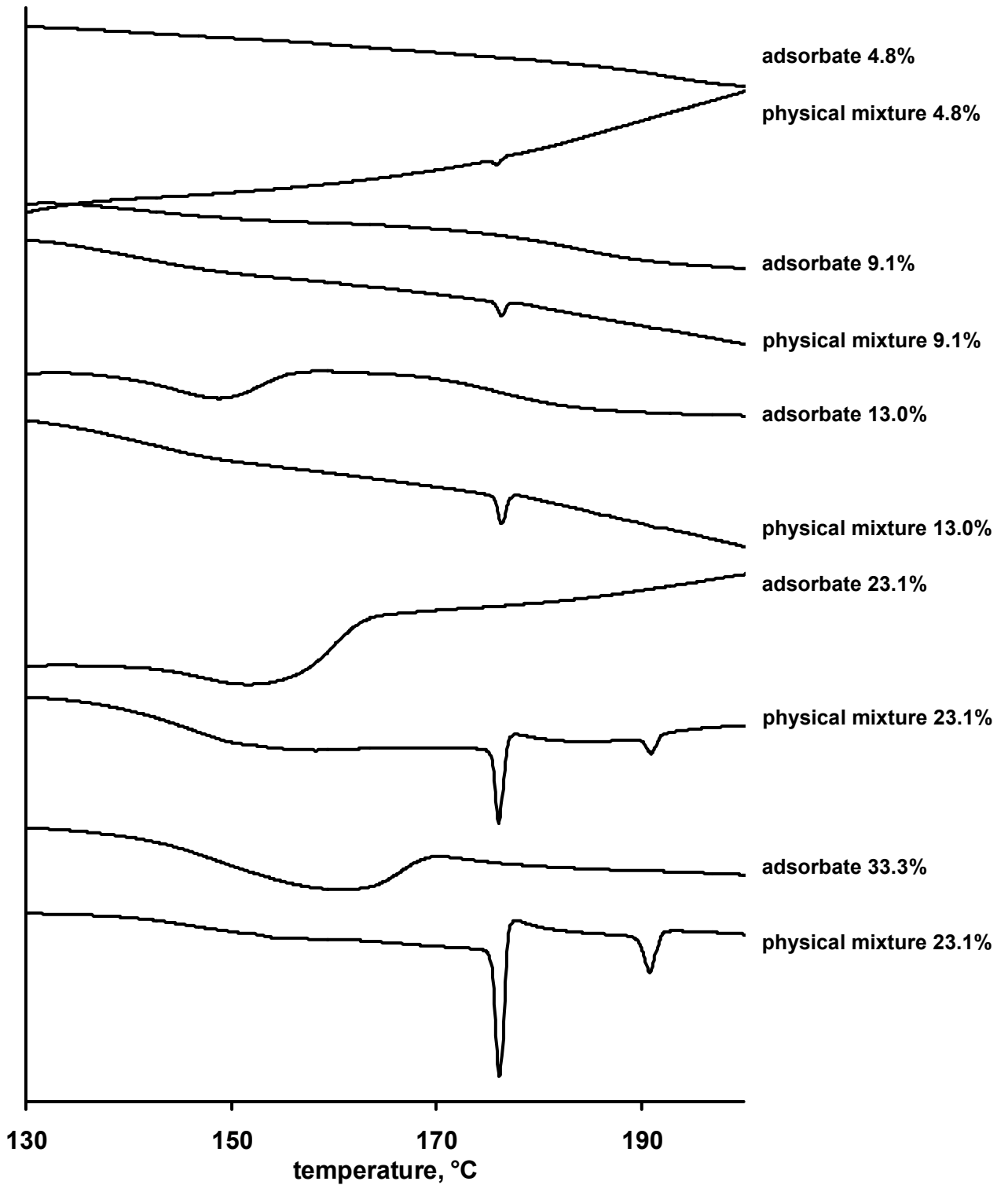


Fig. 27 DSC thermograms of carbamazepine-CPVP adsorbates and the corresponding physical mixtures with 33.3, 23.1, 13.0, 9.1 and 4.8% drug loading

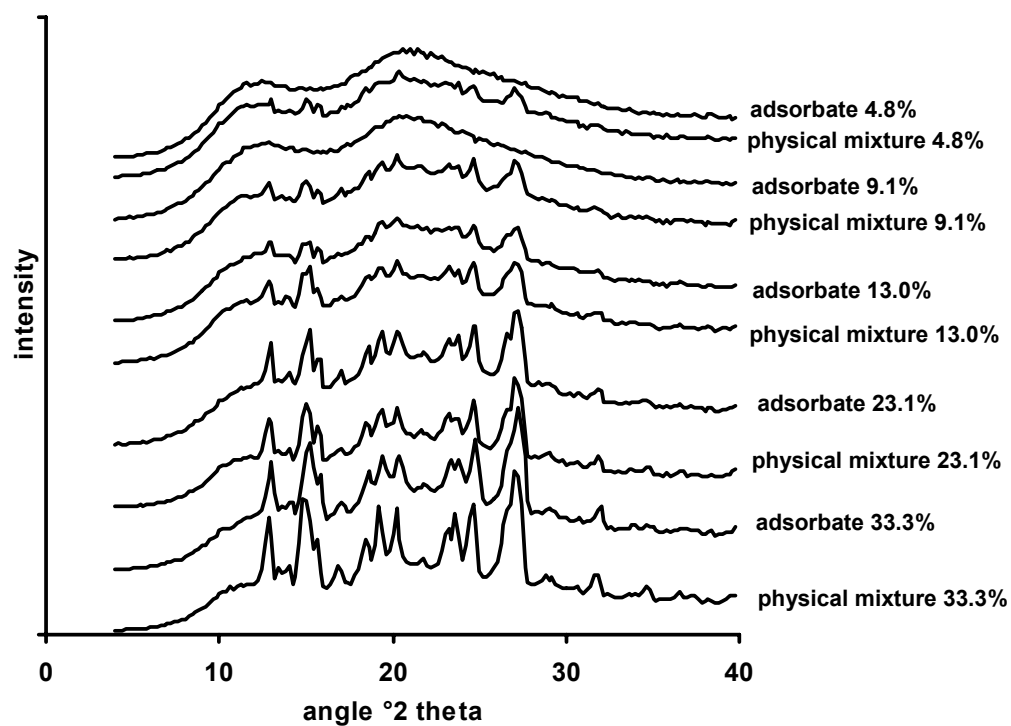


Fig. 28 XRPD of carbamazepine-CPVP adsorbates and the corresponding physical mixtures with different drug loadings

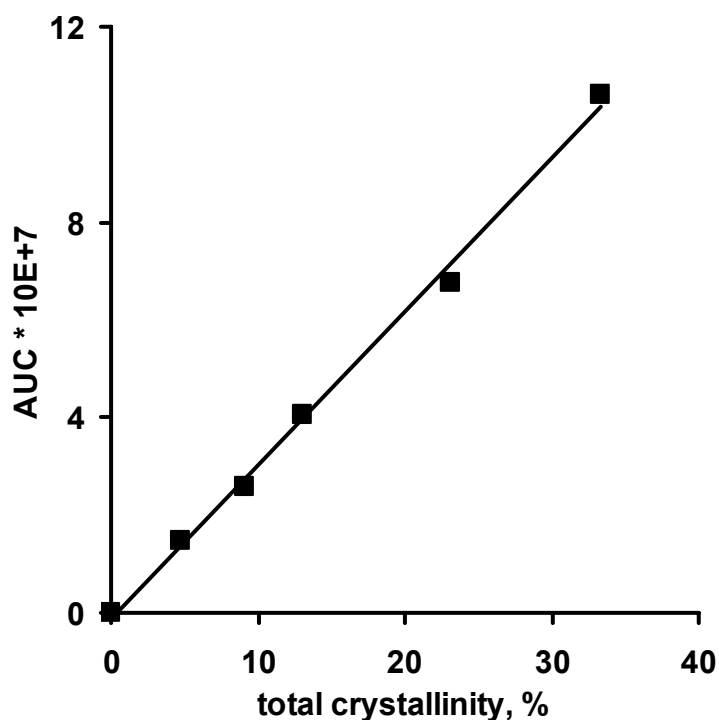


Fig. 29 Correlation of \sum AUCs of the 3 main XRD peaks (at 13.0, 15.2, and 27.2°) in carbamazepine-CPVP physical mixtures and the total crystallinity of the physical mixtures, %

From the spectra of physical mixtures (crystalline carbamazepine form III plus CPVP, which is 100% amorphous), a correlation between the sum of the AUCs of carbamazepine's three main peaks and the total crystallinity of the mixture was obtained (Fig. 29). This relationship was used to determine the crystallinity of carbamazepine in the adsorbates (Table 7). XRD did not detect carbamazepine crystals in adsorbates with 4.8 and 9.1% drug loading, while adsorbates with higher drug loading contained crystalline carbamazepine. The total “non-crystallinity” of carbamazepine (drug loading, % - total crystallinity, %) yielded similar values for drug loadings from 13.0 to 33.3%. This showed the capacity of CPVP to inhibit drug recrystallization when drug crystals were present. The drug loading of 9.1% showed a higher capacity of CPVP to inhibit the recrystallization of carbamazepine, probably because in this case no seed crystals were available.

Table 7 Crystallinity of carbamazepine in carbamazepine-CPVP adsorbates determined by XRPD

Drug loading, %	AUC formulation	Total crystallinity, %	Drug crystallinity, %	Drug loading – total crystallinity, %
33.3	90216955	29.1	87.3	4.2
23.1	57669697	18.7	80.5	4.4
13.0	25451563	8.5	64.2	4.5
9.1	not detectable	0	0	9.1
4.8	not detectable	0	0	4.8

SEM (Fig. 30) pictures showed carbamazepine crystals as thin needles which formed in adsorbates with drug loadings > 9.1%. In adsorbates with lower drug loading, no carbamazepine crystals were observed. Polarized light microscopy showed similar results as SEM.

In conclusion, drug crystals were not detected by any method when the drug loading was 9.1% or less. In these adsorbates, the drug probably existed in a molecularly dispersed form. Studies of more complicated systems with ethinyl estradiol and levonorgestrel adsorbed onto CPVP in a polyisobutene matrix were conducted and are described in section 3.3.2. These systems were crystal-free at similar drug loadings (12%) as determined with carbamazepine.

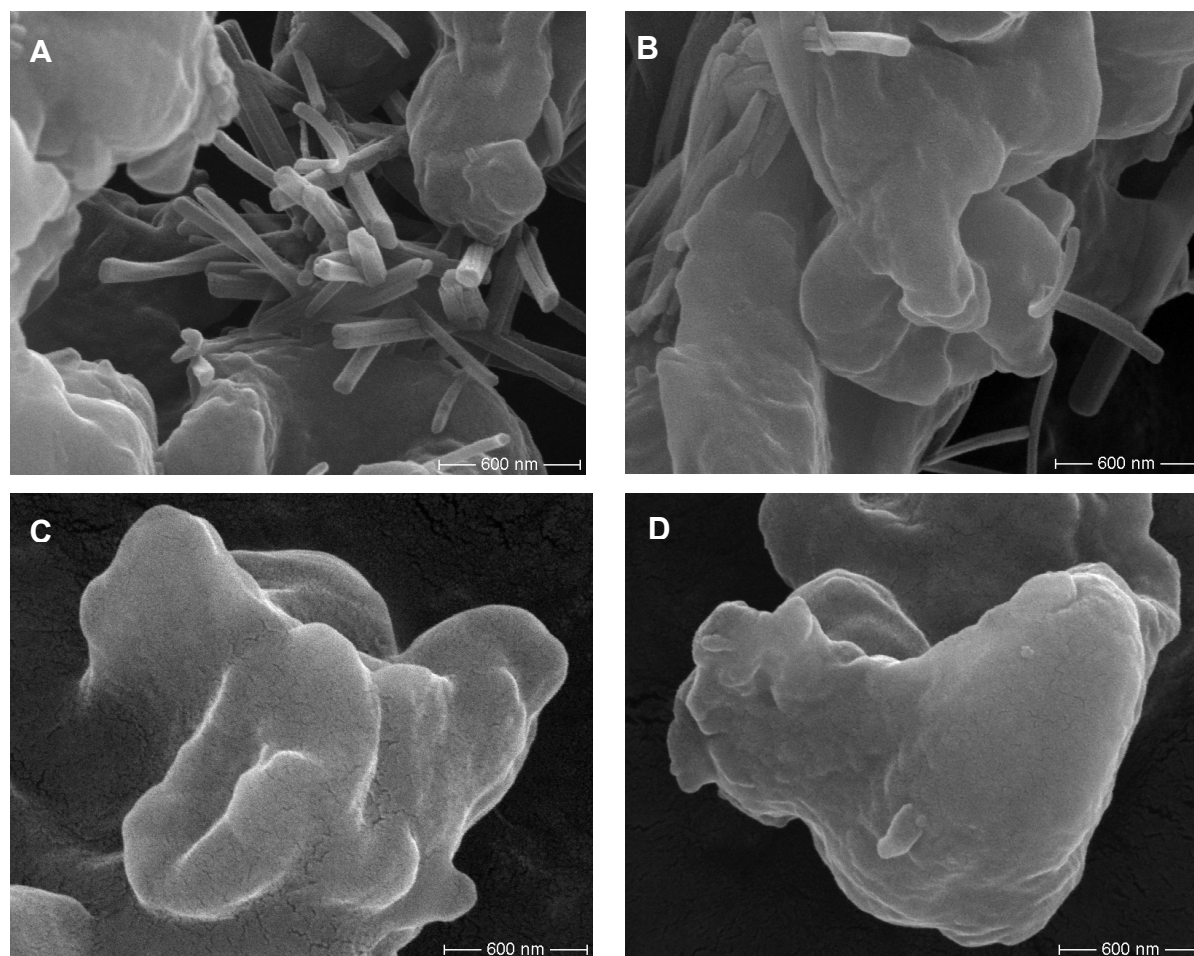


Fig. 30 SEM pictures of carbamazepine adsorbates onto CPVP with: 33.3% (A), 13.3% (B), 9.1% (C) and 4.8% (D) drug loading

3.1.5 Drug release

The adsorbate with 9.1% drug loading and the corresponding physical mixture were compressed into tablets without further additives. The compression step was performed because the carbamazepine adsorbates onto CPVP tended to agglomerate when they were added to the release medium, which led to irreproducible results. These tablets and pure micronized carbamazepine were released in a dissolution tester. Disintegration of these tablets occurred within the first seconds after contact with the release medium due to the pronounced swelling properties of CPVP. The drug release was faster from tablets comprised of adsorbates compared to tablets comprised of physical mixture (Fig. 31). The molecularly dispersed state in which the drugs were present in the adsorbate tablets represents the ultimate reduction in particle size and the maximum increase in drug surface area. This correlates, according to the Noyes-Whitney equation, directly with the dissolution rate. Furthermore, in this physical state, no energy is required to break up crystal structures before

the drug can dissolve (Leuner and Dressman 2000). The drug release from tablets containing the physical mixture was faster than the dissolution of pure micronized carbamazepine. There are two possible explanations for this result: Firstly, micronized drugs tend to agglomerate, which significantly hampers their dissolution (Armando J. Aguiar 1967). It is likely that CPVP in the tablets containing physical mixtures helped to disperse and disaggregate the drug particles. Secondly, it is known that even carriers that are not surface active (but hydrophilic), like linear PVP, can improve the wetting of hydrophobic drugs, e.g., in solid dispersions (Leuner and Dressman 2000). Since the wetting is a prerequisite for dissolution, this effect probably contributed to a faster drug release kinetic.

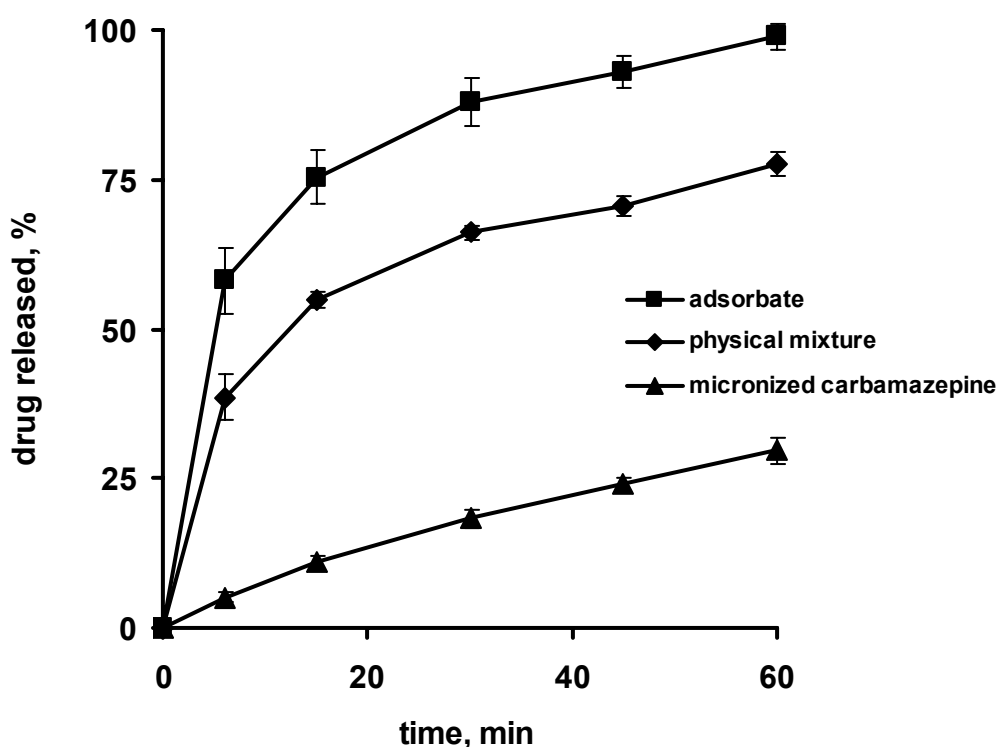


Fig. 31 Drug release from tablets prepared of the carbamazepine-CPVP adsorbate (9.1% drug loading), the corresponding physical mixture (9.1% drug content) and pure micronized carbamazepine

3.1.6 Conclusions

The adsorption process of carbamazepine onto CPVP is probably mainly governed by hydrogen bonds, which form between the NH_2 -group of carbamazepine's urea function and CPVP's carbonyl group. This is a favorable mechanism for immediate release formulations

because it ensures the complete and fast drug release from the polymeric network in aqueous environments due to the strong hydrogen donor properties of water. The interactions between carbamazepine and CPVP in the adsorbates prevented the drug from recrystallization when the drug loading did not exceed 9.1%. This adsorbate showed increased dissolution kinetics compared to the physical mixture and the pure drug. Two mechanisms of dissolution enhancement seemed to play a role: Firstly, the molecularly dispersed state of carbamazepine, which explains the faster release from the adsorbate than from the physical mixture and secondly, deagglomeration and wetting effects, which explain the faster release from the physical mixture compared to the pure drug powder.

3.2 METHOD DEVELOPMENT – TRANSDERMAL PATCHES

The incorporation of drug adsorbates onto insoluble carriers into transdermal patches could be a promising strategy to inhibit drug recrystallization therein. This might be an interesting alternative, especially for very lipophilic adhesives, like PIB, which show incompatibilities with conventional crystallization inhibitors, like linear PVP (Schurad et al. 2005),

This chapter describes the development of methods for the preparation and the analytic of such formulations.

3.2.1 Detection of drug crystals

Commonly used methods for the detection of crystals in pharmaceutical formulations are differential scanning calorimetry (DSC), X-ray diffraction (XRD) and polarized light microscopy.

To investigate the sensitivity of these methods in the case of transdermal hormone patches, PIB matrices with a defined amount of crystalline ethinyl estradiol or crystalline levonorgestrel were prepared. This was achieved by adding the drugs to PIB solutions in hexane. This preparation method yielded PIB matrices with suspended drug because ethinyl estradiol and levonorgestrel are practically insoluble in hexane (approximately 0.008 and 0.02 mg/ml, respectively). DSC was not sensitive enough to detect ethinyl estradiol, but could detect levonorgestrel down to 2% in the PIB matrix (Fig. 32). The higher sensitivity of DSC for levonorgestrel compared to ethinyl estradiol is a result of levonorgestrel's higher enthalpy of fusion (Table 8). XRD was able to detect levonorgestrel in PIB matrices with a drug content of 5%, but was not sensitive enough to detect drug crystals at any other concentration (Fig. 33). Polarized light microscopy could detect drug crystals without difficulty at all tested concentrations because the colorful crystals contrasted with the amorphous matrix. (Fig. 34). A further advantage of this technique is that the whole specimen can be searched for drug crystals.

The crystal growth in supersaturated matrices stops once the system is saturated (Raghavan et al. 2001b). Since the drug content of hormone patches is usually $\leq 1\%$ and drug recrystallization might only occur with a fractional amount of the drug, DSC and XRD were not appropriate methods for the detection of drug recrystallization. Polarized light microscopy is not able to quantify the amount of recrystallized drug, but was the most sensitive method to detect drug crystals in the amorphous matrix. Therefore, this method was used in the following studies to investigate the drug physical state in the patches.

Table 8 Thermic events of ethinyl estradiol and levonorgestrel

Adsorbent	Ethinyl estradiol		Levonorgestrel	
	Melting point, °C	Enthalpy of fusion, J/g	Melting point, °C	Enthalpy of fusion, J/g
Pure drug	184.9	81.1	241.2	128.6

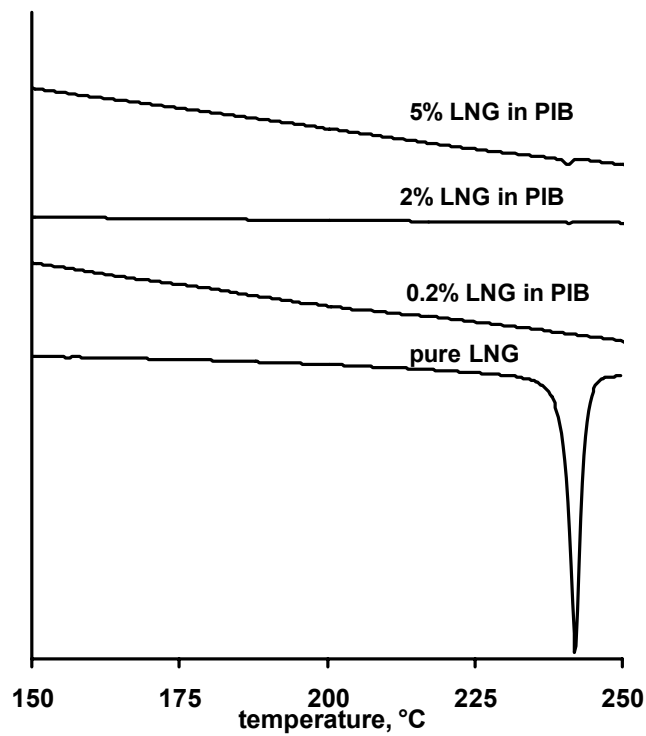
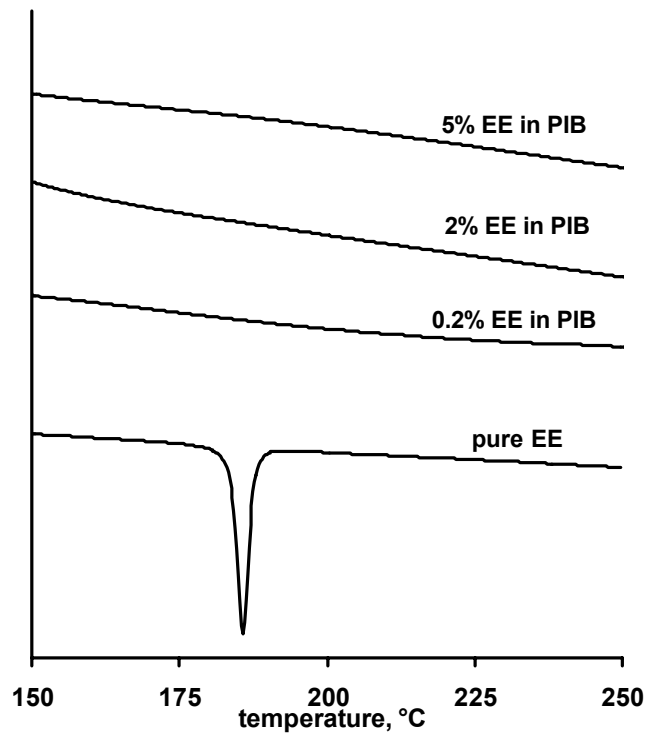


Fig. 32 DSC of PIB matrices with different amounts of suspended ethinyl estradiol (EE) and levonorgestrel (LNG)

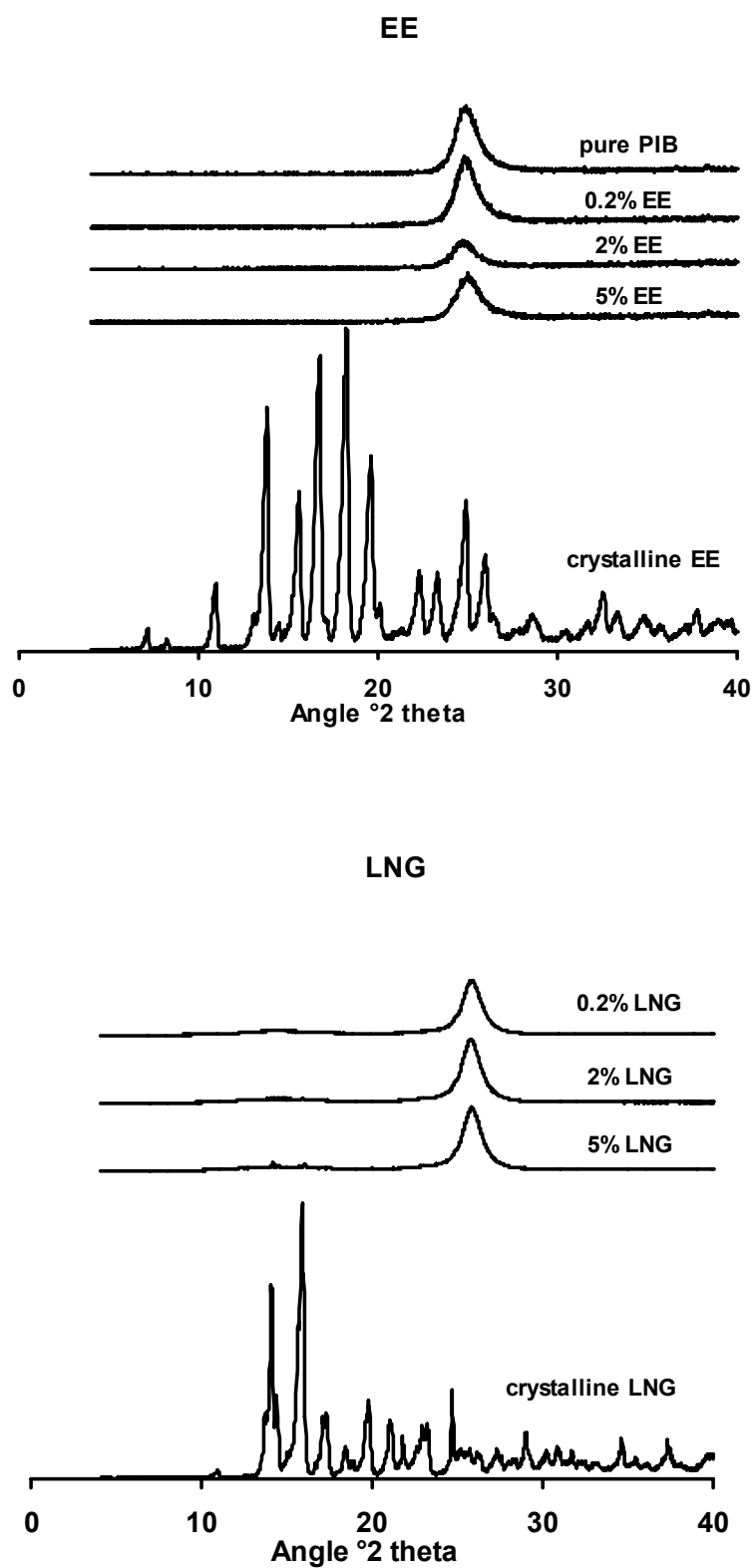


Fig. 33 XRD of PIB matrices with different amounts of suspended ethinyl estradiol (EE) or levonorgestrel (LNG)

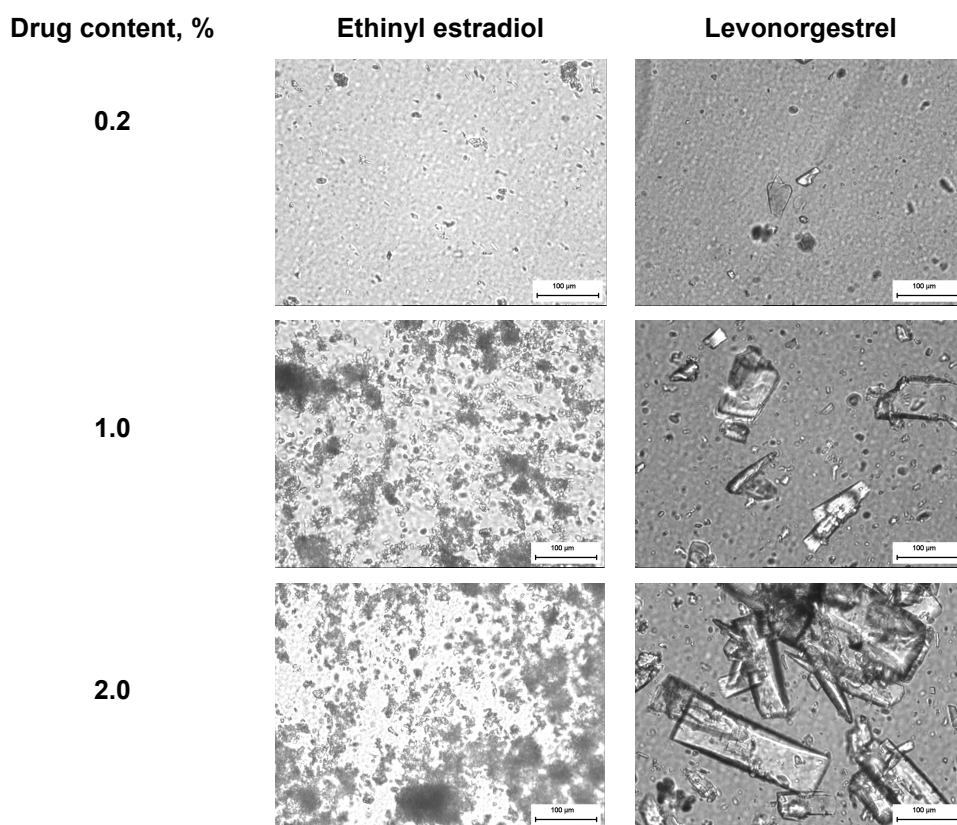


Fig. 34 Polarized light microscopy of PIB matrices with different amounts of suspended ethinyl estradiol or levonorgestrel

3.2.2 Solubility considerations

3.2.2.1 Drug solubility in solvents

Ethinyl estradiol and levonorgestrel were practically insoluble (according to USP 24 categories) in water and hexane (Table 9). While ethinyl estradiol showed good solubility in several organic solvents, levonorgestrel was only sparingly or slightly soluble in all solvents except chloroform. Levonorgestrel's lower solubility in all solvents compared to ethinyl estradiol is also reflected by its higher melting point and its higher enthalpy of fusion (Table 8). According to the theory of ideal solutions this reflects higher interactions between the levonorgestrel molecules and hence lower solubility in an ideal solvent (Martin 1993b).

As a consequence, chloroform was used as a solvent for the preparation of the ethinyl estradiol and levonorgestrel adsorbates onto carrier material. 2% aqueous SDS solution increased the solubilities of the two drugs significantly (Table 9) and was chosen as the release medium to ensure sink conditions.

Table 9 Solubility of ethinyl estradiol (EE) and levonorgestrel (LNG) in different solvents

Solvent	Solubility of LNG, mg/ml	Solubility of EE, mg/ml
Water	$1.4 \cdot 10^{-3} \pm 0.7$	$6.0 \cdot 10^{-3} \pm 2.0$
2.0% SDS	$86.4 \cdot 10^{-3} \pm 1.9$	$553.5 \cdot 10^{-3} \pm 23.2$
Methanol	15.1 ± 0.4	n.d.
Ethanol	11.3 ± 0.6	> 200 ^a
Isopropanol	6.0 ± 0.1	n.d.
Ethyl acetate	10.6 ± 0.2	> 200 ^a
Acetone	11.7 ± 0.2	n.d.
Methylene chloride	23.6 ± 3.0	n.d.
Chloroform	57.3 ± 2.1	> 50 ^a
Hexane	0.02^b	0.008^b

n.d.: not determined; ^a solubility was estimated by adding increments of 50 mg EE to 1.0 ml the solvent until the drug did not completely dissolve or 200 mg/ml were reached (n=1); ^b n=1

3.2.2.2 Drug solubility in polyisobutene

Polyisobutene (PIB), the adhesive base of the patches, is a very lipophilic polymer since it consists only of isobutene units. It is soluble in paraffinic solvents like hexane (Higgins et al. 1989) or, to a lesser degree, in chloroform, but not in oxygenated solvents (e.g., low molecular weight esters, ketones, alcohols).

To investigate the solubility of ethinyl estradiol and levonorgestrel in PIB, polarized light microscopic investigations of PIB matrices with different ethinyl estradiol or levonorgestrel contents were carried out. The casting solutions were prepared in chloroform and were crystal-free. Polarized light microscopic analysis of the dried matrices (after 48 h) showed characteristic needles of crystallized hormones at all investigated drug concentrations (Fig. 35). The low solubility of both hormones in PIB is probably a result of PIB's hydrocarbon structure. The lack of any functional groups inhibits specific interactions between the drugs and the polymer, which facilitate the dissolution process (Martin 1993b).

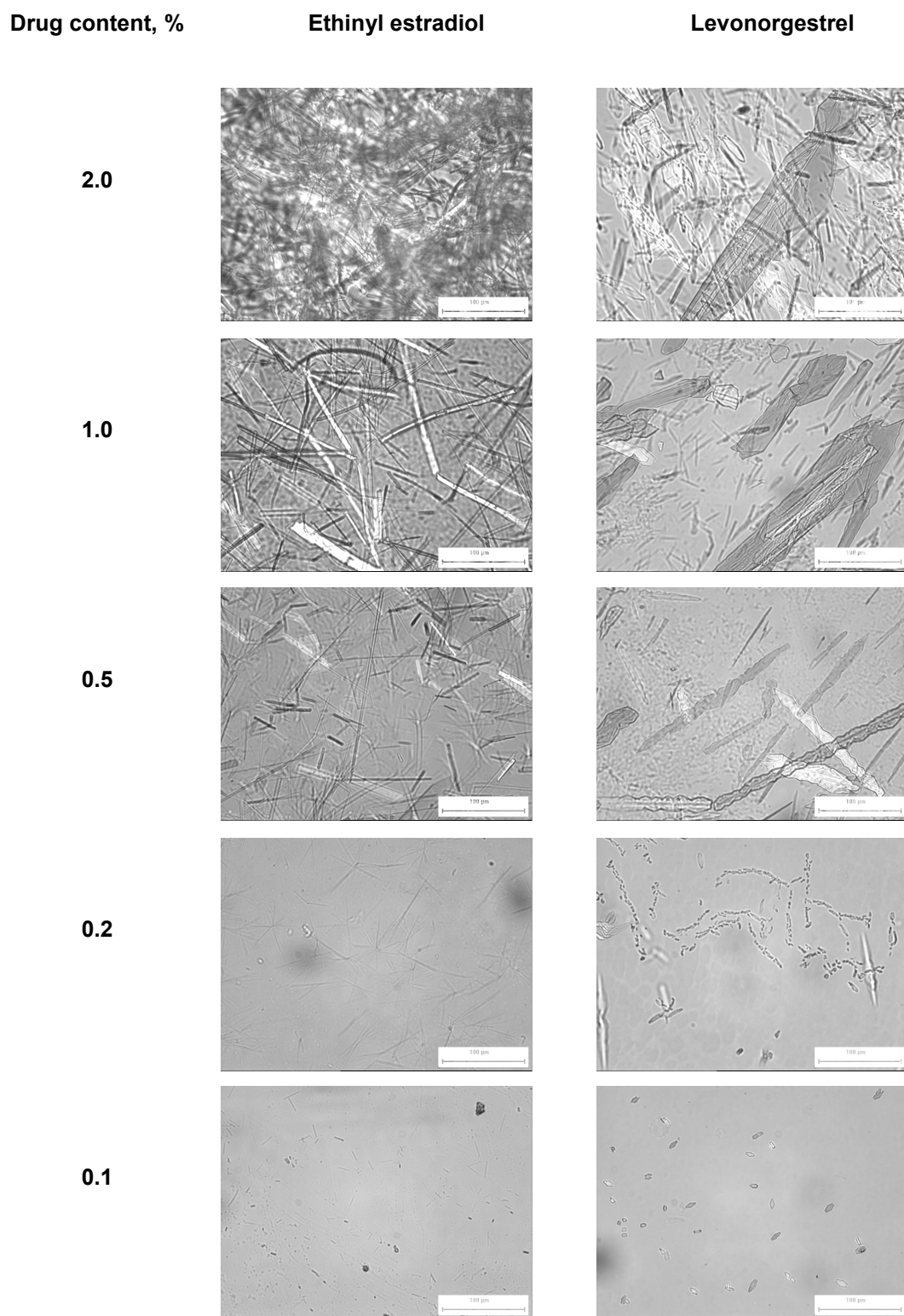


Fig. 35 Polarized light microscopic analysis of recrystallized drug in PIB matrices with varying amounts of ethinyl estradiol and levonorgestrel

3.2.3 Preparation of polyisobutene patches

Several ways to prepare PIB patches containing ethinyl estradiol and levonorgestrel adsorbates onto CPVP were investigated with regard to their influence on the physical state of the drug (Table 10). PIB solutions were prepared in either hexane or chloroform. In formulations 1 and 4, drug solution and CPVP were simply added to the PIB solution and mixed. In formulation 2 and 3, the ethinyl estradiol and levonorgestrel adsorbate onto CPVP was first prepared and then added to the PIB solution.

Table 10 Effect of the preparation method on the physical state of the drug in MM-PIB patches containing ethinyl estradiol (0.2%) and levonorgestrel (1.0%) adsorbates onto CPVP (20%)

Formulation	Solvent for PIB	Addition of	Recrystallization
1	Hexane	Drug solution in chloroform + CPVP	Yes
2	Hexane	Drug adsorbate onto CPVP	No
3	Chloroform	Drug adsorbate onto CPVP	No
4	Chloroform	Drug solution in chloroform + CPVP	No

The omission of the adsorption step resulted in drug recrystallization when hexane was used as solvent for PIB. Due to the very low solubility of both drugs therein (Table 9), they probably recrystallized before they were able to interact with CPVP's binding sites. Adding the adsorbate to PIB solution in hexane resulted in crystal free patches. In this case, the low solubility of both drugs in hexane was irrelevant, because ethinyl estradiol and levonorgestrel were already bound to CPVP. The patch preparation in chloroformic PIB solution yielded crystal free patches, even when drug solution and CPVP were added separately. The drugs were soluble in the chloroformic PIB solution and adsorbed onto CPVP during the mixing process. The kinetic of the adsorption process was fast; 5 min mixing time was sufficient to achieve crystal free patches (Fig. 36).

Ethinyl estradiol and levonorgestrel peaks of the adjusted method were baseline separated and showed optimal peak symmetry (Fig. 37).

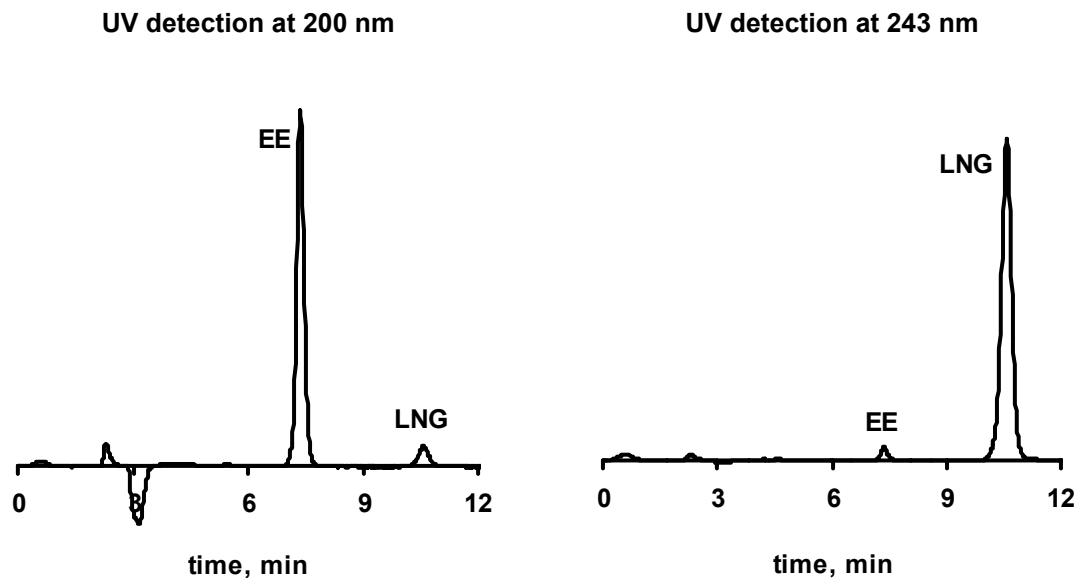


Fig. 37 Simultaneous reversed phase HPLC analysis of ethinyl estradiol (EE) and levonorgestrel (LNG) (mobile phase: water/methanol/acetonitrile 37/21/42, v/v)

3.2.4.2 Enhancement of the sensitivity for ethinyl estradiol

Ethinyl estradiol and levonorgestrel are commonly detected at their UV maxima at 280 and 243 nm, respectively (USP26 2003) (Fig. 38).

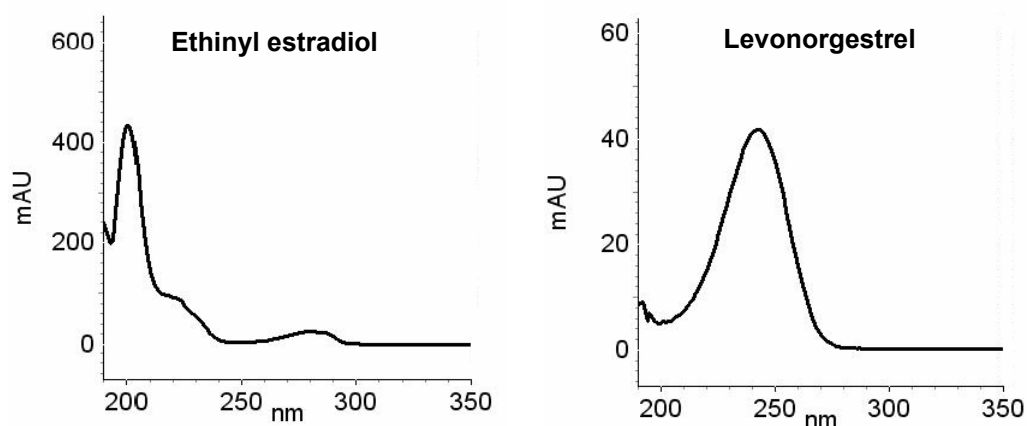


Fig. 38 UV spectra of ethinyl estradiol and levonorgestrel in water/methanol/acetonitrile (37/21/42, v/v)

To enable ethinyl estradiol's detection at low concentrations in the first 4 h of the drug release studies, as well as at higher concentrations in the later drug release phase, two HPLC methods were established: The first one for low drug concentrations detected the drug at 200 nm, where its UV absorption is maximal, and used 75 μ l injection volume. The second method for higher drug concentrations used 280 nm as detection wavelength and 25 ml injection volume. The linearity was > 0.9995 for both methods (Fig. 39).

The UV cut-off for water and acetonitrile is generally considered to be 190 nm and for methanol 205 nm (LoBrutto and Kazakevich 2007). In this case, methanol did not interfere with the analytic of ethinyl estradiol at 200 nm due to the relatively low methanol content in the mobile phase and the high UV absorption of ethinyl estradiol at this wavelength.

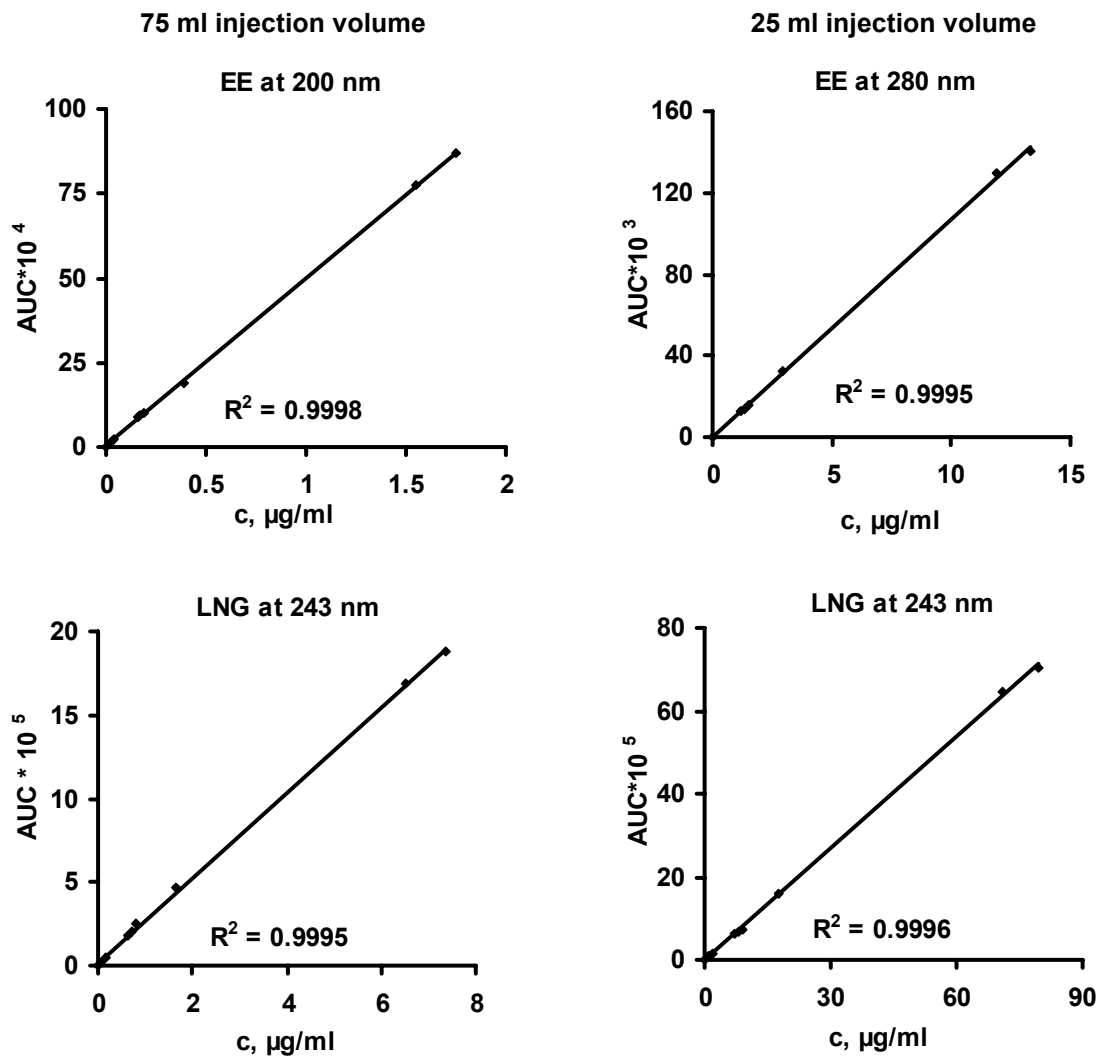


Fig. 39 Linearity of ethinyl estradiol (EE) and levonorgestrel (LNG) for different injection volumes and detection wavelengths

By this means, a limit of quantification for ethinyl estradiol of 0.02 $\mu\text{g/ml}$ could be reached while the linearity and the reproducibility remained virtually unchanged (Table 12).

In subsequent studies, ethinyl estradiol and levonorgestrel were generally detected at 280 and 243 nm, respectively, with 25 ml injection volume. Only ethinyl estradiol concentrations below 0.4 $\mu\text{g/ml}$ were detected at 200 nm with 75 ml injection volume.

Table 12 Influence of the injection volume and the detection wavelength on the sensitivity, linearity and reproducibility of the HPLC method

	Ethinyl estradiol		Levonorgestrel	
	280 nm, 25 μl	200 nm, 75 μl	243 nm, 25 μl	243 nm, 75 μl
LOQ ^A , $\mu\text{g/ml}$	0.4	0.02	0.06	0.02
Correlation coefficient	0.9995	0.9998	0.9995	0.9996
Variation coefficient	0.46-3.64	0.09-4.64	0.28-2.22	0.09-1.42

A: limit of quantification determined according to signal-to-noise approach

3.2.5 Development of the drug release study

European and United States Pharmacopoeia describe several assemblies for drug release studies of transdermal patches (Pharm.Eur.4 2003; USP26 2003). These assemblies have in common that the patch is attached to a sample holder and faces the drug release medium. Drug release studies conducted with PIB patches containing 20% drug adsorbate onto CPVP according to the USP “paddle-over-disk” method showed erosion of the patch (Fig. 40). This was a result of CPVP’s pronounced swelling and disintegrating properties. The average weight loss of these patches after 24 h was approximately 45%.

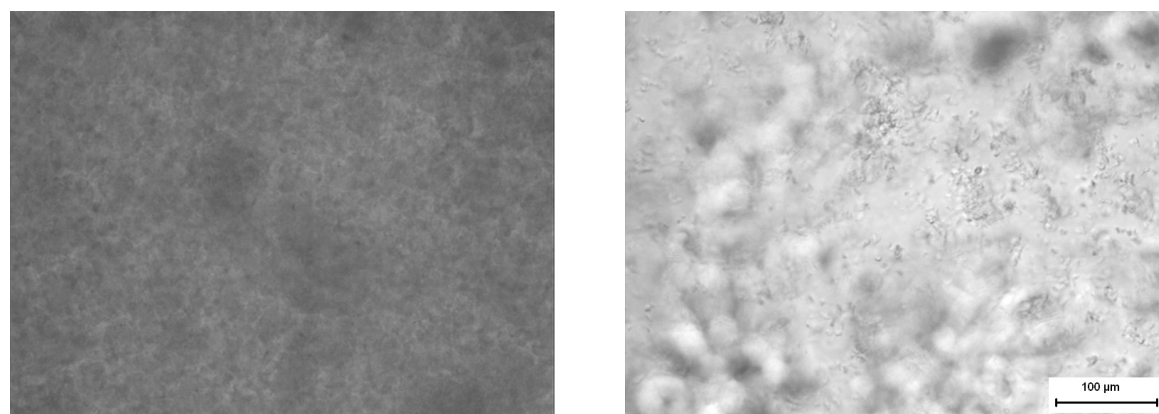


Fig. 40 PIB patch containing 20% CPVP before (left) and after 24 h (right) release testing according to the USP “paddle-over-disk” method (recorded with the same brightness)

To circumvent the problem of patch disintegration, the suitability of Franz diffusion cells was investigated. In this case, the drug release occurs across a membrane onto which the release side of the patch is attached. Hence, erosion of the patch is avoided and the study approximates physiological conditions better because only low water/moisture amounts are in contact with the patch during the drug release study. The goal was to establish a drug release method able to distinguish between patch formulations with different drug release kinetics. Therefore, three different microporous polyethylene membranes (Table 13) were tested with saturated ethinyl estradiol and levonorgestrel solutions in the donor compartment (Fig. 41).

Table 13 Properties of Solupor[®] membranes according to the manufacturer

	Solupor [®] 7P03A	Solupor [®] 9H01A	Solupor [®] 10P05A
Material	Polyethylene	Polyethylene	Polyethylene
Lipophilic / Hydrophilic	Lipophilic	Hydrophilic	Lipophilic
Porosity, %	85	74	83
Thickness, μm	50	35	60
Maximum Pore size, μm	0.5	0.1	0.8

The comparison of the two lipophilic membranes showed faster drug release across Solupor[®] 10P05A than across Solupor[®] 7P03A. Both membranes have a similar porosity, but Solupor[®] 10P05A possesses bigger pores, which are probably easier wetted and penetrated by the aqueous release medium.

The drug release across the hydrophilic Solupor[®] 9H01A yielded the best reproducibility. Its hydrophilic properties facilitated the wetting by the medium and prevented the adsorption of the lipophilic hormones (if observed, please mention above). Furthermore, the small maximum pore size ensured that the fine fraction of CPVP in the patches would be retained on the membrane. Thus, further drug release studies were conducted with Solupor[®] 9H01A as membrane.

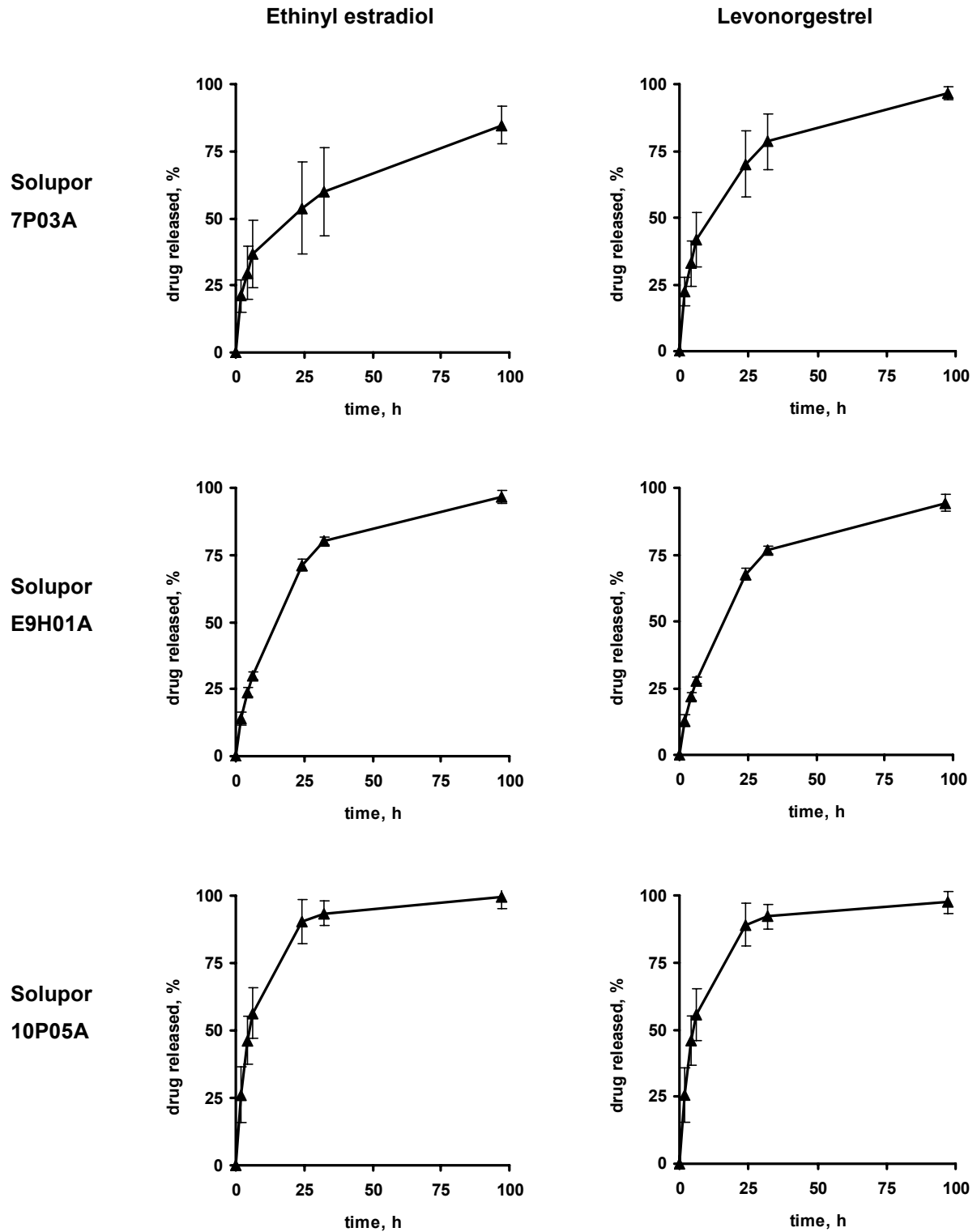


Fig. 41 Drug release from saturated ethinyl estradiol and levonorgestrel solutions in 2% SDS across different membranes: A) Solupor 7P03A, B) Solupor E9H01A, C) Solupor 10P05A

3.3 ADSORBATES IN TRANSDERMAL PATCHES

Drug recrystallization in transdermal patches is detrimental for the drug release and should be prevented. Especially very lipophilic matrices, like PIB, show compatibility issues with some commonly used crystallization inhibitors, such as PVP (Schurad et al. 2005). The incorporation of adsorbates onto insoluble carriers into transdermal patches could be an alternative.

3.3.1 Suitability screening of insoluble carriers

3.3.1.1 Influence of the carrier on the drug physical state

In the first step, adsorbates of ethinyl estradiol and levonorgestrel (drug content: 1.0 and 5.0%, w/w, respectively) onto titanium dioxide, Aerosil, MCC and CPVP were prepared and the carrier's ability to inhibit drug recrystallization was investigated. Polarized light microscopy revealed the presence of drug crystals in the adsorbate onto titanium dioxide and the absence of drug crystals in the adsorbates onto CPVP and Aerosil. It was not possible to determine the presence or the absence of drug crystals in adsorbates onto MCC with this method because the carrier itself is crystalline (Fig. 42).

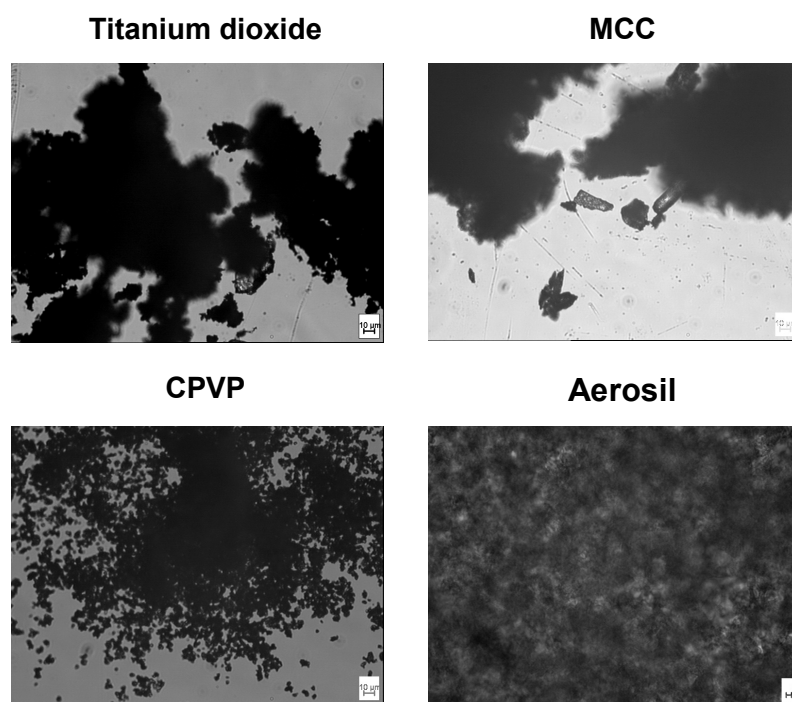


Fig. 42 Polarized light microscopic investigation of adsorbates containing 1.0% levonorgestrel (LNG) and 0.2% ethinyl estradiol (EE) content onto titanium dioxide, MCC, CPVP and Aerosil

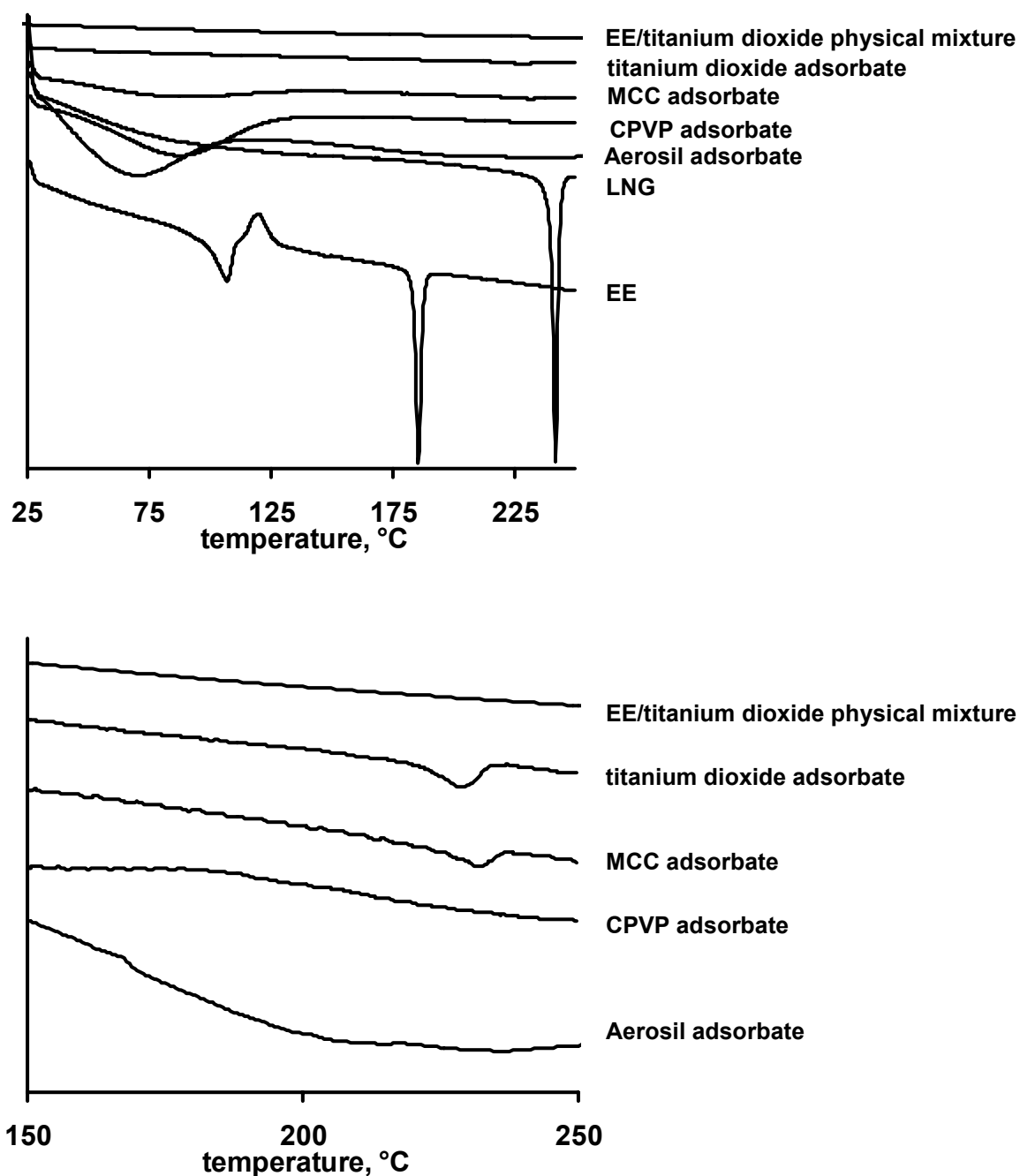


Fig. 43 DSC thermograms of ethinyl estradiol (EE) and levonorgestrel (LNG) recrystallized from chloroform, adsorbates with 1.0% EE and 5.0% (w/w) LNG onto Aerosil, CPVP, MCC and titanium dioxide and a physical mixture of titanium dioxide and EE (1.0%)

DSC scans of pure ethinyl estradiol (recrystallized from chloroform) showed a melting transition at 108.0 °C, which was probably related to a hydrate form of the drug (Ishida et al. 1989) (Fig. 43). The hydrate form recrystallized immediately afterwards and melted at 184.9

°C. Pure levonorgestrel (recrystallized from chloroform) showed only one melting transition at 241.2 °C.

DSC scans of a physical mixture containing ethinyl estradiol and titanium dioxide (drug content: 1.0%, w/w) were not able to detect ethinyl estradiol's melting peak. Hence this method was not sensitive enough to draw conclusions with regard to ethinyl estradiol's physical state in the adsorbates. Drug adsorbates onto MCC and titanium dioxide showed levonorgestrel's melting transition at 231.3 and 228.2 °C, respectively. The melting peak depression in comparison to the pure levonorgestrel has been described in the literature for adsorbates. It was attributed to drug-carrier interactions and the minuscular form of the drug crystals, which facilitates their melting (Monkhouse and Lach 1972b; Friedrich et al. 2006). Adsorbates onto CPVP and Aerosil did not show thermal events related to the melting of levonorgestrel. By correlating the adsorbates' enthalpy of fusion to the pure drug's enthalpy of fusion, levonorgestrel's crystallinity in adsorbates with titanium dioxide and MCC was calculated to be 45.9 and 28.2%, respectively (Table 14).

Table 14 DSC data of adsorbates containing 1.0% ethinyl estradiol and 5.0% levonorgestrel onto different adsorbents

Adsorbent	Ethinyl estradiol			Levonorgestrel		
	Melting point, °C	Enthalpy of fusion, J/g	Crystallinity, %	Melting point, °C	Enthalpy of fusion, J/g	Crystallinity, %
Pure drug	184.9	81.1	100.0	241.2	128.6	100.0
Titanium dioxide	b.d.l.	b.d.l.	n.d.	228.2	2.9	45.9
MCC	b.d.l.	b.d.l.	n.d.	231.3	1.8	28.2
CPVP	b.d.l.	b.d.l.	n.d.	-	0	0
Aerosil	b.d.l.	b.d.l.	n.d.	-	0	0

b.d.l.: below detection limit; **n.d.:** not determined

Hence the ability of the adsorbents to inhibit the recrystallization of levonorgestrel increased in the order of titanium dioxide < MCC < CPVP = Aerosil. No conclusion could be drawn for the physical state of ethinyl estradiol due to its low loading. It is likely that the formation of hydrogen bonds between the carriers and the drugs was responsible for the crystallization inhibition. Both drugs contain moieties able to act as hydrogen acceptors (carbonyl and hydroxyl groups) or hydrogen donors (hydroxyl groups). The ability of CPVP to act as hydrogen acceptor has already been described in section 3.1. MCC's 1,4 β -acetal and the

hydroxyl groups enable its contribution in hydrogen bonds. Oguchi et al. (1995) investigated the crystallinity of benzoic acid after grinding with MCC and found reduced crystallinity, which they attributed to the formation of hydrogen bonds. The ability of titanium dioxide to act as hydrogen acceptor has been described by Diebold (2003). Aerosil's silanol groups are capable of forming hydrogen bonds with drugs, which has been investigated by Monkhouse and Lach (1972a) and Watanabe (2001). Interactions between drug and carrier are thought to play a major role for drug recrystallization inhibition because they immobilize the drug molecules (Taylor and Zografi 1997).

The second step was the incorporation of the adsorbates into the adhesive matrix to form transdermal patches. As a comparison, transdermal patches with similar drug loading were prepared without adsorbents. The crystal free casting solution for these patches was prepared by adding chloroformic drug solution to the chloroformic PIB solution.

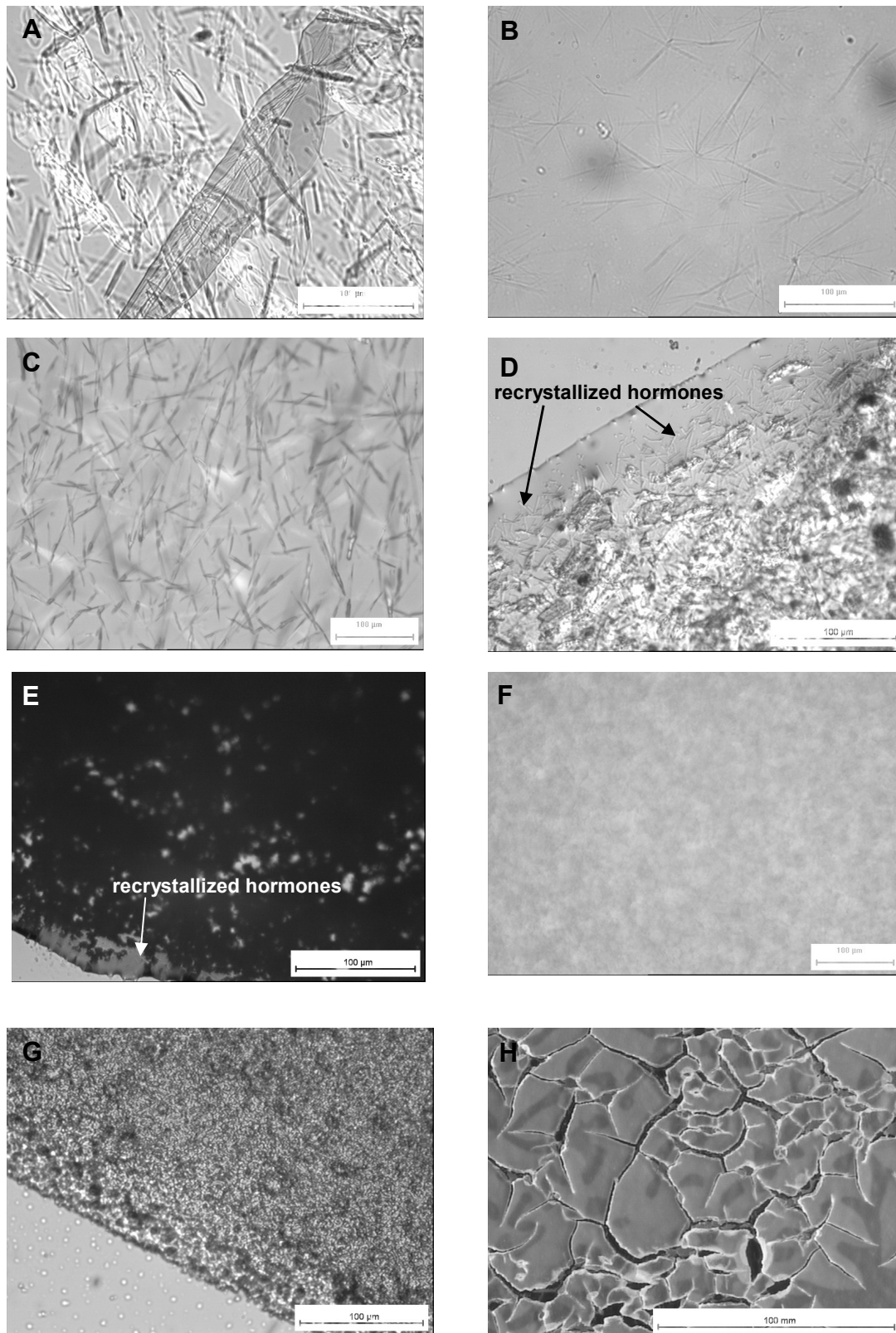


Fig. 44 Polarized light microscopic investigation of MM-PIB matrices containing 1.0% levonorgestrel (A), 0.2% ethinyl estradiol (B), 0.2% ethinyl estradiol and 1.0% levonorgestrel (C) and adsorbates with 0.2% ethinyl estradiol and 1.0% levonorgestrel onto 20% MCC (D), 20% titanium dioxide (E), 20% CPVP (F), 20% Aerosil (G) 20% Aerosil (macroscopic picture (H))

It was not possible to detect drug crystals in patches by DSC or XRD because the total drug concentrations (0.2 and 1.0% for ethinyl estradiol and levonorgestrel, respectively) were below the detection limit. Hence the patches were investigated by polarized light microscopy. Patches without adsorbents containing 0.2% ethinyl estradiol and 1.0% levonorgestrel showed drug crystals. To identify whether these crystals were ethinyl estradiol or levonorgestrel, patches with solely 0.2% ethinyl estradiol and patches with solely 1.0% levonorgestrel were prepared. Since these patches also showed crystals (Fig. 44A-C) it was concluded that neither of the hormones was completely soluble in the adhesive matrix at the investigated concentrations. Patches containing drug adsorbates onto titanium dioxide and drug adsorbates onto MCC showed recrystallized hormones in the matrix, although to a lower extent than the patches with the pure drug (Fig. 44D-E). The drug crystals' characteristic needle-like shape upon recrystallization in the adhesive matrix enabled their distinction from MCC crystals. Latsch et al. (2004) showed that the crystallization process of the norethindrone acetate in a matrix patch was considerably accelerated when a second steroid (estradiol hemihydrate) was present. Therefore, it can be speculated that both hormones *recrystallized to a certain extent in the matrices containing drug-titanium dioxide and drug-MCC adsorbates. MM-PIB films prepared with adsorbates onto CPVP and Aerosil did not show drug crystals (Fig. 44F-G). It was not possible to prepare coherent patches with the Aerosil adsorbate, because its addition to the PIB solution caused the formation of a thixotropic gel. This mixture had to be diluted with chloroform to become castable. This diluted solution, however, yielded an incoherent film without adhesive properties (Fig. 44H). Therefore, patches based on Aerosil adsorbates were not further investigated.

3.3.1.2 *Influence of the carrier on the drug release*

The release of both ethinyl estradiol and levonorgestrel from patches containing adsorbates was higher than from patches without adsorbent and increased in the order of titanium dioxide < MCC < CPVP (Fig. 45).

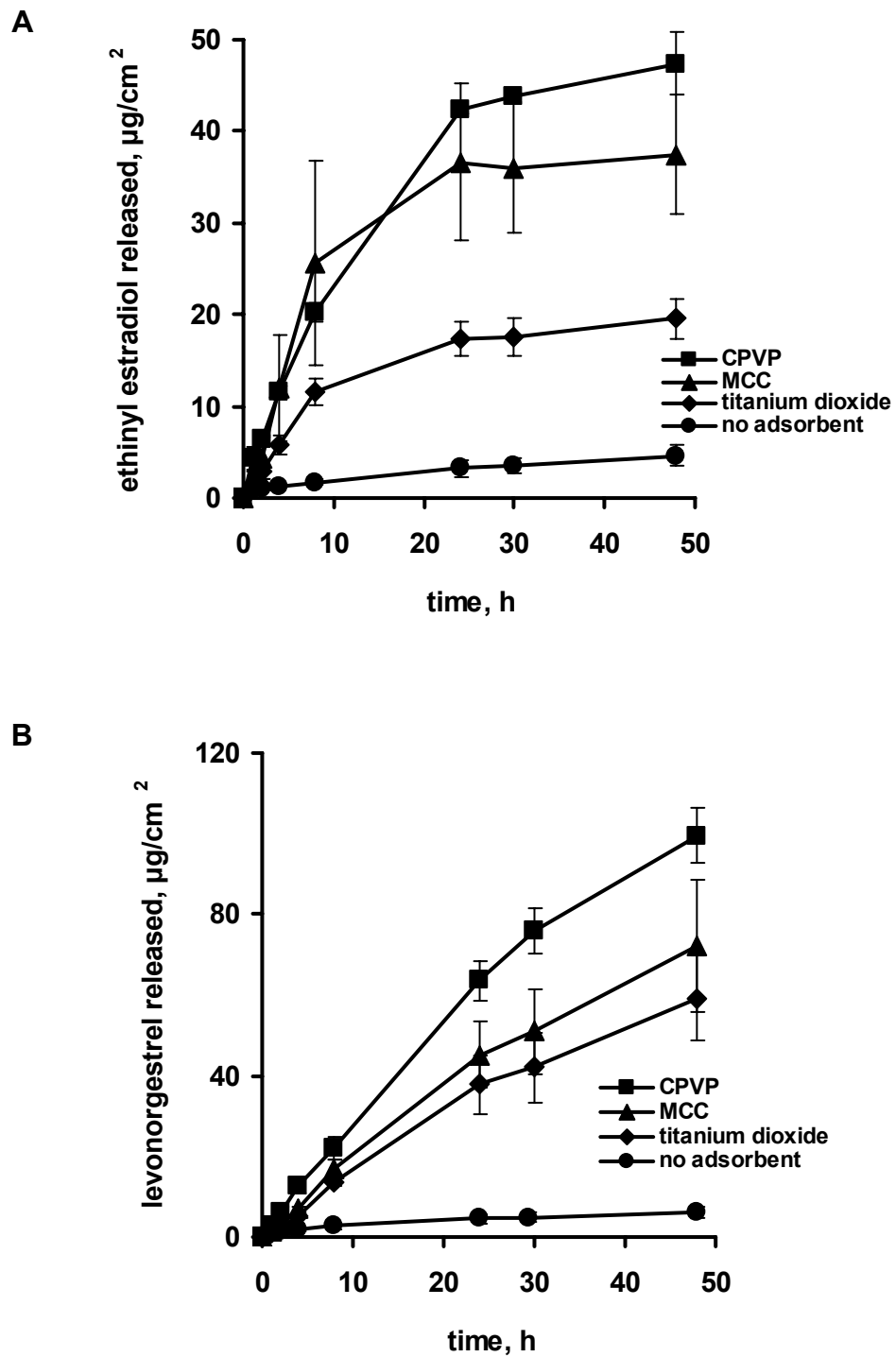


Fig. 45 Effect of adsorbent type on the ethinyl estradiol (A) and levonorgestrel (B) release from MM-PIB patches containing ethinyl estradiol (0.2%) and levonorgestrel (1.0%) or the same amount of drugs adsorbed onto CPVP, MCC or titanium dioxide (20%)

Since the water uptake of a matrix can influence the drug release it was determined for the adsorbents and the manufactured patches. The adsorbent's water uptake as a bulk property was determined by centrifuging aqueous adsorbent suspensions and weighing the centrifuge residue thereafter. The use of mild centrifugation conditions (3 min, 5000 rpm) resulted in increasing water uptake in the order of titanium dioxide < MCC = CPVP (Fig. 46). Rigorous centrifugation conditions (15 min, 13000 rpm) followed by the incubation of the centrifugation vessels for 12 h before the decantation showed a significantly higher water uptake of CPVP than of MCC. The difference was probably a result of CPVP's higher swelling pressure compared to MCC which led to a greater expansion of the particles during the incubation period. Conventional methods to determine the water uptake of dosage forms are not suited for transdermal patches due to their stickiness. Therefore, a dynamic vapor sorption (DVS) method was developed, which determined the dried patches' weight gain at 90% RH as a surrogate parameter. While patches without adsorbates and patches with adsorbates onto titanium dioxide did not show a significant water uptake, patches with adsorbates onto MCC and CPVP took up approximately 1.6 and 4.8% water, respectively (Fig. 47). Thus, the difference in water uptake between the adsorbates became more pronounced when they were restricted by the adhesive matrix, which was likely due to their different swelling pressures.

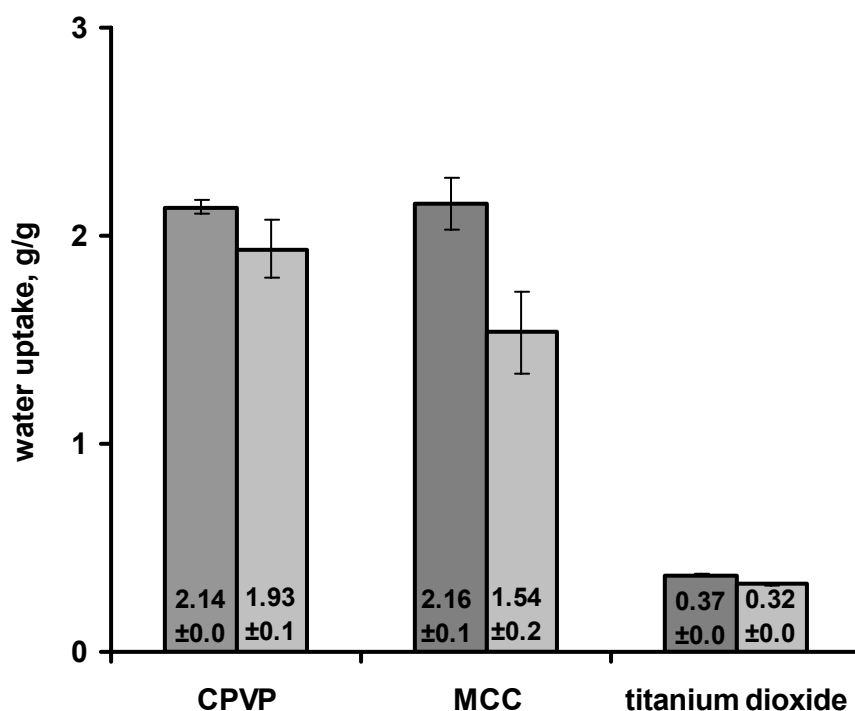


Fig. 46 Water uptake (g water/g adsorbent) of CPVP, MCC and titanium dioxide determined by centrifugation of an aqueous suspension (left column: 3 min at 5000 rpm; right column: 15 min at 13000 rpm and incubation for 12 h before the decantation)

The initial drug release (up to 8 h) from PIB patches without adsorbent was probably mainly governed by the dissolution of drug crystals close to the patch surface. Since PIB did not show a significant water uptake (Fig. 47), the drug crystals in the bulk of the patch were practically sealed off from the release medium. These drug crystals slowly dissolved in the adhesive matrix and the drug molecules had to diffuse through the adhesive matrix in order to be released (8 to 48 h). The drug release from patches containing titanium dioxide adsorbates was probably faster than the drug release from patches without adsorbents for two reasons: Firstly, the adsorbate particles disrupted the matrix. This may have facilitated the penetration of release medium into regions in the vicinity of the patch surface. Secondly, the patches showed less drug crystals compared to patches without adsorbates, indicating that the drugs existed partly in the molecularly dispersed state. This “reduction in drug particle size” is known to speed up the dissolution by increasing the available drug surface area. Patches with MCC adsorbates showed reduced drug crystallinity. Furthermore, the water uptake determined by DVS indicated that the release medium penetrated into the bulk of the patch. Accordingly, patches containing adsorbates onto MCC released the drugs faster than patches

with adsorbates onto titanium dioxide. The fastest drug release was achieved by incorporating adsorbates onto CPVP into the PIB matrices. CPVP is highly hygroscopic and has pronounced swelling properties, which resulted in the highest water uptake (Fig. 47). Moreover, patches containing CPVP adsorbates were crystal free. Due to the insolubility of the drugs in PIB, it is likely that the major amount of the drugs in the patches was bound to the CPVP particles. Besides diffusion through the matrix, the drugs were probably released through fluid filled channels that formed between the CPVP particles upon release medium uptake and swelling.

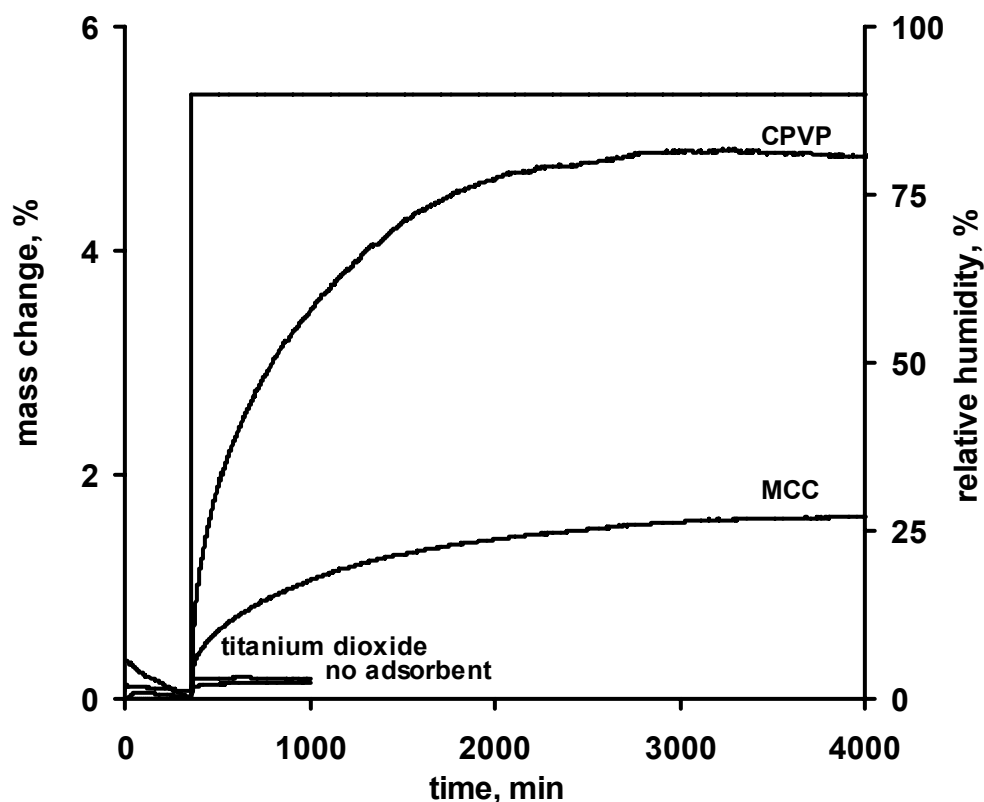


Fig. 47 Effect of adsorbent type on the water uptake at 90% RH of MM-PIB patches containing ethinyl estradiol (0.2%) and levonorgestrel (1.0%) or the same amount of drugs adsorbed onto CPVP, MCC or titanium dioxide (20%)

3.3.2 Patches containing adsorbates onto crosopvidone

Patches containing adsorbates onto CPVP showed the most pronounced increase in drug release and were crystal-free. Therefore they were investigated in more detail.

3.3.2.1 *Effect of drug and drug loading*

Patches with CPVP adsorbates containing different drug loadings of ethinyl estradiol and levonorgestrel at a constant CPVP content were investigated. No crystals could be detected in the patches by polarized light microscopy. The drug release increased with drug loading (Fig. 48) for both drugs. Levonorgestrel was released slower than ethinyl estradiol, probably as a result of levonorgestrel's lower solubility in the release medium (Table 9). In other words, the release medium that penetrated into the patch was closer to the saturation concentration of levonorgestrel than of ethinyl estradiol, which could have slowed down the dissolution of levonorgestrel.

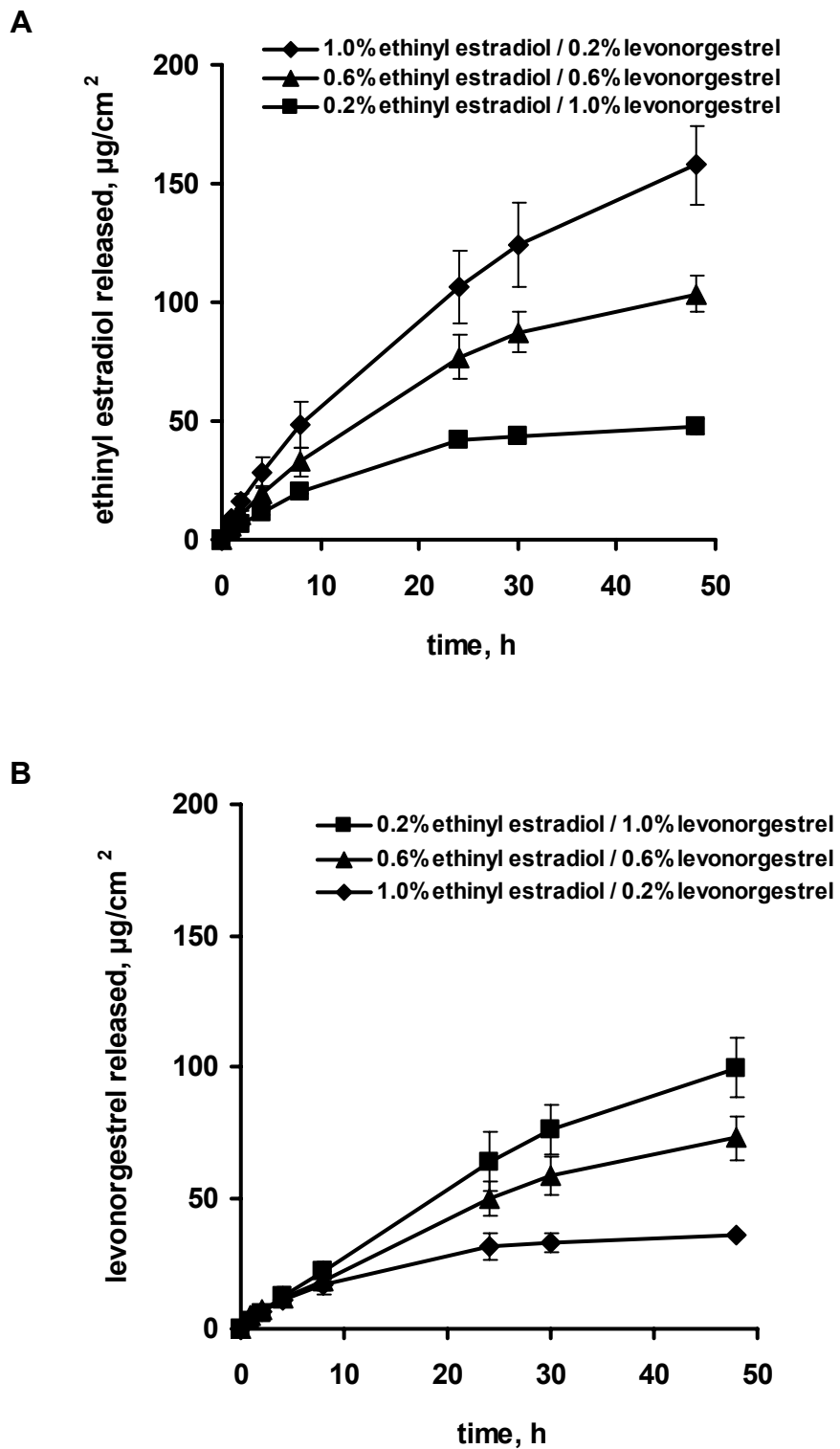


Fig. 48 Effect of ethinyl estradiol and levonorgestrel content on the ethinyl estradiol (A) and levonorgestrel (B) release from MM-PIB patches containing adsorbates of the drugs onto CPVP (20.0%)

3.3.2.2 *Effect of the crospovidone content*

Patches with 1.0% levonorgestrel and 0.2% ethinyl estradiol content were crystal-free at a CPVP content of 10% or higher (which corresponded to a drug loading of 12% onto CPVP). Drug crystals could be detected by polarized light microscopy in matrices with 5% CPVP content. This result was in agreement with earlier findings obtained from carbamazepine-CPVP systems in which a carbamazepine loading of 9.1% yielded crystal-free formulations (Table 7).

The drug release increased with increasing CPVP content (Fig. 49). This was probably due to two reasons: Firstly, the drugs were (partly) crystalline in formulations without CPVP or with 5% CPVP which slowed down their dissolution. Secondly, the incorporation of CPVP into the PIB matrix is likely to increase the diffusion coefficient of the drugs by forming fluid filled channels between the CPVP particles upon water uptake. According to the Stokes-Einstein equation, the diffusion coefficient is inversely proportional to the viscosity and hence higher in the release medium than in the adhesive matrix. While in formulations without CPVP, drug molecules had to travel through the viscous polymer matrix, they could travel through areas of release medium that surrounded the CPVP particles in patches containing adsorbates onto CPVP. Higher CPVP contents (up to 15% CPVP) resulted in a more connected CPVP network which increased the release. Formulations with 15% and 20% CPVP adsorbate released the drugs almost identically.

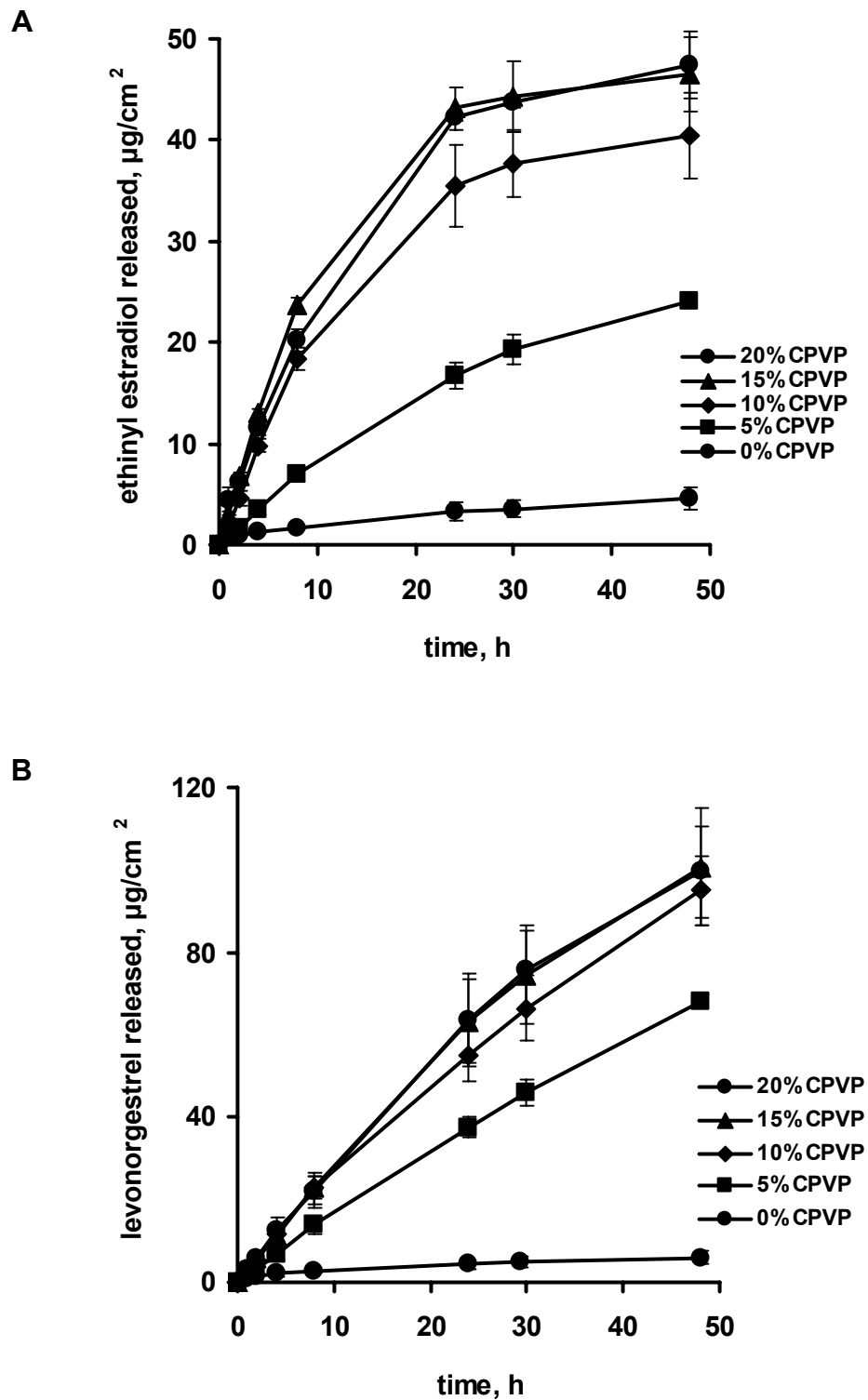


Fig. 49 Effect of CPVP content on the ethinyl estradiol (A) and levonorgestrel (B) release from MM-PIB patches containing ethinyl estradiol (0.2%) and levonorgestrel (1.0%)

3.3.2.3 *Effect of crospovidone particle size*

Smaller CPVP particles led to faster drug release in the beginning (0 to 24 h, Fig. 50) while the drug release from patches with bigger CPVP particles was slower in the beginning but did not level off later (24 to 48 h). This result was probably due to the particle distribution in the patch. Microscopic pictures of the patch cross-sections showed that smaller CPVP particles were distributed evenly throughout the patch. In contrast, larger CPVP particles occupied the area close to the release side of the patch to a lesser degree (Fig. 51). In the initial drug release phase patches containing smaller CPVP particles probably released rapidly because the adsorbates were present at the release surface. In contrast, the release medium needed more time to reach the adsorbate in patches containing larger CPVP particles, which was reflected by their slower water-uptake determined by DVS (Fig. 52). This slowed down the initial release from patches containing adsorbates onto larger CPVP particles. However, once the release medium reached the CPVP particles, they could release the drugs relatively fast because drug diffusion could occur through large areas of swollen CPVP in the patch without intermittent PIB matrix.

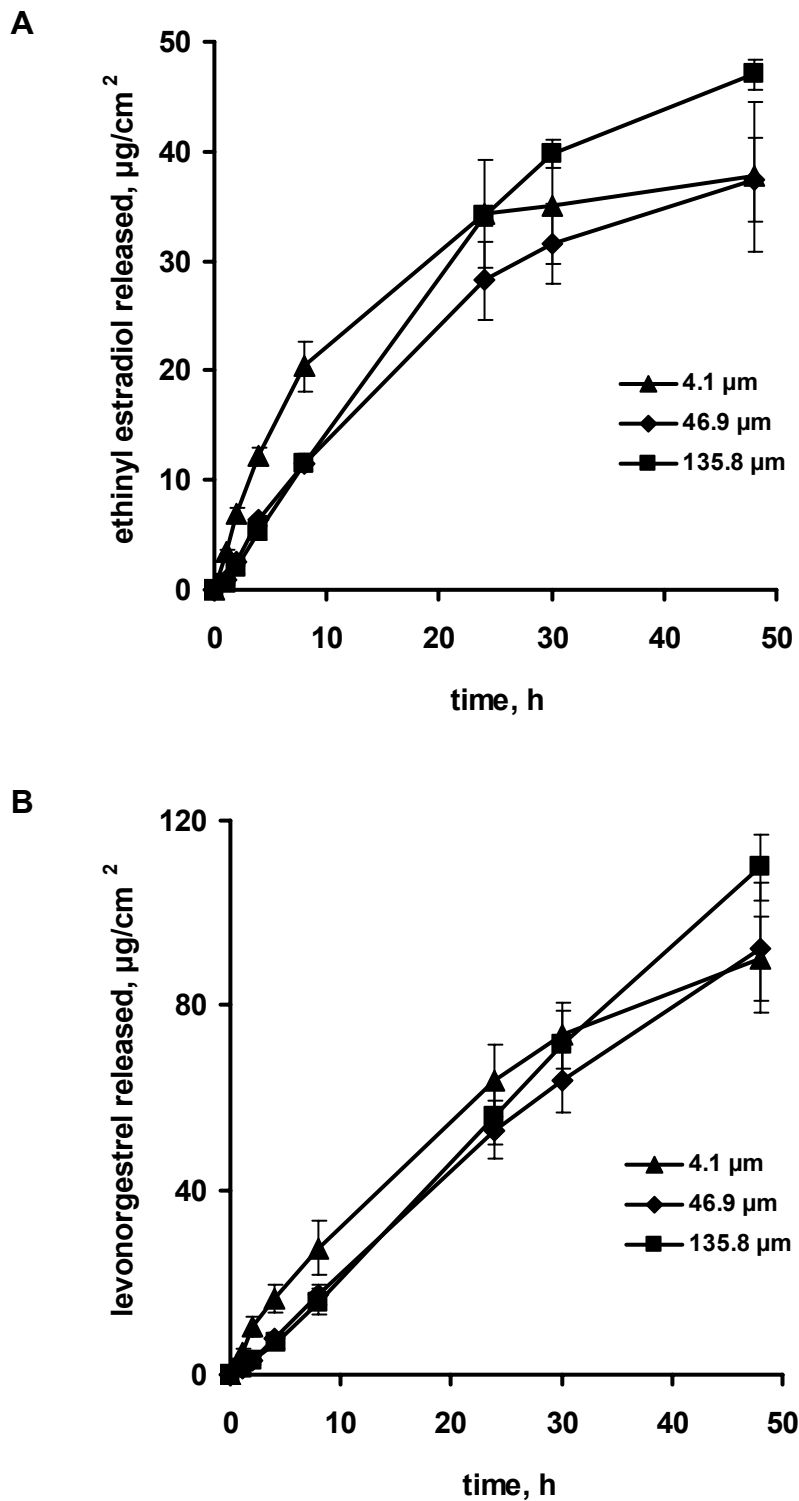


Fig. 50 Effect of CPVP particle size on the ethinyl estradiol (A) and levonorgestrel (B) release from MM-PIB patches containing ethinyl estradiol (0.2%) and levonorgestrel (1.0%) adsorbed onto CPVP (20%)

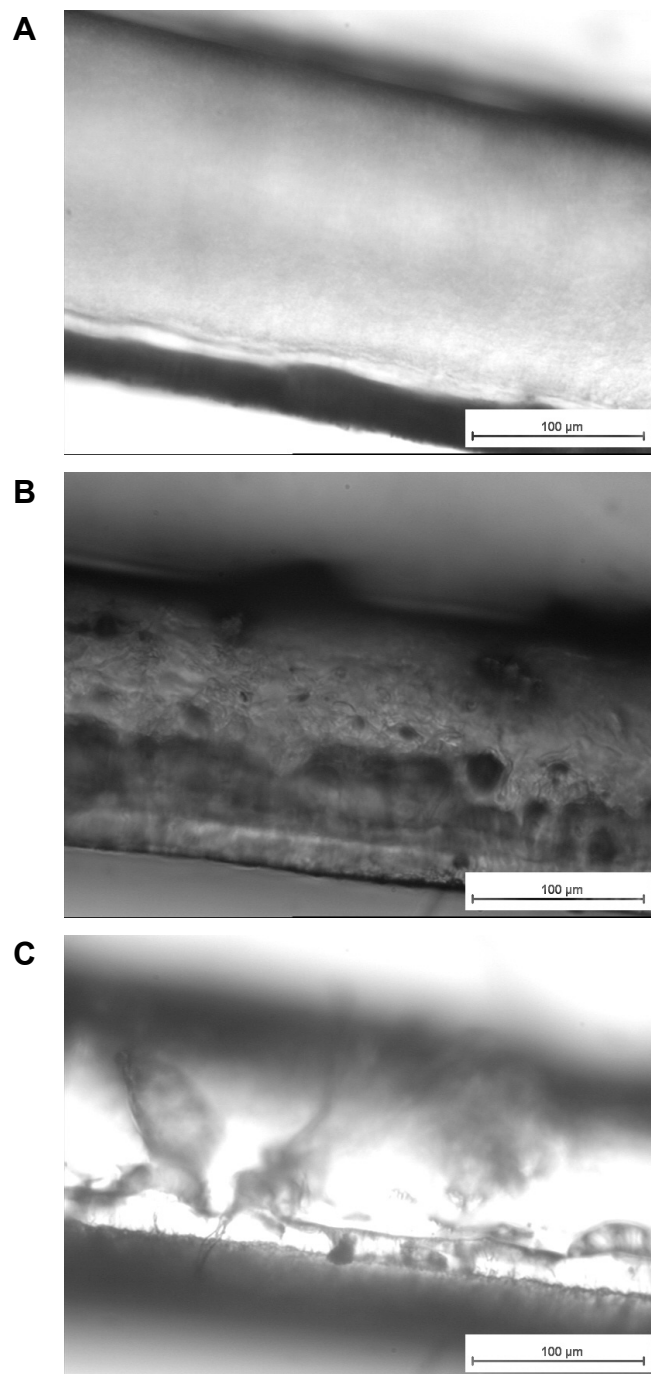


Fig. 51 Cross-sections of patches containing ethinyl estradiol (0.2%) and levonorgestrel (1.0%) adsorbed onto CPVP (20%) with $d_{50} = 4.1 \mu\text{m}$ (A), $46.9 \mu\text{m}$ (B) and $135.8 \mu\text{m}$ (C)

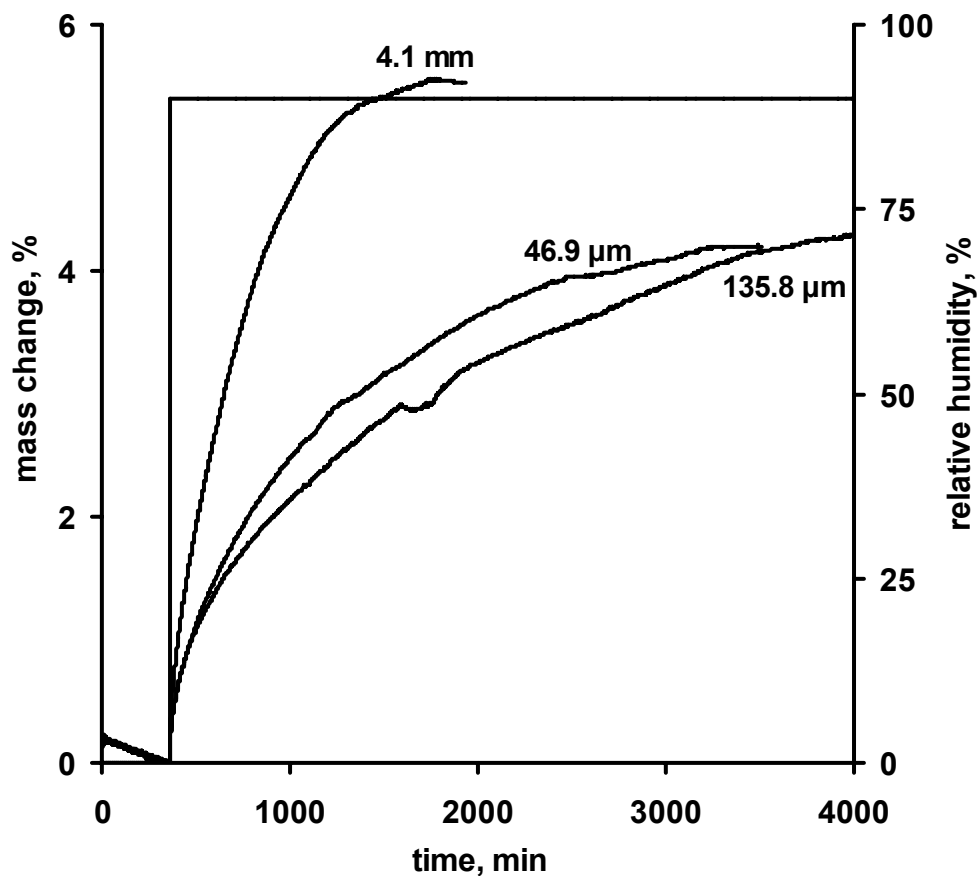


Fig. 52 Effect of the CPVP particle size on the water uptake at 90% RH of MM-PIB patches containing ethinyl estradiol (0.2%) and levonorgestrel (1.0%) adsorbed onto CPVP (20%)

3.3.3 Conclusions

The incorporation of adsorbates onto CPVP into PIB matrices yielded crystal free patches with significantly increased drug release. Besides the molecularly dispersed state of the drugs this was probably a result of the increased water uptake of the matrices governed by CPVP.

3.4 INFLUENCE OF THE ADHESIVE

The adhesive is an important structural element of transdermal patches. In monolithic drug-in-adhesive (DIA) patches, the drug can either dispersed or dissolved in the adhesive matrix. Thus the adhesive affects the drug release.

To investigate the influence of the adhesive base on the drug physical state and the drug release from transdermal systems containing adsorbates, patches based on PIB (with varying molecular weight distributions) and on acrylate adhesives were prepared. The PIB patches consisted of high:medium:low molecular weight PIB (HM:MM:LM PIB) = 1:5:0, 1:5:2 and 1:5:4 (Table 15).

Table 15 Properties of high, medium and low molecular weight PIB

Adhesive	Functionality	M _w , g/mol	Appearance
HM-PIB	Isobutene	1 110 000	Rubberlike solid
MM-PIB	Isobutene	55 000	Solid, but viscous flow at 25°C
LM-PIB	Isobutene	2 300	Semiliquid

Acrylate patches were prepared of the ready-to-use mixtures Durotak[®] 87-202A, Durotak[®] 87-2074, Durotak[®] 87-2677 (Table 16).

Table 16 Properties of acrylate adhesives

Adhesive	Functionality	Backbone polymer	Functional monomer, %
Durotak [®] 87-2677	Carboxyl	Polyacrylate-vinylacetate copolymer	3-5
Durotak [®] 87-2074	Hydroxyl / Carboxyl	Polyacrylate	10-15
Durotak [®] 87 -202A	Hydroxyl	Polyacrylate	30-35

3.4.1 Drug physical state

Drug crystals were detected by polarized light microscopy in all matrices based on PIB without CPVP (Fig. 53). The insolubility of the hormones in PIB appeared to be independent of its molecular weight composition. This was probably a result of PIB's hydrocarbon nature and its lack of functional groups. As seen earlier for MM-PIB, the incorporation of the ethinyl estradiol and levonorgestrel adsorbates onto CPVP into the PIB matrices prevented drug recrystallization (Fig. 44). All patches based on acrylate adhesives, independent of whether they contained the pure drugs or the adsorbates, were crystal-free. A stability study

was conducted with the initially crystal-free matrices. In all cases, they did not show drug recrystallization after 3 months at 25 °C/60 RH and 40 °C/75 RH (Table 17).

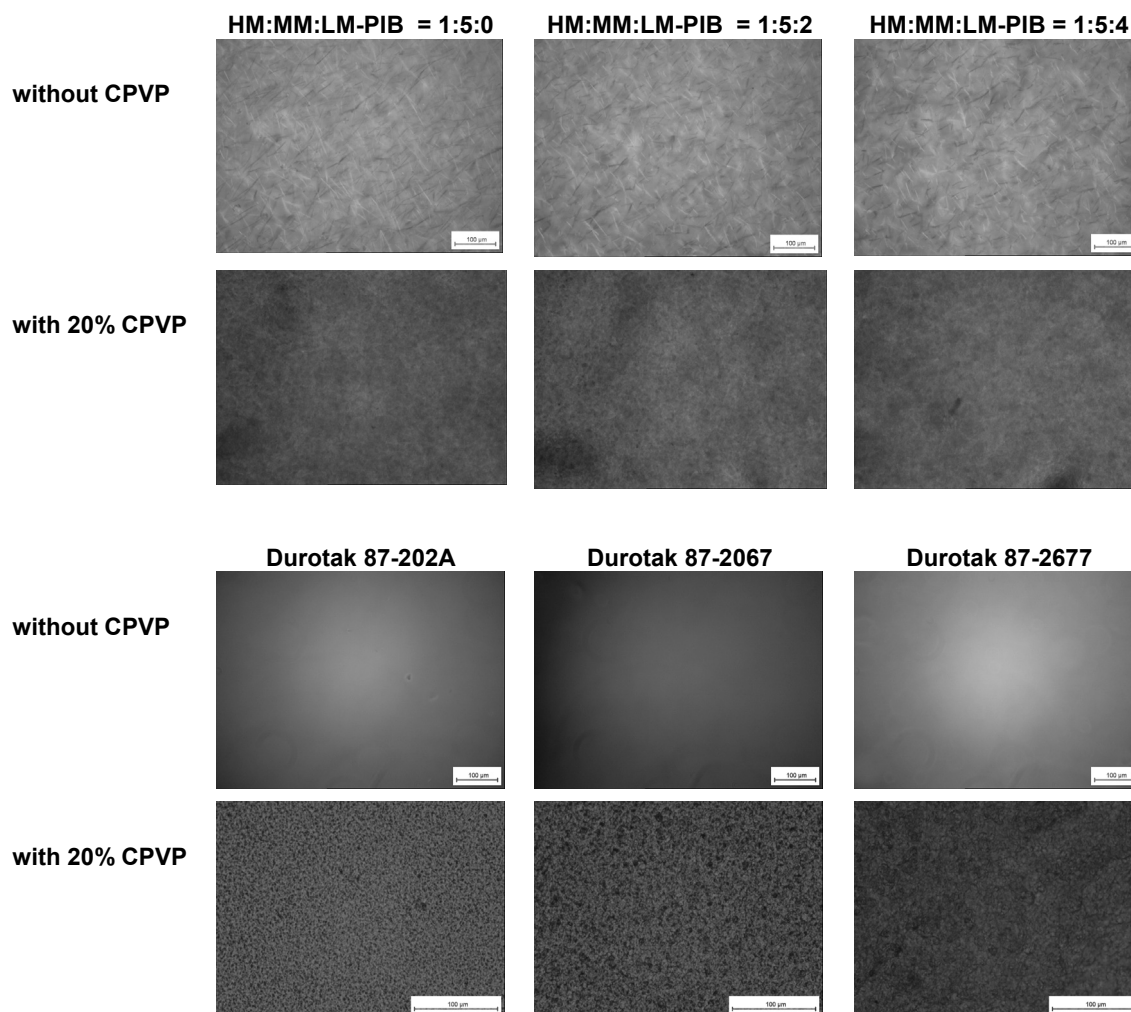


Fig. 53 Polarized light microscopic investigation of patches based on HM:MM:LM-PIB = 1:5:0, 1:5:2, 1:5:4, Durotak[®] 87-202A, Durotak[®] 87-2074 and Durotak[®] 87-2677 containing 0.2% ethinyl estradiol and 1.0% levonorgestrel or the same amount of drugs adsorbed onto CPVP (20%)

Table 17 Drug recrystallization in patches based on HM:MM:LM-PIB = 1:5:0, 1:5:2, 1:5:4, Durotak 87-2677, Durotak 87-2074, Durotak 87-202A containing ethinyl estradiol (0.2%) and levonorgestrel (1.0%) or the same amount of drugs adsorbed onto CPVP (20%)

Adhesive base	CPVP, %	Crystals detectable after				
		Start	1 month		3 months	
			25 °C / 60%	40 °C / 75%	25 °C / 60%	40 °C / 75%
HM:MM:LM-PIB = 1:5:0	0	X	n.d.	n.d.	n.d.	n.d.
HM:MM:LM-PIB = 1:5:2	0	X	n.d.	n.d.	n.d.	n.d.
HM:MM:LM-PIB = 1:5:4	0	X	n.d.	n.d.	n.d.	n.d.
HM:MM:LM-PIB = 1:5:0	20	0	0	0	0	0
HM:MM:LM-PIB = 1:5:2	20	0	0	0	0	0
HM:MM:LM-PIB = 1:5:4	20	0	0	0	0	0
Durotak 87-2677	0	0	0	0	0	0
Durotak 87-2074	0	0	0	0	0	0
Durotak 87-202A	0	0	0	0	0	0
Durotak 87-2677	20	0	0	0	0	0
Durotak 87-2074	20	0	0	0	0	0
Durotak 87-202A	20	0	0	0	0	0

X = recrystallization; 0 = no recrystallization; n.d. = not determined

3.4.2 Drug release from patches based on polyisobutene

The drug release from PIB patches was largely increased when drug adsorbates onto CPVP were incorporated into the matrix compared to pure drugs (Fig. 54). This was probably due to two reasons: Firstly, in patches with adsorbates, the drugs existed in the molecularly dispersed state. This increased the dissolution of the drugs by increasing their surface area. Furthermore, the molecularly dispersed state does not require energy to break up crystal structures before the drug can dissolve (Leuner and Dressman 2000). Secondly, the adsorbates increased the uptake of release medium by the PIB matrices. The water uptake of the patches was determined at 90% RH as a surrogate parameter. It was approximately 30-fold higher for PIB patches containing the adsorbates compared to PIB patches containing the drugs only (Fig. 55). This probably increased the diffusion coefficient of the drugs by forming fluid filled channels between the CPVP particles in the patch upon uptake of the release medium as described in section 3.2. The relatively slow drug release from PIB patches containing only drugs was probably mainly governed by the dissolution of drug crystals close to the patch surface. Since PIB matrices did not show a significant water uptake, the drug crystals in the bulk of the patch were sealed off from the release medium.

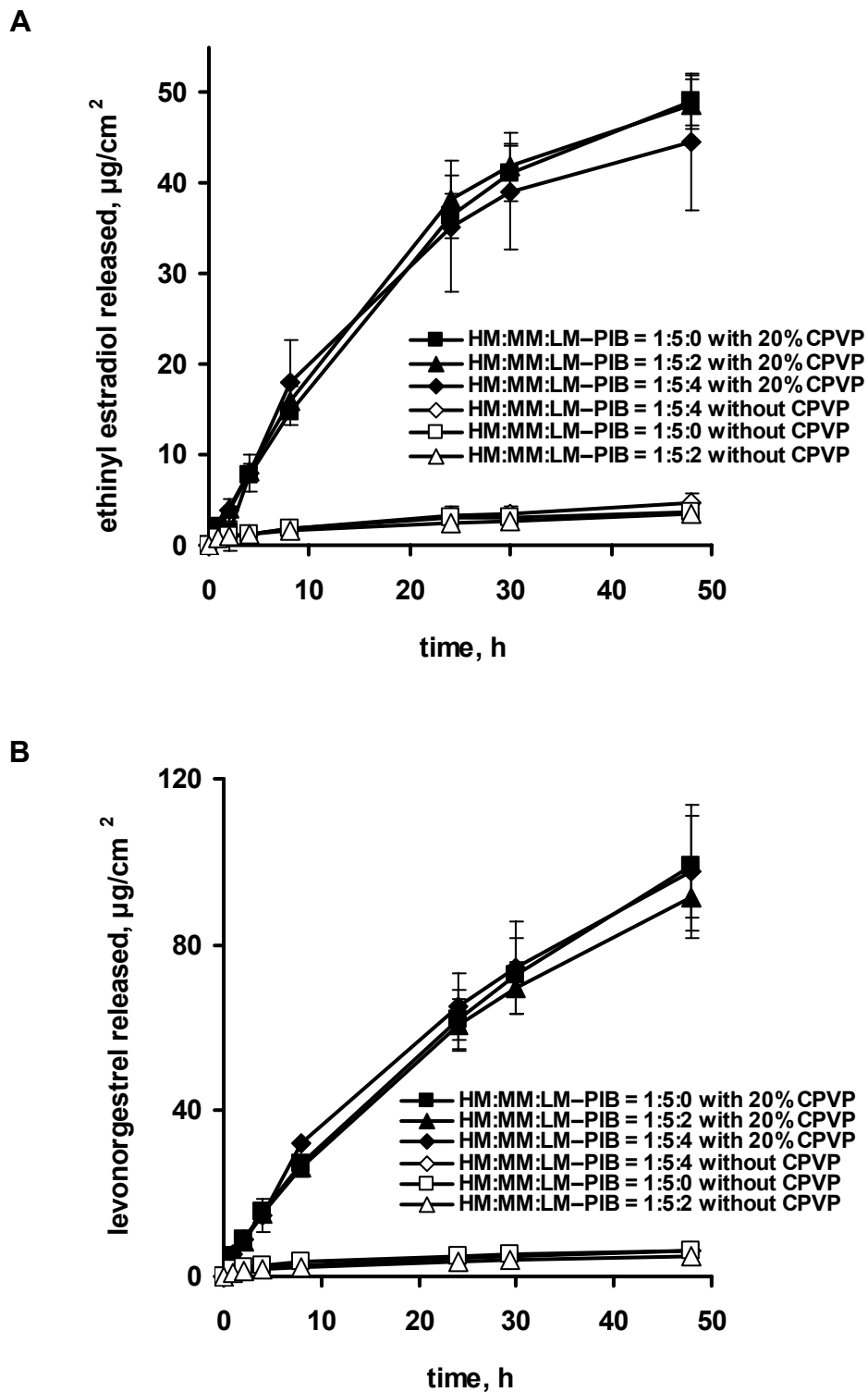


Fig. 54 Effect of the PIB molecular weight distribution on the ethinyl estradiol (A) and levonorgestrel (B) release from patches containing ethinyl estradiol (0.2%) and levonorgestrel (1.0%) or the same amount of drugs adsorbed onto CPVP (20%)

PIB adhesives with different molecular weight distributions have different viscosities (Table 15). According to the Stokes-Einstein equation, the diffusion coefficient of the drug is inversely proportional to the viscosity of the medium. Hence the drug release from patches based on PIB adhesives with different molecular weight distribution should differ if the drug release occurs mainly by diffusion through the polymer. However, the molecular weight distribution of the PIB matrices did not have a significant effect on the drug release from patches with adsorbates. This finding supports the hypothesis that the drug release occurred mainly through fluid filled channels between the CPVP particles. Correspondingly, the water uptake of PIB adhesives with different molecular weight distributions was similar. Since probably only a negligible amount of drug was actually released by diffusion through PIB, its molecular weight distribution was of minor importance. In patches containing only the drugs, the molecular weight distribution of PIB did not have an effect on the drug release either, probably because the drug release was mainly governed by the dissolution of recrystallized drugs on the patch surface.

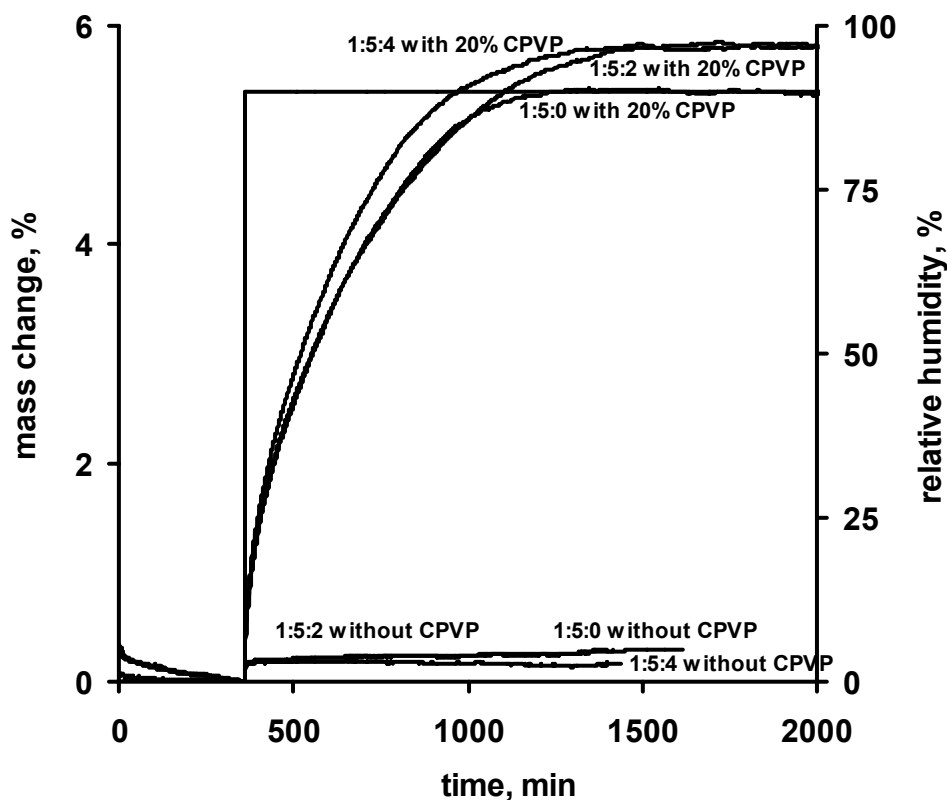


Fig. 55 Effect of PIB molecular weight distribution (HM:MM:LM) on the water uptake at 90% RH of patches containing ethinyl estradiol (0.2%) and levonorgestrel (1.0%) or the same amount of drugs adsorbed onto CPVP (20%)

3.4.3 Drug release from patches based on acrylates

The drug release from acrylate patches only increased for Durotak 87-2677 when adsorbates were incorporated into the matrix compared to the pure drugs (Fig. 56). The acrylate adhesives showed a significant water uptake (Fig. 57) as a result of their hydroxyl and carboxyl functionalities (Table 16). The additional water uptake in patches containing adsorbates did not enhance the drug release to a large degree. Moreover, since all acrylate patches were crystal-free, it was concluded that the drugs were dissolved in the adhesive matrix and hence the recrystallization inhibitory properties of CPVP, which sped up the drug release from PIB matrices, had no effect.

However, the drug release from different adhesive bases differed significantly and increased in the order of Durotak 87-2677 < Durotak 87-2074 < 87-202A. The exact chemical structure of the Durotak adhesives is not revealed by the manufacturer, but it is known that they

contain different functionalities. Consequently, a compound's solubility varies in different adhesives. The predicted solubilities for both drugs increased in the order of Durotak 87-202A < Durotak 87-2074 < Durotak 87-2677 (Table 18) and thus were inversely correlated with the drug release. In general, the degree of saturation of a formulation can either be increased by increasing the drug concentration or decreasing the drug solubility therein. Both approaches lead to enhanced thermodynamic activity of the drug. The driving force for the drug release is the gradient of the chemical potential between the formulation and the release medium (which is related to the degree of saturation) and not the concentration gradient (Barry 2001; Hadgraft 2001; Moser et al. 2001b).

The levonorgestrel loading in all matrices was 1.0% and hence higher than the predicted solubility for the drug in Durotak-2074 (0.7%) and Durotak 87-202A (0.2%). It is likely that the respective matrices were supersaturated. The inhibition of drug recrystallization is mainly due to intermolecular interactions between drug and excipient. By this means, the excipient immobilizes the drug molecules and "poisons" the crystallization (Doherty and York 1987; Taylor and Zografi 1997; Bhugra and Pikal 2008). Acrylate adhesives could have crystallization inhibitory properties due to their ester and carboxyl/hydroxyl groups (Table 16). These moieties can act as a hydrogen acceptors and donors and therefore offer potential binding site for ethinyl estradiol and levonorgestrel. Structurally similar polymethacrylates, namely Eudragit[®] E and Eudragit[®] RL, successfully prevented the recrystallization of ibuprofen (Cilurzo et al. 2005). The assumption of supersaturation in acrylate patches based on Durotak - 87 202A can explain the high levonorgestrel release in the first 24 h. Supersaturated systems are known to increase the drug flux across membranes due to their higher thermodynamic activity (Iervolino et al. 2000). Since supersaturated systems are metastable by definition, drug recrystallization will occur eventually. The slowing-down of the levonorgestrel release kinetic of Durotak 87-202A between 24 and 48 h could be a result of levonorgestrel recrystallization. Durotak - 87 202A showed the highest release medium uptake out of all investigated adhesives. This could have decreased the levonorgestrel solubility in the adhesive matrix and potentially have precipitated the drug. However, polarized light microscopic analysis of the patches conducted during the release study was not able to detect drug crystals.

Table 18 Estimated solubility of ethinyl estradiol and levonorgestrel in moisture free acrylate adhesives (based the correlation of the drugs' $P_{\text{octanol/water}}$ and $P_{\text{adhesive/water}}$)

Drug	Input parameters		Predicted drug solubility in Durotak 87 -x, %		
	Water solubility, $\mu\text{g/ml}$	log P	2677	2074	202A
Ethinyl estradiol	6.0 ¹	4.2 ²	14.3	6.1	1.7
Levonorgestrel	1.4 ¹	3.9 ³	1.6	0.7	0.2

¹: (Schulz et al. 2008); ²: (Liebig et al. 2005); ³: (Scifinder 2008)

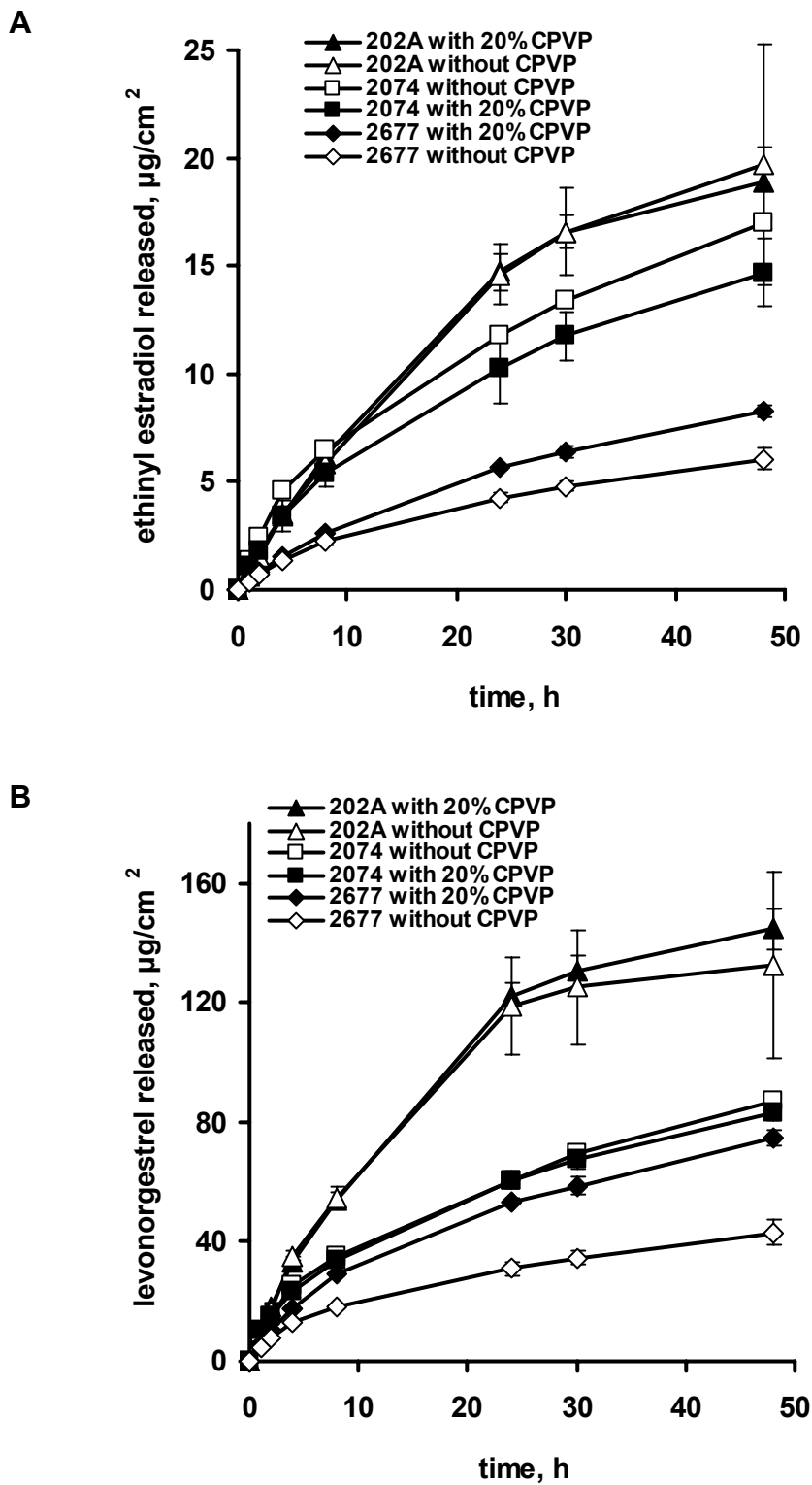


Fig. 56 Effect of acrylate adhesives (Durotak 87-x) on the ethinyl estradiol (A) and levonorgestrel (B) release from patches containing 0.2% ethinyl estradiol and 1.0% levonorgestrel or the same amount of drugs adsorbed onto CPVP (20%)

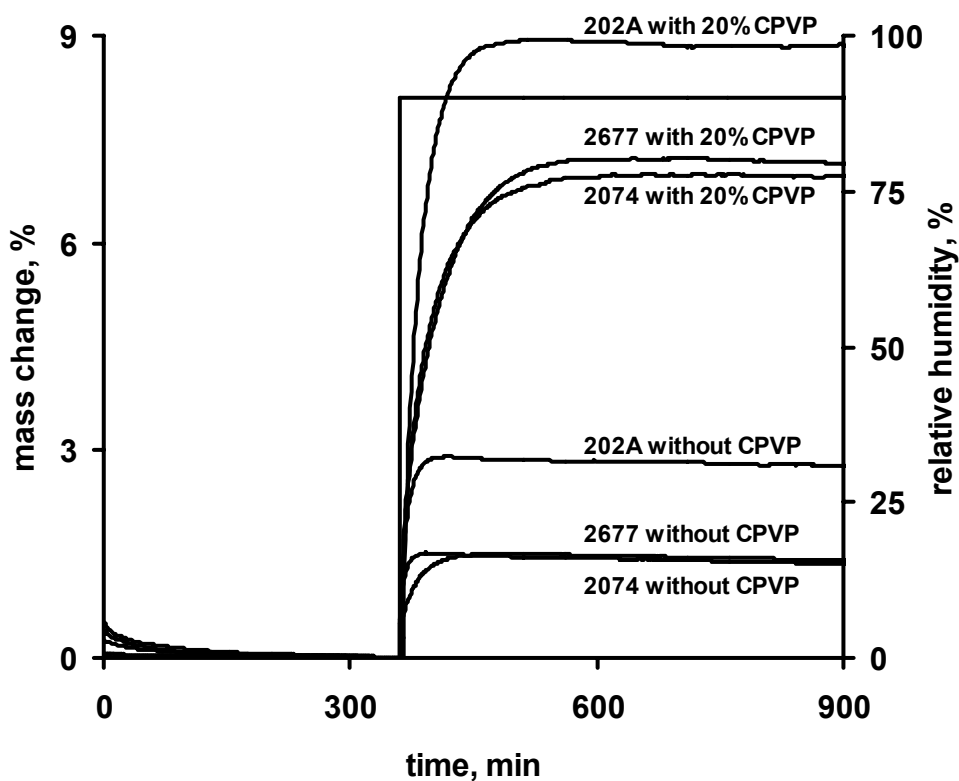


Fig. 57 Effect of acrylic adhesive base on the water uptake at 90% RH of patches containing ethinyl estradiol (0.2%) and levonorgestrel (1.0%) or the same amount of drugs adsorbed onto CPVP (20%)

3.4.4 Drug release from acrylic patches containing adsorbates onto titanium dioxide

Since the incorporation of drug adsorbates onto CPVP did not change the release kinetic from acrylic adhesives to a large degree, the effect of the incorporation of adsorbates onto titanium dioxide, which do not possess swelling properties, was investigated. It was suspected that the incorporation of these adsorbates might decrease the drug release because titanium dioxide does not increase the release medium uptake, but might limit the diffusion of the drug molecules. However, the drug release from these patches was also similar to the drug release from patches without adsorbents (Fig. 58).

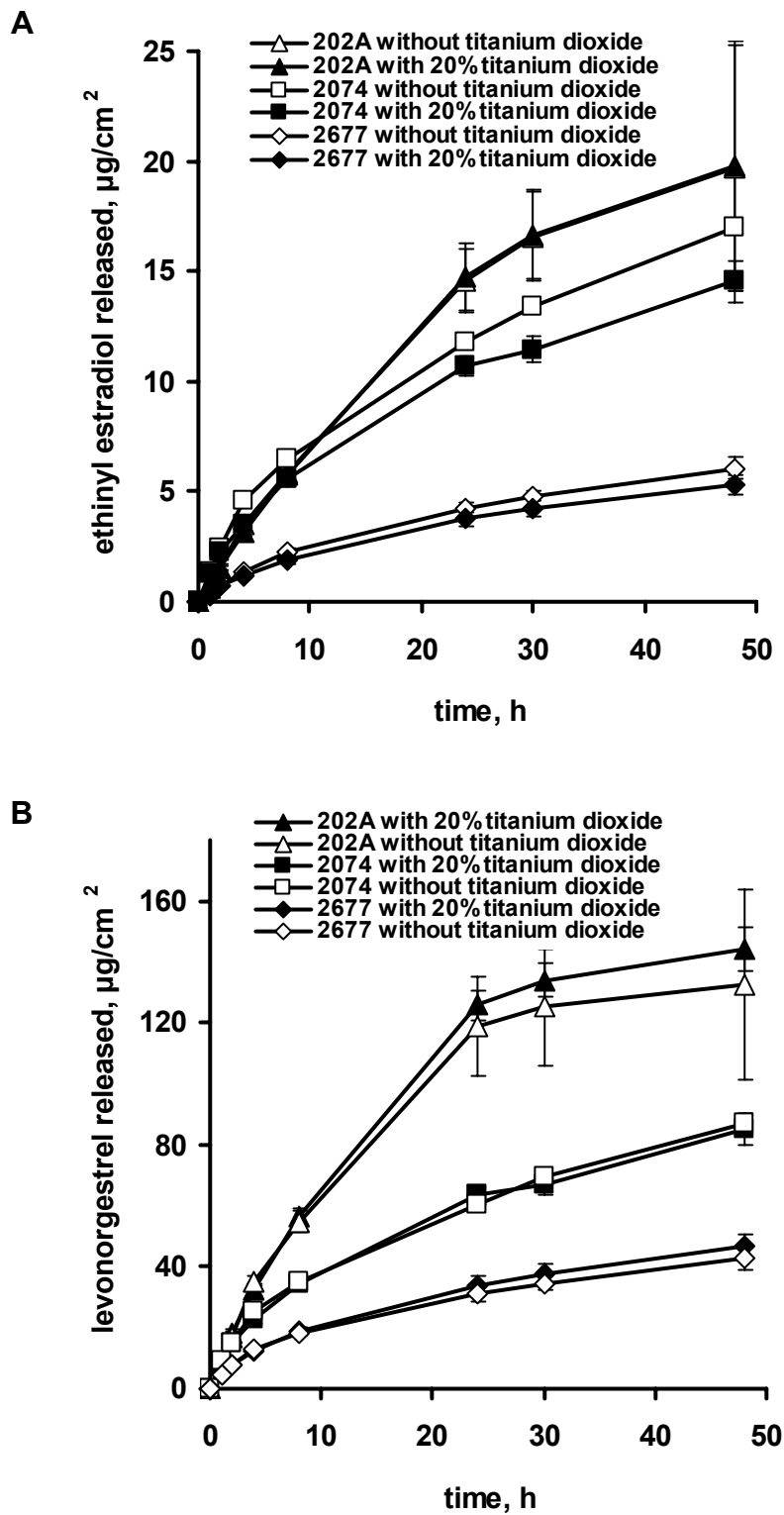


Fig. 58 Effect of acrylate adhesives (Durotak 87-x) on the ethinyl estradiol (A) and levonorgestrel (B) release from patches containing 0.2% ethinyl estradiol and 1.0% levonorgestrel or the same amount of drugs adsorbed onto titanium dioxide (20%)

3.4.5 Comparison of the drug release from polyisobutene and acrylate patches

The unequal enhancement of drug release from PIB and acrylate adhesives loaded with adsorbates compared to the pure drugs is probably a result of the different drug distribution in the matrices. In PIB matrices containing adsorbates, the drugs were probably still bound to the CPVP particles due to their low solubility in the adhesive. The release medium uptake was solely governed by the adsorbates and resulted in the desorption of the drug molecules from the carrier. As a consequence, the drug release from PIB matrices with adsorbates correlated with their water uptake determined by DVS. By contrast, ethinyl estradiol and levonorgestrel were soluble in the acrylate adhesives. Hence the drug molecules were probably distributed throughout the matrix. This diminished the influence of the release medium uptake governed by the CPVP particles on the drug release. Acrylate patches released the drugs primarily by diffusion through the adhesive polymer, which is reflected by the inverse correlation of the drug release with the drug solubility in the respective acrylate adhesive.

When the released drug amounts are corrected for the drug content of the formulations (0.2% ethinyl estradiol and 1.0% levonorgestrel, w/w) and compared, ethinyl estradiol is released faster than levonorgestrel from PIB matrices but slower than levonorgestrel from acrylate matrices. In PIB matrices, levonorgestrel was probably released slower than ethinyl estradiol as a result of its lower solubility in the release medium ($86.4 \cdot 10^{-3}$ mg/ml \pm 1.9 compared to $553.5 \cdot 10^{-3}$ mg/ml \pm 23.2). Hence the concentration of the release medium which penetrated into the patch was closer to the saturation solubility of levonorgestrel than of ethinyl estradiol, which could have slowed down the dissolution of levonorgestrel. The faster release of levonorgestrel compared to ethinyl estradiol from acrylates is probably a result of levonorgestrel's lower solubility in these matrices. This yields a higher degree of saturation for levonorgestrel compared to ethinyl estradiol.

3.4.6 Conclusions

Varying the molecular weight distribution of PIB did not significantly change the drug release kinetic of ethinyl estradiol and levonorgestrel from patches containing drug adsorbates onto CPVP. Probably the drug release was mainly governed by the release medium uptake of the adsorbates and the drug diffusion through the PIB matrix was of minor importance. This result suggests that the molecular weight distribution of PIB in such systems can be adjusted to tailor patches with optimal adhesive and cohesive properties.

The drug release from acrylate adhesives was independent of whether the patch contained pure drugs, adsorbates onto CPVP or adsorbates onto titanium dioxide. The degree of saturation (or supersaturation) in these systems was inversely correlated to the drug release. A higher degree of saturation (or supersaturation) resulted in a higher thermodynamic activity of the drugs and thus faster drug release. Hence the drug release from such systems can be adjusted by the selection of an appropriate adhesive base.

3.5 ADHESIVE PROPERTIES

The adhesive's main task is to establish a bond with the patient's skin and enable a residue-free removal of the patch after the intended wearing period. A reduction of the adhesion area leads to diminished drug delivery and hence improper dosing of the patient. Adhesion failure is one of the major post-approval problems that occur for transdermal drug delivery systems (Brown et al. 2006). The following chapter investigates the influence of the CPVP incorporation into different adhesive bases on their adhesive properties in vivo and in vitro.

3.5.1 Preparation of placebo patches

The in vitro and in vivo adhesion studies were only conducted with placebo patches. The placebo patches based on PIB were prepared with hexane for convenience because hexane dissolves PIB much faster than chloroform (chloroform was used for the preparation of PIB patches containing ethinyl estradiol and levonorgestrel since it dissolves both the drugs and PIB).

3.5.2 Development of probe tack method

The two main factors that influence probe tack measurements besides the adhesive's stickiness are the nature of the backing liner (due to deformation) and the film thickness (due to energy dissipation in the bulk) (Satas 1989b). The correlation between film thickness and probe tack is exponential and levels off at approximately 300 μm , depending on the viscoelastic properties of the adhesive (Tordjeman et al. 2000). To exclude these effects, films for the in vitro study were cast onto rigid polyester liner with a dry film thickness of approximately 400 μm . During the measurement, the specimens were placed between two stainless steel plates (the top plate had an orifice for the probe) to restrict them from moving (Fig. 59). The evaluated parameters of the force-distance diagrams were maximal force, elongation at detachment and the area under the force-distance curve (AUC) (Fig. 60).

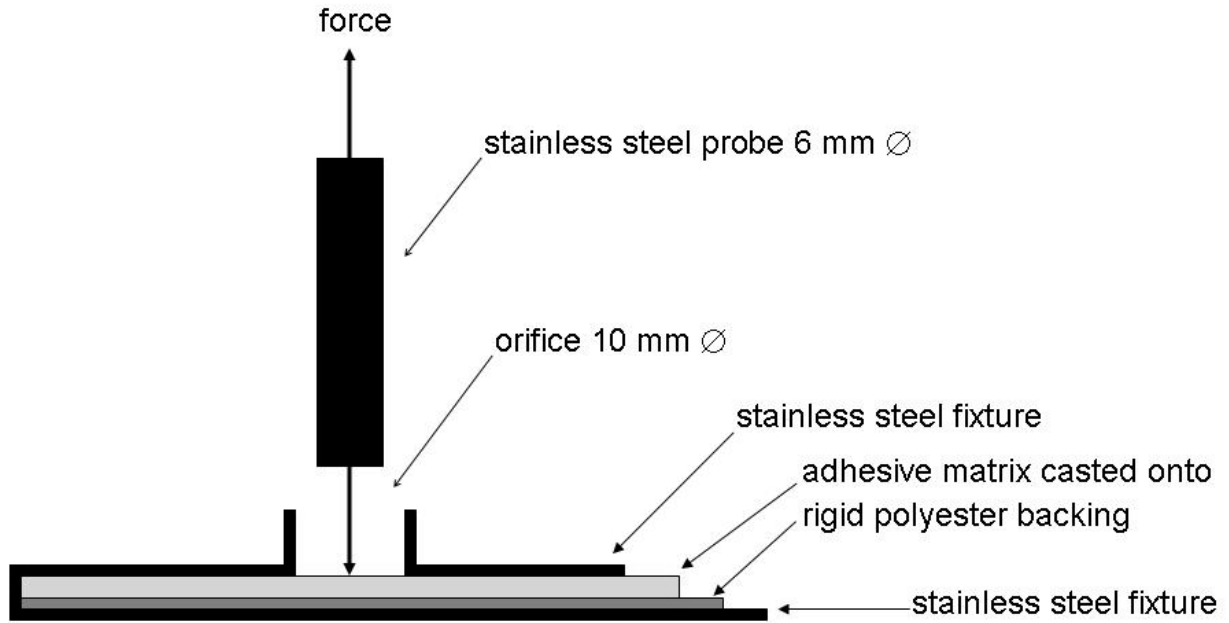


Fig. 59 Schematic of the texture analyzer setup for the determination of the probe tack

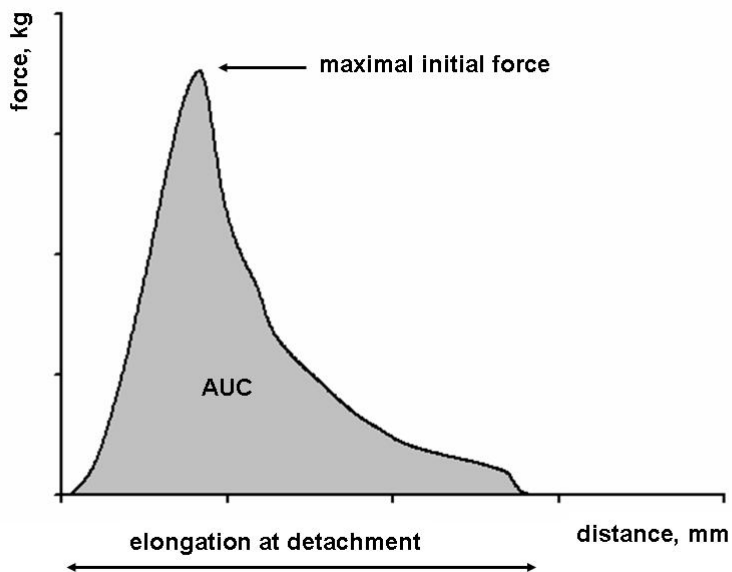


Fig. 60 Evaluated parameters of a typical force-distance curve

The method parameters were contact time, applied force and separation rate. Contact time and applied force were optimized with regard to the reproducibility of the maximal force (Fig. 61).

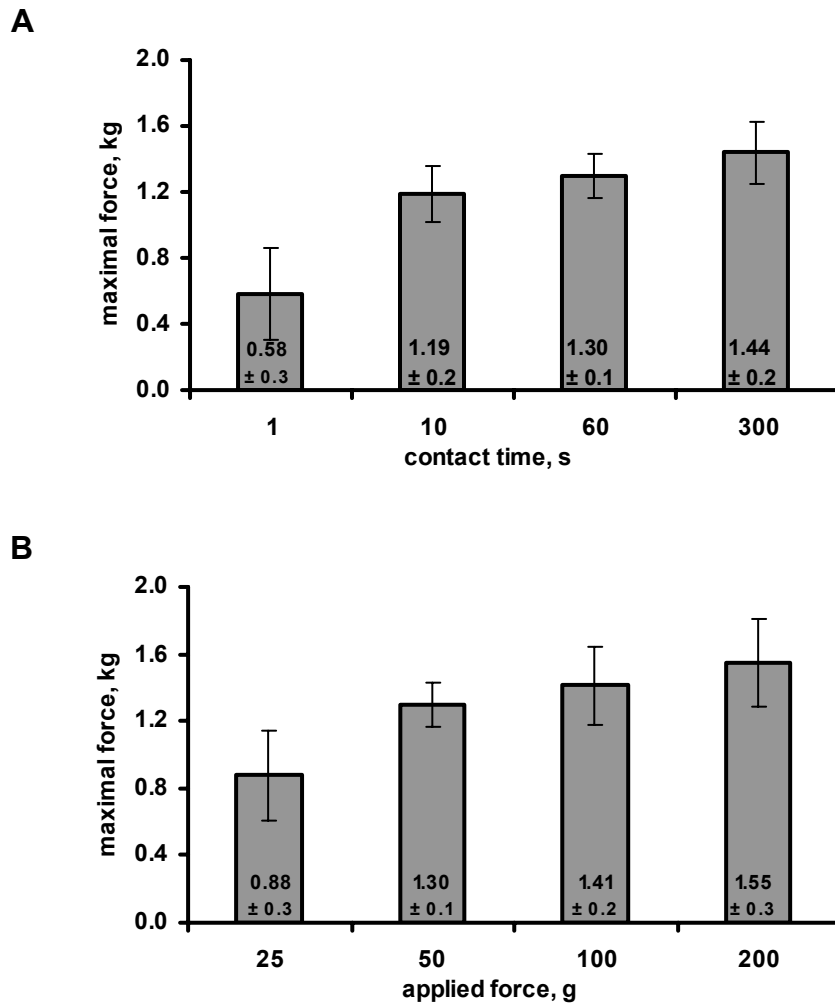


Fig. 61 Effect of the contact time (A) and the applied force (B) on the maximal force of placebo PIB patches (HM:MM:LM = 1:5:0) containing 0% CPVP (separation rate: 5 mm/s, applied force for (A): 50 g, contact time for (B): 60 s, n=6)

All subsequent studies were conducted with 60 s contact time and an applied force of 50 g. Increasing separation rates resulted in increasing maximal force and decreasing elongation at detachment values and favored adhesive failure (Fig. 62). This behavior has been described in the literature with regard to peel testing of pressure sensitive adhesives and is a result of the adhesive's viscoelastic properties (Satas 1989a). 5 mm/s was used as separation rate in subsequent studies as an approximation of the in vivo situation.

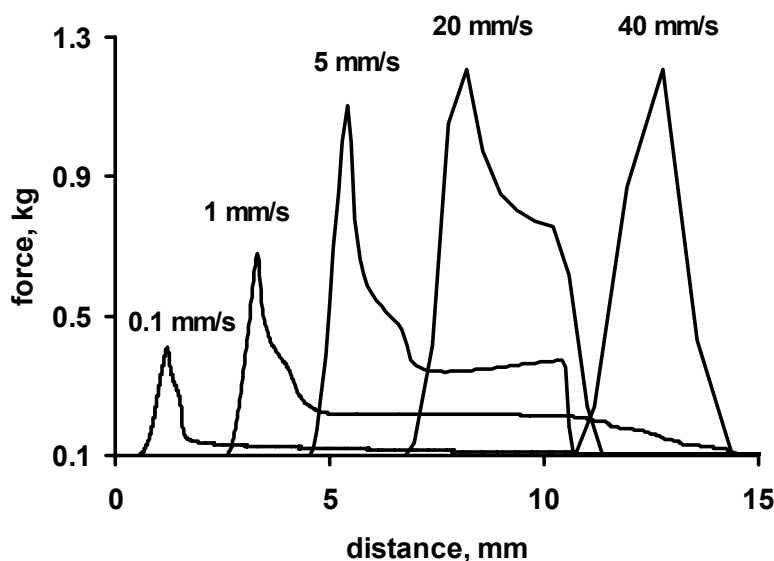


Fig. 62 Effect of the separation rate on the force-distance curves of placebo PIB patches (HM:MM:LM = 1:5:0) containing 0% CPVP (applied force: 50 g, contact time: 60 s)

3.5.3 In vitro adhesive properties of medium molecular weight polyisobutene

Patches based on medium molecular weight PIB (MM-PIB) failed cohesively (regardless of the CPVP content) (Fig. 63); the failure occurred in the bulk of the adhesive and not at the adhesive-substrate interface. Increasing CPVP content resulted in increased maximal force (Fig. 63A) and decreased elongation at detachment (Fig. 63B). Both tendencies were a result of CPVP particles reinforcing the matrix. The reinforcement was presumably due to friction between the CPVP particles and interactions between CPVP and the PIB chains. Similar reinforcements have been described in the literature, e.g., for natural rubber with fumed silica or carbon black (Jong 2007). A CPVP content of 50% (w/w) in the matrix resulted in the complete loss of adhesive properties. These matrices were rigid and did not possess the necessary flow properties to establish an intimate molecular contact with the stainless steel probe.

MM-PIB did not show fibrillation during probe detachment. Fibrillation is a three-step process that includes (1) the formation of cavities, (2) their expansion (3) and the formation, growing and rupture of fibrils. Since fibrillation is a result of polymer chain entanglement, it requires a minimum molecular weight of about 850 kDa for PIB (O'Connor and Willenbacher 2004), which was not reached in this case (MM-PIB has a molecular weight of approximately 55 kDa).

The AUC (Fig. 63C) was influenced by both the maximal force and the elongation at break.

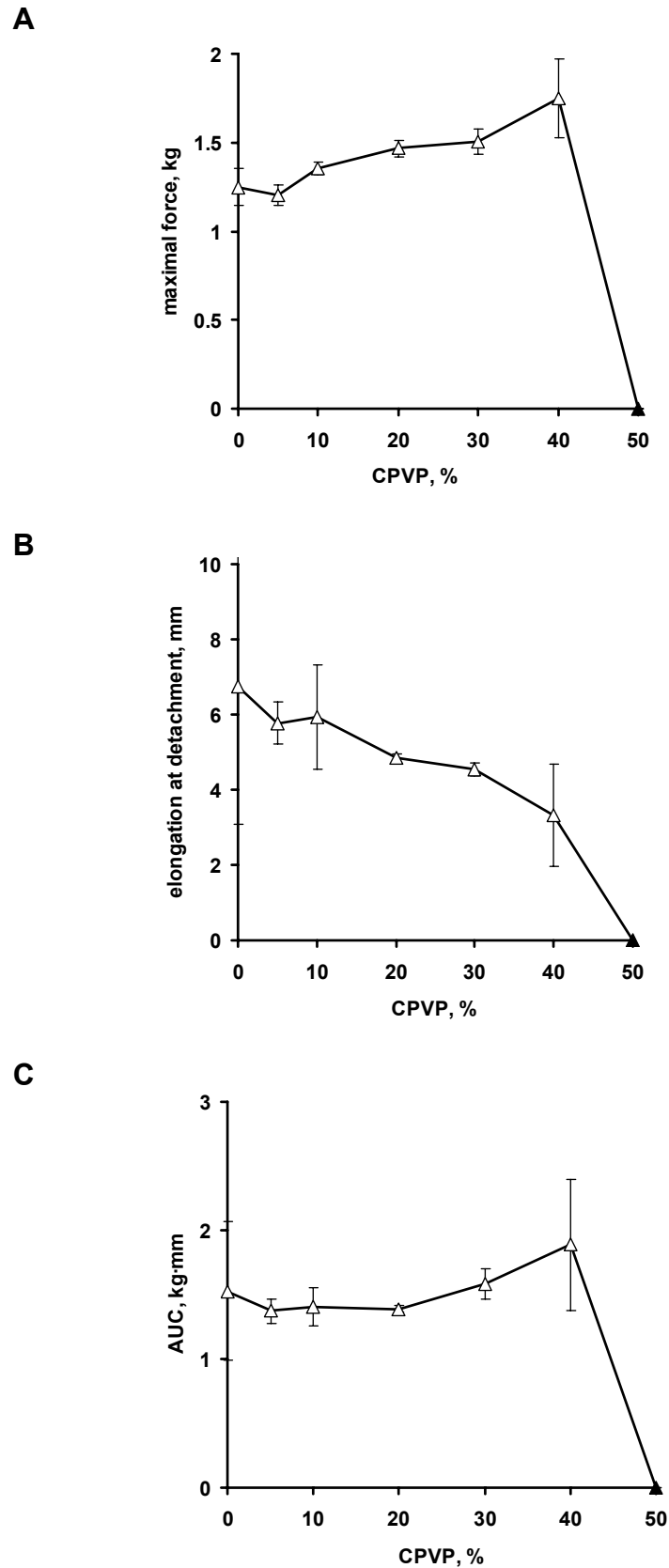


Fig. 63 Effect of the CPVP content on the maximal force (A), elongation at detachment (B), AUC (C) of MM-PIB placebo patches determined with the texture analyzer (separation rate: 5 mm/s, applied force: 50 g, contact time: 60 s); Δ : cohesive failure \blacktriangle : adhesive failure

3.5.4 In vitro adhesive properties of different polyisobutene blends

Blends of high, medium and low molecular weight PIB (HM:MM:LM-PIB) are used in commercially available transdermal patches based on PIB to obtain patches with the desired adhesive/cohesive properties. A typical composition consists of HM:MM:LM-PIB = 1:5:2 (Venkatraman and Gale 1998). Texture analyzer studies were conducted with HM:MM:LM-PIB = 1:5:0, 1:5:2 and 1:5:4.

CPVP reinforced blends of different molecular weight PIB in a similar fashion as discussed for MM-PIB: the maximal force increased with increasing CPVP content until the matrix became too rigid to form an intimate bond with the stainless-steel probe and the elongation at detachment decreased with increasing CPVP content (Fig. 68). In contrast to MM-PIB, the specimens failed predominantly adhesively (Table 19) due to the presence of HM-PIB. HM-PIB increased the matrix cohesion by facilitating entanglements between polymer chains (Zosel 1998). This caused the formation of fibrils during the detachment process.

CPVP probably additionally increased the maximal force by enabling the bond formation between the adhesive and the polar moieties of the substrate. PIB is known to adhere weakly to many surfaces due to its hydrocarbon nature (Higgins et al. 1989). This often necessitates the addition of tackifiers (e.g., ester resins) to introduce some polarity to the adhesive formulation (Tan and Pfister 1999). Crospovidone is classified as a hydrophilic polymer (Bühler 1992) and could improve the adhesion by this means. An adhesion enhancing effect by insoluble polar additives has been described in the literature for an epoxy adhesive with dispersed nanosized (approximately 150 nm) aluminum oxide particles. In that case, the pull-off strength from carbon steel was increased by the factor of 5 (Zhai et al. 2008).

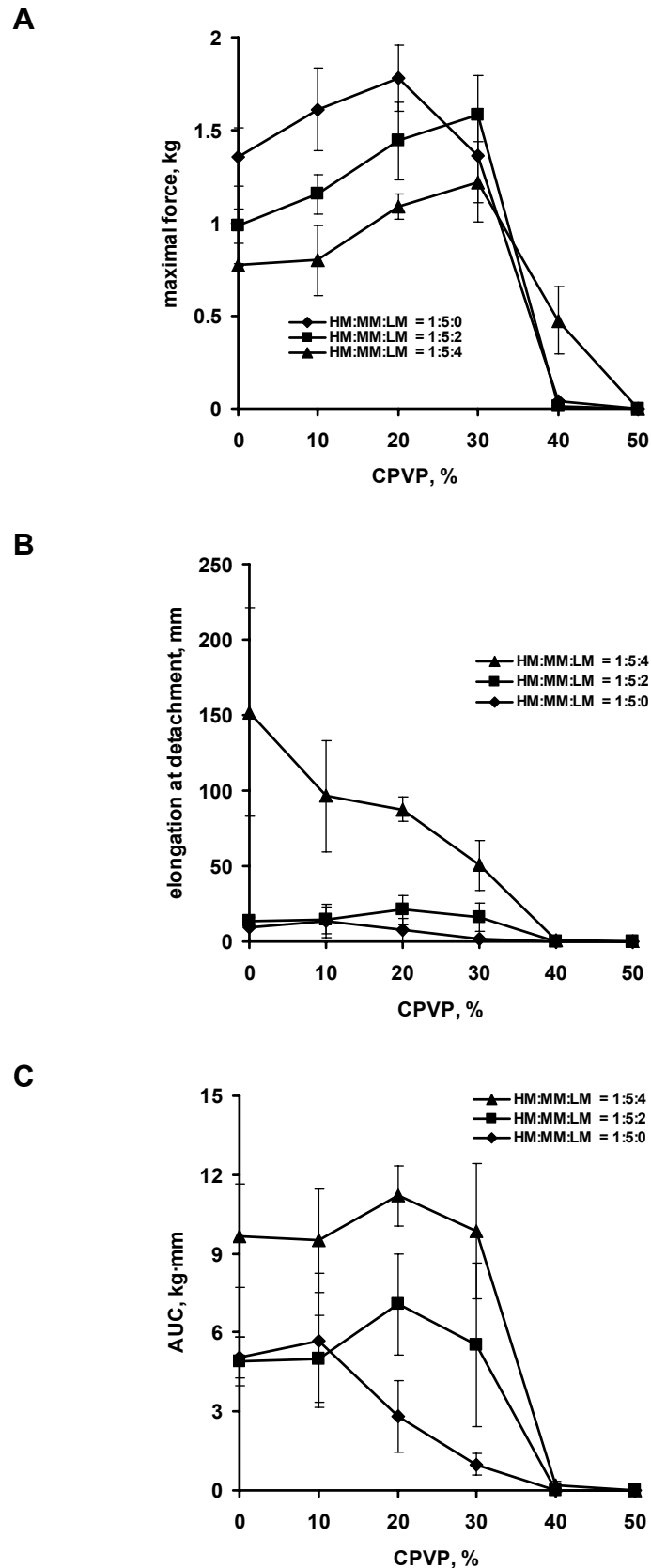


Fig. 64 Effect of the CPVP content on the maximal force (A), elongation at detachment (B), AUC (C) of placebo patches based on HM:MM:LM PIB = 1:5:0, 1:5:2 and 1:5:4 determined with the texture analyzer (separation rate: 5 mm/s, applied force: 50 g, contact time: 60 s)

Table 19 Incidence of adhesive failure (%) during probe tack measurement of placebo patches based on HM:MM:LM PIB = 1:5:0, 1:5:2, and 1:5:4

CPVP, %	Incidence of adhesive failure, %		
	HM:MM:LM = 1:5:0	HM:MM:LM = 1:5:2	HM:MM:LM = 1:5:4
0	100	100	100
10	100	100	83
20	100	100	50
30	100	100	50
40	100	100	100
50	100	100	100

3.5.5 In vitro adhesive properties of Durotak-87 202A

The effect of the CPVP content on the adhesive properties of acrylate adhesives was investigated for placebo patches based on Durotak-87 202A. These patches always failed adhesively. CPVP reinforced these matrices in a similar way as discussed for the PIB adhesives (Fig. 65). However, the effects were more pronounced. When the CPVP content in the matrix was increased from 0 to 10%, the maximal force increased by 8.5, 18.8, 17.4 and 3.4% for MM-PIB, HM:MM:LM-PIB = 1:5:0, HM:MM:LM-PIB = 1:5:2 and HM:MM:LM-PIB = 1:5:4, respectively, while the maximal force increased by 68.4% for Durotak 87-202A matrices. The larger reinforcement effect of CPVP in acrylate adhesives compared to PIB adhesives could be a result of stronger interactions between the adhesive and CPVP. Durotak 87-202A possesses hydroxyl and carbonyl functionalities that can form hydrogen bonds with CPVP, while PIB lacks this ability.

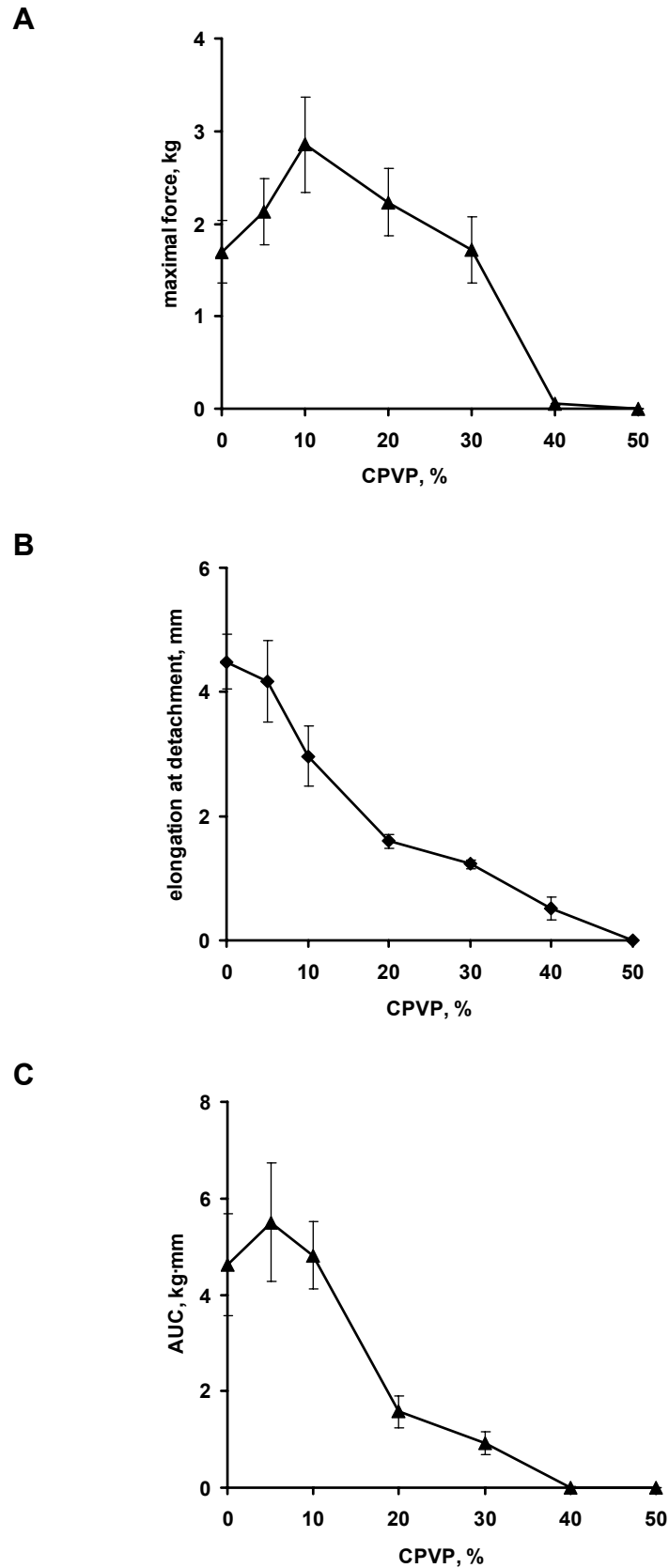


Fig. 65 Effect of the CPVP content on the maximal force (A), elongation at detachment (B), AUC (C) of placebo patches based Durotak-87 202A determined with the texture analyzer (separation rate: 5 mm/s, applied force: 50 g, contact time: 60 s)

3.5.6 In vivo adhesion, matrix creep and skin irritation

The effect of the CPVP content on the in vivo adhesion, in vivo matrix creep and skin irritation was investigated for HM:MM:LM-PIB = 1:5:0, 1:5:2 and 1:5:4.

3.5.6.1 In vivo adhesion

CPVP contents of 10, 20 and 30% (w/w) in matrices comprised of LM:MM:HM-PIB = 1:5:0, 1:5:2 and 1:5:4, respectively, resulted in maximum in vivo skin adhesion (Fig. 66). As previously discussed, CPVP increased the cohesive strength of the matrices and enabled them to bond with polar moieties of the skin. Patches without CPVP, particularly those based on LM:MM:HM-PIB matrices = 1:5:2 and 1:5:4, moved during the wearing period as a result of their low cohesive strength. Accordingly, the in vivo skin adhesion initially increased with increasing CPVP content. Skin adhesion decreased for higher CPVP contents because the matrices lost the necessary flow properties to achieve bonding. LM:MM:HM-PIB = 1:5:0 matrices with 40 and 50% CPVP and LM:MM:HM-PIB matrices = 1:5:2 and 1:5:4 with 50% CPVP did not adhere to the skin at all.

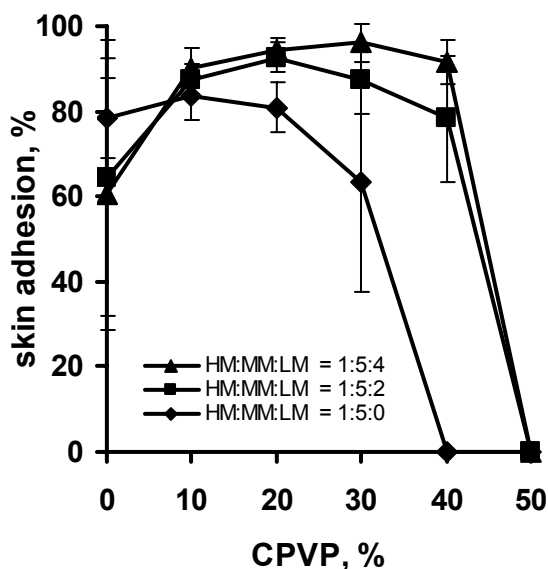


Fig. 66 Effect of the CPVP content on the in vivo skin adhesion (%) of placebo patches based on HM:MM:LM PIB = 1:5:0, 1:5:2 and 1:5:4 determined after 7 d wearing period

A further advantage of matrices containing CPVP in the in vivo situation was probably their capability to take up fluids. Pure PIB shows negligible moisture uptake and possess very low

moisture permeability (Higgins et al. 1989). Hence, applied PIB patches resulted in occluding conditions. The transepidermal water loss, which is approximately $10 \text{ g/m}^2/\text{h}$ (Casiraghi et al. 2002), could lead to the formation of a sweat film between the skin and the adhesive. This sweat film can facilitate the detachment of patches. Being highly hygroscopic, CPVP was able to take up the excess fluids. This could be visually observed; patches containing CPVP showed white spots and increased thickness during/after physical activity.

Increasing LM-PIB content in the adhesive base decreased the matrix coherence and thereby shifted the optimum CPVP content to higher values. HM:MM:LM PIB = 1:5:4 with 30% (w/w) CPVP showed the best skin adhesion ($96.1\% \pm 4.4$) of all tested formulations.

3.5.6.2 *In vivo matrix creep*

Matrix creep leads to the formation of a dark “dirt ring” at the patch’s edge. In addition to being unsightly, this can cause the patch to stick to clothing and move during stress. Furthermore, the formation of a “dirt ring” can change the patch’s release kinetic. To assess the matrix creep, a photoanalytical method was developed that quantified the area of this zone. After the wearing period, the removed patches were scanned using a white background and the histograms of their grey-scale pictures were evaluated. Increasing CPVP and decreasing LM-PIB content in the matrix led to decreased matrix creep due to enhancement of the matrix coherence (Fig. 67).

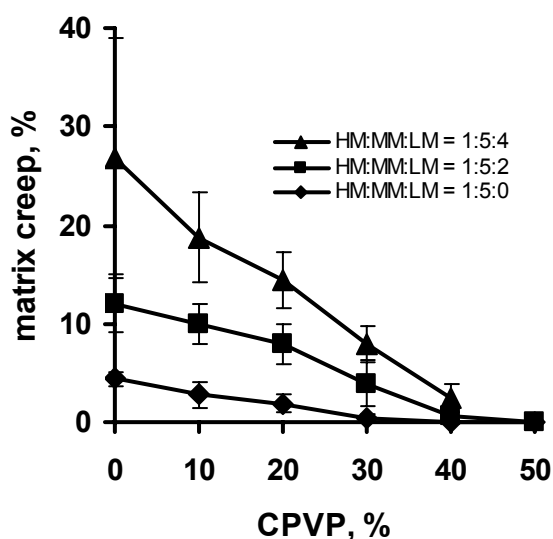


Fig. 67 Effect of the CPVP content on the *in vivo* matrix creep (%) of placebo patches based on HM:MM:LM PIB = 1:5:0, 1:5:2 and 1:5:4 (photoanalytically determined after 7 d wearing period)

3.5.6.3 Comparison of *in vivo* and *in vitro* data

The *in vivo* skin adhesion and the *in vivo* matrix creep were compared to the maximal force, AUC and elongation at detachment values obtained from the texture analyzer study. The AUC, which represents the work of adhesion (Kelly et al. 2004), showed the best correlation with the *in vivo* skin adhesion; it was able to predict both the shape of the curve with increasing CPVP content and the increase of the *in vivo* skin adhesion of formulations with increasing LM-PIB content. Satas (1989b) reported a study that compared the highly subjective thumb test (i.e., estimating the tack of an adhesive by touching its surface with the thumb and sensing the force required to break the bond) with probe tack results. Satas also found a better correlation of the thumb test with the AUC compared to the maximal force.

Both the matrix creep detected *in vivo* and the elongation at detachment derived from the force-distance curves showed a general trend of decreasing values with increasing CPVP content. This was a result of CPVP increasing the matrix coherence.

3.5.6.4 Skin irritation

Erythema determined directly after patch removal were mild and never exceeded rating score 2 (Fig. 68). They were strictly restricted to the application site, which suggests that their nature was traumatic and not allergic. Increasing CPVP content in the patches decreased the frequency and the severity of the erythema. This trend was observed for all tested adhesive bases while it was not possible to detect a trend with regard to the different amounts of LM-PIB in the adhesive base. A second investigation of the application sites after 48 h showed that skin recovery had taken place; no erythema could be observed in any case.

Skin occlusion leads to skin irritations in approx. 1/3 of healthy subjects (Wolf et al. 1998; Bucks and Maibach 1999). Sweat accumulation underneath the patch is thought to trigger this reaction by clogging sweat ducts. This may lead to lesions in the duct walls and induce an intra-epidermal inflammatory reaction (Hurkmans et al. 1985). CPVP particles in the adhesive matrix can diminish the accumulation of sweat underneath the patch due to their hygroscopic nature. By this means the incorporation of CPVP particles into PIB matrices could have improved the skin tolerability.

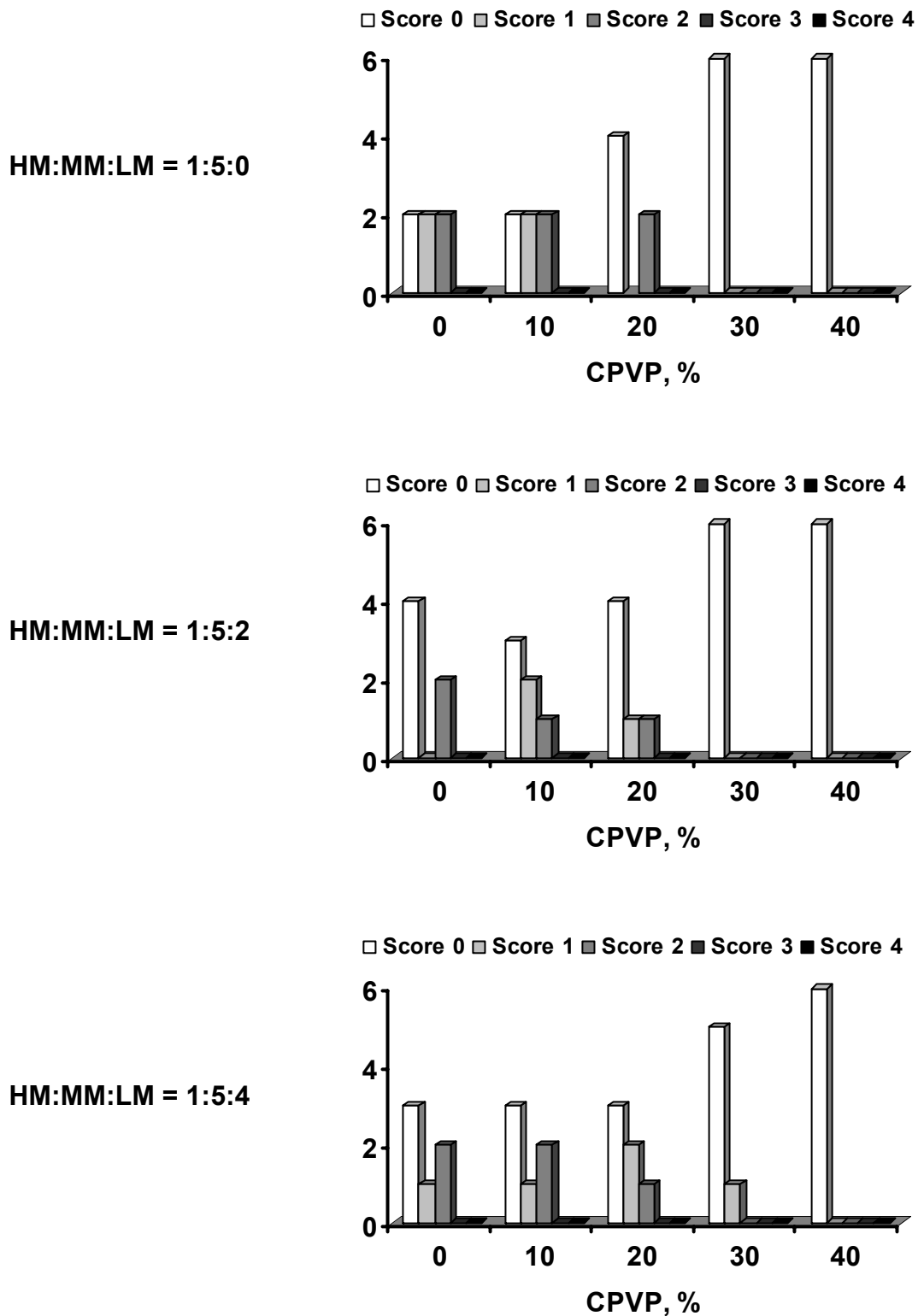


Fig. 68 Erythema incidence in study subjects directly after removal (wearing period: 7 d) of placebo patches based on HM:MM:LM PIB = 1:5:0, 1:5:2 and 1:5:4 with different CPVP contents (Scores: 0=no erythema, 1=slight erythema (barely perceptible light pink), 2=moderate erythema (dark pink), 3= moderate to severe erythema (light red), 4=severe erythema (extreme redness)).

3.5.7 Conclusions

The incorporation of CPVP into PIB and acrylate matrices increased the maximal force and the AUC of force-distance curves determined with the texture analyzer. The optimum CPVP content varied for different adhesive formulations and depended on the adhesive's cohesiveness and probably on the adhesive's ability to interact with CPVP. Reasons for the enhanced tack are probably the reinforcement of the matrix and the ability of CPVP to form bonds with polar moieties of the probe. The elongation at detachment decreased with increasing CPVP content as a result of the reinforced adhesive matrix.

The *in vivo* skin adhesion of PIB adhesives was maximal for CPVP contents of 10 and 20%, depending on the adhesive's molecular weight distribution. It is conceivable that CPVP's hygroscopy prevented the sweat film formation between the skin and the patch. This could be beneficial for the skin adhesion as well as for the skin tolerability.

4 SUMMARY

Adsorption mechanism of carbamazepine onto crospovidone

Firstly, the adsorption mechanism of the model drug carbamazepine onto crospovidone (CPVP) was investigated. Batches of CPVP with different specific surface areas showed similar drug adsorption. Since the extent of the drug adsorption increased linearly with the amount of CPVP but was independent of CPVP's surface area, it was concluded that the carbamazepine adsorption took place throughout the bulk of the CPVP particles. Adsorption isotherms of the drug onto CPVP showed a higher drug adsorption when ethyl acetate was used as a solvent, compared to ethanol. This behavior was attributed to ethanol's ability to form hydrogen bonds with CPVP and thus competing with the drug for binding sites on the carrier. CPVP possesses two hydrogen acceptor sites: the nitrogen and the oxygen atom of the cyclic amide. Attenuated total reflection Fourier transformation infrared experiments confirmed that solvents with hydrogen donor sites formed hydrogen bonds with CPVP's carbonyl function. The extent of the band shift of CPVP's carbonyl stretching vibrational band was correlated to the strength of the hydrogen bond, and increased in the order of ethyl acetate < chloroform < ethanol < water. A dry crystal free carbamazepine adsorbate onto CPVP (9.1% drug content, w/w) also showed a shift of CPVP's carbonyl band, indicating a hydrogen bond formation between the amine group of carbamazepine's urea function, which is carbamazepine's only hydrogen donor site, and CPVP's carbonyl function. This drug-carrier interaction was probably responsible for the recrystallization inhibitory effect.

To find the optimum drug-carrier ratio, carbamazepine adsorbates onto CPVP with different drug-carrier ratios were prepared by the solvent-deposition method and investigated using differential scanning calorimetry, X-ray diffraction, scanning electron microscopy and polarized light microscopy. Adsorbates with a drug loading up to 9.1% were crystal free. The adsorbate with 9.1% drug loading showed increased dissolution behavior, compared to the corresponding physical mixture and the micronized drug.

Development of the drug release method

The conventional USP drug release methods resulted in the disintegration of patches containing CPVP due to the polymer's pronounced swelling properties. Therefore, a drug release study employing Franz diffusion cells was developed. A hydrophilic, microporous polyethylene film with a film thickness of 35 μm was found optimal as a membrane: it prevented the erosion of the patch and yielded reproducible drug release results when tested with saturated ethinyl estradiol and levonorgestrel solutions. To quantify ethinyl estradiol and levonorgestrel simultaneously at low concentrations, an HPLC method was established. Using a RP-18 column and adjusting the mobile phase to water/methanol/acetonitrile (37/21/42, v/v) resulted in baseline separated ethinyl estradiol and levonorgestrel peaks with optimal peak symmetry. A limit of quantification (LOQ) of 0.02 $\mu\text{g/ml}$ was achieved for both drugs ($r^2 \geq 0.9995$).

Drug-in-adhesive patches containing adsorbates

Ethinyl estradiol and levonorgestrel are insoluble in medium molecular weight polyisobutene (MM-PIB). The effect of the incorporation of ethinyl estradiol and levonorgestrel adsorbates into this matrix on the physical state of the drugs was investigated by polarized light microscopy. MM-PIB patches containing adsorbates (drug content: 0.2% ethinyl estradiol, 1.0% levonorgestrel; carrier content: 20%, w/w) were crystal free for adsorbates onto CPVP and possessed reduced crystallinity for adsorbates onto titanium dioxide and MCC. Drug adsorbates of similar composition onto Aerosil were crystal free. However, their addition to the MM-PIB solution resulted in the formation of a thixotropic gel, which prevented the preparation of coherent films. The drug release from the patches increased in the order of no adsorbent < titanium dioxide < MCC < CPVP. This was attributed to differences in drug crystallinity and water uptake. Since conventional water uptake studies are not suitable for transdermal patches, the water uptake was determined by dynamic vapor sorption (DVS) at 90% rh. Patches without adsorbent and patches with titanium dioxide did not show water uptake. By contrast, patches containing MCC or CPVP showed a significant water uptake which indicated that release medium penetrated into the bulk of these patches during drug release studies. Probably fluid filled channels that facilitated the drug diffusion formed in these patches. Patches containing adsorbates onto CPVP were investigated in detail. Increasing the adsorbate's drug loading increased the drug release. Levonorgestrel was released slower than ethinyl estradiol because levonorgestrel's degree of saturation in the

release medium that penetrated the patch was higher. The decrease of the CPVP content below 15% (w/w) resulted in decreased drug release. Patches were crystal free for CPVP contents $\geq 10\%$ (w/w), which corresponded to a drug loading of CPVP of 12% (w/w). This result was in agreement with earlier findings obtained from carbamazepine-CPVP systems. Smaller CPVP particles led to faster initial drug release. This was probably due to the particle distribution in the patch: Smaller CPVP particles were distributed evenly throughout the patch, while larger CPVP particles rarely occupied areas close to the patch surface. Hence, in patches containing larger CPVP particles, the release medium needed more time to reach the adsorbate, which was reflected by the slower water-uptake determined by DVS.

Ethinyl estradiol and levonorgestrel were also insoluble in blends of high:medium:low molecular weight PIB = 1:5:0, 1:5:2 and 1:5:4. The incorporation of drug adsorbates onto CPVP into the PIB blends yielded crystal free patches. The drug release from these patches was independent of the PIB molecular weight distribution. The molecular weight distribution of PIB in such systems can be adjusted to tailor patches with optimal adhesive and cohesive properties without changing the drug release profile.

By contrast, the drug release from three Durotak acrylic adhesives was independent of whether the patches contained the pure drugs, drug adsorbates onto CPVP or drug adsorbates onto titanium dioxide. Both ethinyl estradiol and levonorgestrel were dissolved in these adhesives. The degree of saturation (or supersaturation) in these systems was correlated to the drug release. A higher degree of saturation (or supersaturation) resulted in a higher thermodynamic activity of the drugs. Hence, the drug release from such systems can be adjusted by the selection of an appropriate adhesive base.

A stability study with the crystal free acrylate and PIB patches was conducted. They did not show drug recrystallization in any case after 3 months at 25 °C/60 rh and 40 °C/75 rh.

Adhesive properties of drug-in-adhesive patches containing adsorbates

Force-distance diagrams, derived from texture analyzer probe tack measurements, were evaluated with regard to maximal initial force (F_m), area under the curve (AUC) and elongation at detachment. Increasing CPVP content in PIB and acrylate matrices increased both the F_m and the AUC up to a CPVP content of 10-40% (w/w), depending on the adhesive composition. Reasons for the enhanced tack were the reinforcement of the matrix and the ability of CPVP to form bonds with polar moieties of the probe. Higher CPVP contents resulted in decreasing F_m and AUC values because the matrices lost the necessary flow

properties to establish intimate bonds with the stainless steel probe. The CPVP content that yielded the highest F_m and AUC values varied for different adhesive formulations. It depended on the adhesive's cohesiveness and ability to interact with CPVP. As a result of the reinforced adhesive matrix, the elongation at detachment decreased with increasing CPVP content.

The *in vivo* adhesion of patches based on blends of high:medium:low molecular weight PIB = 1:5:0, 1:5:2 and 1:5:4 with varying CPVP content was investigated after a wearing period of 7 d. The *in vivo* adhesion was maximal for CPVP contents of 10-30%, depending on the adhesive's molecular weight distribution. The adhesive with high:medium:low molecular weight PIB = 1:5:4 with 30% CPVP showed the best skin adhesion ($96.1\% \pm 4.4$) of all tested formulations. Besides the above mentioned reasons for the enhanced tack, the increase in adhesion was probably a result of CPVP's hygroscopy, which prevented the sweat film formation between the skin and the patch. The reduced sweat film formation was probably also the reason for the better skin tolerability of patches containing CPVP. A photoanalytical method was developed to quantify the matrix creep after the wearing period. The matrix creep decreased with increasing CPVP and decreasing low molecular weight PIB content as a result of the increased matrix coherence.

A comparison of the *in vitro* and *in vivo* data showed a better correlation of the AUC than of the maximal initial force with the *in vivo* skin adhesion. The elongation at detachment showed the same trend as the *in vivo* matrix creep.

5 ZUSAMMENFASSUNG

Adsorptionsmechanismus von Carbamazepin an Crospovidon

Zunächst wurde der Adsorptionsmechanismus des Modellarzneistoffs Carbamazepin an Crospovidon (CPVP) untersucht. Da das Ausmaß der Wirkstoffadsorption unabhängig von der Oberfläche von CPVP war, aber mit der CPVP-Menge linear korrelierte, wurde gefolgert, dass die Adsorption eine Bulkeigenschaft von CPVP ist. Adsorptionsisothermen des Wirkstoffs an CPVP zeigten eine höhere Wirkstoffadsorption, wenn Ethylacetat statt Ethanol als Lösemittel eingesetzt wurde. Dieses Verhalten liegt vermutlich an der Fähigkeit von Ethanol, Wasserstoffbrückenbindungen mit CPVP zu bilden und dadurch mit dem Wirkstoff um Bindungsstellen an CPVP zu konkurrieren. Als Wasserstoffakzeptor-Stellen kommen das Stickstoff- und das Sauerstoffatom des zyklischen Amids im CPVP in Frage. Fourier-Transform-Infrarot-Spektroskopie mit abgeschwächter Totalreflexion zeigte, dass Lösemittel, die als Wasserstoffdonoren fungieren, Wasserstoffbrückenbindungen mit der Carbonylfunktion von CPVP bildeten. Das Ausmaß der Verschiebung der betreffenden Streckschwingung korrelierte mit der Stärke der Wasserstoffbrückenbindung und nahm in folgender Reihenfolge zu: Ethylacetat < Chloroform < Ethanol < Wasser. Ein sorgsam getrocknetes, kristallfreies Carbamazepin-Adsorbat an CPVP (Wirkstoffgehalt: 9.1% m/m) zeigte gleichfalls eine Verschiebung der Carbonyl-Streckschwingung (in der Größenordnung der Verschiebung von Chloroform). Dies wies auf eine Wasserstoffbrückenbindung zwischen der NH₂-Gruppe der Harnstofffunktion von Carbamazepin, seiner einzigen Wasserstoffdonatorstelle, und der Carbonylfunktion von CPVP hin. Diese Wechselwirkung war vermutlich für die rekristallisationshemmende Wirkung verantwortlich. Um das optimale Wirkstoff-Träger Verhältnis zu bestimmen wurden Carbamazepin-Adsorbate an CPVP in unterschiedlichen Verhältnissen nach der „Solvent-Deposition“ Methode hergestellt und mit Differenzkalorimetrie, Röntgenbeugung, Rasterelektronenmikroskopie und Polarisationsmikroskopie analysiert. Adsorbate mit bis zu 9.1% Arzneistoffbeladung waren kristallfrei. Das Adsorbat mit 9.1% Arzneistoffbeladung zeigte schnellere Arzneistofffreisetzung als die entsprechende physikalische Mischung und der mikronisierte Arzneistoff.

Entwicklung der Methode zur Wirkstofffreisetzung

Da CPVP ausgeprägte Quelleigenschaften besitzt, führten die konventionellen USP-Methoden zur Wirkstofffreisetzung zum Zerfall der CPVP enthaltenden Pflaster. Deshalb wurde ein Freisetzungstest unter der Verwendung von Franz-Diffusionszellen etabliert. Ein hydrophiler, mikroporöser Polyethylen-Film mit einer Filmdicke von 35 µm stellte sich als optimale Membran heraus: Dieser Film verhinderte die Erosion der Pflaster und ergab im Test mit an Ethinylestradiol und Levonorgestrel gesättigten Lösungen die beste Reproduzierbarkeit. Um Ethinylestradiol und Levonorgestrel gleichzeitig und in geringen Konzentrationen zu quantifizieren, wurde eine HPLC-Methode etabliert. Die Verwendung einer RP-18 Säule mit einer mobilen Phase aus Wasser/Methanol/Acetonitril (37/21/42, v/v) ergab basisliniengetrennte Ethinylestradiol und Levonorgestrel-Peaks mit optimaler Peaksymmetrie. Es wurde eine Quantifizierungsgrenze von 0.02 µg/ml für beide Hormone erreicht ($r^2 \geq 0.9995$).

Drug-In-Adhesive Pflaster mit Adsorbaten

Ethinylestradiol und Levonorgestrel sind unlöslich in mittelmolekularem Polyisobuten (MM-PIB). Mit Hilfe von Polarisationsmikroskopie wurde der Effekt der Einarbeitung von Ethinylestradiol- und Levonorgestrel-Adsorbaten auf die Kristallisation der Hormone in dieser Matrix untersucht. MM-PIB Pflaster (Wirkstoffgehalt: 0.2% Ethinylestradiol, 1.0% Levonorgestrel; Adsorbensgehalt: 20% m/m) waren kristallfrei, wenn CPVP als Adsorbens verwendet wurde und besaßen reduzierte Kristallinität bei Verwendung von Titaniumdioxid und MCC. Wirkstoffadsorbate gleicher Komposition an Aerosil zeigten keine Kristalle. Ihre Zugabe zur PIB-Lösung hatte jedoch die Bildung eines thixotropen Gels zur Folge, was die Herstellung von zusammenhängenden Filmen verhinderte. Die Wirkstofffreisetzung aus den Pflastern erhöhte sich in folgender Reihenfolge: kein Adsorbat < Titaniumdioxid < MCC < CPVP. Dies wurde auf die (teilweise) Hemmung der Wirkstoffkristallisation und die Unterschiede in der Wasseraufnahme zurückgeführt. Da konventionelle Methoden zur Bestimmung der Wasseraufnahme für Pflaster schlecht geeignet sind, wurde die Wasseraufnahme mittels dynamischer Dampfsorption bei 90% r.F. bestimmt. Pflaster ohne Adsorbate und Pflaster mit Titaniumdioxid zeigten keine Wasseraufnahme. Im Gegensatz dazu zeigten Pflaster, die MCC oder CPVP enthielten, eine deutliche Wasseraufnahme, was darauf hindeutete, dass während der Freisetzungstudien Freisetzungsmittel in die Pflaster eindrang. Dort bildeten sich vermutlich Kanäle, welche die Wirkstoffdiffusion erleichterten.

Pflaster, die Adsorbate an CPVP enthielten, wurden genauer untersucht. Eine Erhöhung der Arzneistoffbeladung der Adsorbate hatte eine erhöhte Wirkstofffreisetzung zur Folge. Levonorgestrel wurde langsamer als Ethinylestradiol freigesetzt, was an der schlechteren Löslichkeit von Levonorgestrel im Freisetzungsmedium lag. Dies hatte wahrscheinlich zur Folge, dass der Sättigungsgrad in der geringen Menge an Freisetzungsmedium, welche in die Pflaster eindrang, für Levonorgestrel höher war als für Ethinylestradiol. Eine Erniedrigung des CPVP-Gehalts unter 15% (w/w) resultierte in verringerter Wirkstofffreisetzung. Die Pflaster waren frei von Wirkstoffkristallen, wenn die totale Wirkstoffbeladung von CPVP 12% nicht überschritt, was den Versuchen mit Carbamazepin-Adsorbaten an CPVP in etwa entsprach. Kleinere CPVP Partikel führten zu schnellerer initialer Wirkstofffreisetzung, was wohl an der Partikelverteilung in den Pflastern lag: Kleinere CPVP-Partikel waren gleichmäßig im Pflaster verteilt, während größere Partikel seltener in den Randregionen der Pflaster zu finden waren. Folglich benötigte das Freisetzungsmedium in Pflastern mit größeren CPVP-Partikeln länger um die Adsorbate zu erreichen, was sich in der langsameren Wasseraufnahme dieser Pflaster widerspiegelte.

Ethinylestradiol und Levonorgestrel waren auch unlöslich in Mischungen von hoch:mittel:niedrig-molekularem PIB = 1:5:0, 1:5:2 und 1:5:4. Die Einarbeitung von Wirkstoffadsorbaten an CPVP in diese Kleber ergab kristallfreie Pflaster, die den Wirkstoff in gleicher Geschwindigkeit freisetzten. Dieses Ergebnis legt nahe, dass die Molekulargewichtsverteilung von PIB in solchen Systemen benutzt werden kann, um Pflaster mit optimalen adhesiven und kohesiven Eigenschaften zu entwickeln ohne die Wirkstofffreisetzung zu verändern.

Im Gegensatz dazu war die Wirkstofffreisetzung aus verschiedenen Acrylatklebern unabhängig davon, ob sie die reinen Wirkstoffe oder Wirkstoffadsorbate an CPVP oder Titaniumdioxid enthielten. Beide Wirkstoffe lagen gelöst in den untersuchten Acrylatklebern vor. Der Sättigungsgrad (Übersättigungsgrad) in diesen Systemen war mit der Wirkstofffreisetzung korreliert. Ein höherer Sättigungsgrad (Übersättigungsgrad) führte zu höherer thermodynamischer Aktivität des Wirkstoffs. Die Wirkstofffreisetzung aus solchen Systemen kann durch die Auswahl eines geeigneten Klebstoffs angepasst werden.

Stabilitätsprüfungen mit den kristallfreien Acrylat- und PIB-Pflastern wurden durchgeführt. Keines der Pflaster zeigte Wirkstoffrekristallisation nach 3 Monaten bei 25 °C/60 r.F. und 40 °C/75 r.F.

Klebeeigenschaften von Drug-In-Adhesive Pflastern mit Adsorbaten

Kraft-Weg Diagramme, aufgezeichnet mit dem Texture-Analyzer, wurden hinsichtlich maximaler Kraft (F_m), Fläche unter der Kurve (AUC) und Ablösedehnung ausgewertet. Die Einarbeitung von CPVP in PIB- und Acrylat-Matrizes erhöhte die maximale Kraft und die AUC von Kraft-Weg Diagrammen bis zu einem CPVP-Gehalt von 10-40% (m/m), je nach Klebstoffkomposition. Gründe für die erhöhte Klebekraft waren wahrscheinlich die Verstärkung der Matrix und die Fähigkeit von CPVP mit polaren Gruppen der Sonde zu wechselwirken. Ein höherer CPVP-Gehalt hatte sinkende F_m und AUC-Werte zur Folge, da die Matrizes nicht mehr die nötige Fließfähigkeit aufwiesen, um einen vollständigen Kontakt mit der Edelstahlsonde einzugehen. Der CPVP-Gehalt, der die höchsten F_m und AUC-Werte ergab, hing von der Kohäsion des Klebers und seiner Fähigkeit, mit CPVP zu interagieren, ab. Als Folge der verstärkten Klebstoffmatrix nahm die Ablösedehnung mit steigendem CPVP-Gehalt ab.

Die *in vivo* Adhäsion von Pflastern, die aus Mischungen von hoch:mittel:niedrig-molekularem PIB = 1:5:0, 1:5:2 und 1:5:4 mit unterschiedlichem CPVP-Gehalt hergestellt wurden, wurde nach einer Tragezeit von 7 Tagen untersucht. Die *in vivo*-Adhäsion war maximal für CPVP-Gehalte von 10-30%, je nach Molekulargewichtsverteilung des Klebers. Der Kleber mit hoch:mittel:niedrig-molekularem PIB = 1:5:4 mit 30% CPVP zeigte die beste Hauthaftung ($96.1\% \pm 4.4$). Neben den oben erwähnten Gründen für die gesteigerte Klebekraft wurde die Adhäsion vermutlich durch die Hygroskopizität des CPVPs erhöht, die die Schweißfilmbildung zwischen der Haut und dem Pflaster verhinderte. Die reduzierte Schweißfilmbildung war wahrscheinlich auch der Grund für die bessere Hautverträglichkeit von Pflastern, die CPVP enthielten. Eine photoanalytische Methode wurde entwickelt, um das Kriechverhalten der Matrix nach der Tragezeit zu quantifizieren. Das Kriechen der Matrix nahm mit zunehmendem CPVP-Gehalt und abnehmendem Anteil an niedrig-molekularem PIB ab, was ein Ergebnis der erhöhten Kohärenz der Matrix war.

Ein Vergleich der *in vivo* und *in vitro* Ergebnisse zeigte eine bessere Korrelation der AUC als der maximalen Kraft mit der *in vivo* Hauthaftung. Die Ablösedehnung zeigte den gleichen Trend wie das *in vivo* Kriechverhalten.

6 REFERENCES

- Akomeah, F., Nazir, T., Martin, G.P. and Brown, M.B., 2004. Effect of heat on the percutaneous absorption and skin retention of three model penetrants. *European Journal of Pharmaceutical Sciences*, 21(2-3), p. 337-345.
- Albert, A., 1958. Chemical Aspects of Selective Toxicity. *Nature*, 182(4633), p. 421-423.
- Allen, K.W., 1992a. Diffusion theory of adhesion. *Handbook of adhesion*. Essex: Longman Scientific & Technical. p. 112-114.
- Allen, K.W., 1992b. Electrostatic theory of adhesion. *Handbook of adhesion*. Essex: Longman Scientific & Technical. p. 139-140.
- Allen, K.W., 1992c. Mechanical theory of adhesion. *Handbook of adhesion*. Essex: Longman Scientific & Technical. p. 273-275.
- Allen, K.W., 1992d. Theories of adhesion. *Handbook of adhesion*. Essex: Longman Scientific & Technical. p. 473-476.
- Alvarez-Roman, R., Merino, G., Kalia, Y.N., Naik, A. and Guy, R.H., 2003. Skin permeability enhancement by low frequency sonophoresis: Lipid extraction and transport pathways. *Journal of Pharmaceutical Sciences*, 92(6), p. 1138-1146.
- Alvarez-Román, R., Naik, A., Kalia, Y.N., Fessi, H. and Guy, R.H., 2004. Visualization of skin penetration using confocal laser scanning microscopy. *European Journal of Pharmaceutics and Biopharmaceutics*, 58(2), p. 301-316.
- Aqil, M., Ahad, A., Sultana, V. and Ali, A., 2007. Status of terpenes as skin penetration enhancers. *Drug Discovery Today*, 12(23-24), p. 1061-1067.
- Armando J. Aguiar, J.E.Z.A.W.K., 1967. Deaggregation behavior of a relatively insoluble substituted benzoic acid and its sodium salt. *Journal of Pharmaceutical Sciences*, 56(10), p. 1243-1252.
- Ashburn, M.A., Ogden, L.L., Zhang, J., Love, G. and Basta, S.V., 2003. The pharmacokinetics of transdermal fentanyl delivered with and without controlled heat. *Journal of Pain*, 4(6), p. 291-297.
- Aungst, B.J., J. Rogers, N. and Shefter, E., 1986. Enhancement of naloxone penetration through human skin in vitro using fatty acids, fatty alcohols, surfactants, sulfoxides and amides. *International Journal of Pharmaceutics*, 33(1-3), p. 225-234.
- Barry, B.W., 1991. Lipid-Protein-Partitioning theory of skin penetration enhancement. *Journal of Controlled Release*, 15(3), p. 237-248.
- Barry, B.W., 2001. Novel mechanisms and devices to enable successful transdermal drug delivery. *European Journal of Pharmaceutical Sciences*, 14(2), p. 101-114.
- Bartek, M.J., Labudde, J.A. and Maibach, H.I., 1972. Skin Permeability In-Vivo - Comparison in Rat, Rabbit, Pig and Man. *Journal of Investigative Dermatology*, 58(3), p. 114-118.
- Barzegar-Jalali, M., Valizadeh, H., Dastmalchi, S., Shadbad, M.R.S., Barzegar-Jalali, A., Adibkia, K. and Mohammadi, G., 2007. Enhancing dissolution rate of carbamazepine via cogrinding with Crospovidone and hydroxypropylmethylcellulose. *Iranian Journal of Pharmaceutical Research*, 6(3), p. 159-165.
- Bauer, K.H., Forster, H., Hoff, D. and Weuta, H., 1975. Availability of Ampicillin Anhydrate and Ampicillin Trihydrate from Medicinal Preparations. *Drug Development Communications*, 1(5), p. 401-409.

- Beetge, E., du Plessis, J., Müller, D.G., Goosen, C. and van Rensburg, F.J., 2000. The influence of the physicochemical characteristics and pharmacokinetic properties of selected NSAID's on their transdermal absorption. *International Journal of Pharmaceutics*, 193(2), p. 261-264.
- Berzas, J.J., Rodriguez, J. and Castaneda, G., 1997. Simultaneous determination of ethinylestradiol and levonorgestrel in oral contraceptives by derivative spectrophotometry. *Analyst*, 122(1), p. 41-44.
- Bhugra, C. and Pikal, M.J., 2008. Role of thermodynamic, molecular, and kinetic factors in crystallization from the amorphous state. *Journal of Pharmaceutical Sciences*, 97(4), p. 1329-1349.
- Boddé, H.E., van den Brink, I., Koerten, H.K. and de Haan, F.H.N., 1991. Visualization of in vitro percutaneous penetration of mercuric chloride; transport through intercellular space versus cellular uptake through desmosomes. *Journal of Controlled Release*, 15(3), p. 227-236.
- Bond, J.R. and Barry, B.W., 1988. Limitations of Hairless Mouse Skin as a Model for In-Vitro Permeation Studies through Human-Skin - Hydration Damage. *Journal of Investigative Dermatology*, 90(4), p. 486-489.
- Bouwstra, J.A., Gooris, G.S., Vanderspek, J.A. and Bras, W., 1991. Structural Investigations of Human Stratum-Corneum by Small-Angle X-Ray-Scattering. *Journal of Investigative Dermatology*, 97(6), p. 1005-1012.
- Brown, M.B., Martin, G.P., Jones, S.A. and Akomeah, F.K., 2006. Dermal and transdermal drug delivery systems: Current and future prospects. *Drug Delivery*, 13(3), p. 175-187.
- Bucks, D. and Maibach, H., 1999. Occlusion does not uniformly enhance penetration in vivo. *Percutaneous Absorption: Drugs-Cosmetics-Mechanisms-Methodology*. New York: Dekker. p. 81-105.
- Bühler, V., 1992. Kollidon - Polyvinylpyrrolidon für die pharmazeutische Industrie. Ludwigshafen: BASF Aktiengesellschaft. p. 131-189.
- Büyüktimkin, N., Büyüktimkin, S. and Rytting, H., 1997. Chemical means of transdermal drug permeation enhancement. *Transdermal and topical drug delivery systems*. Buffalo Grove: Interpharm Press. p. 260-292.
- Bunge, A.L., Guy, R.H. and Hadgraft, J., 1999. The determination of a diffusional pathlength through the stratum corneum. *International Journal of Pharmaceutics*, 188(1), p. 121-124.
- Burkoth, T.L., Bellhouse, B.J., Hewson, G., Longridge, D.J., Muddle, A.G. and Sarphie, D.F., 1999. Transdermal and transmucosal powdered drug delivery. *Critical Reviews in Therapeutic Drug Carrier Systems*, 16(4), p. 331-384.
- Cantor, A.S., 1999. Drug and excipient diffusion and solubility in acrylate adhesives measured by infrared-attenuated total reflectance (IR-ATR) spectroscopy. *Journal of Controlled Release*, 61(1-2), p. 219-231.
- Carli, F., Colombo, I., Magarotto, L., Motta, A. and Torricelli, C., 1986. Influence of Polymer Characteristics on Drug Loading into Crospovidone. *International Journal of Pharmaceutics*, 33(1-3), p. 115-124.
- Carli, F. and Garbassi, F., 1985. Characterization of Drug Loading in Crospovidone by X-Ray Photoelectron-Spectroscopy. *Journal of Pharmaceutical Sciences*, 74(9), p. 963-967.
- Casiraghi, A., Minghetti, P., Cilurzo, F., Montanari, L. and Naik, A., 2002. Occlusive properties of monolayer patches: In vitro and in vivo evaluation. *Pharmaceutical Research*, 19(4), p. 423-426.

- Cevc, G., Blume, G., Schätzlein, A., Gebauer, D. and Paul, A., 1996. The skin: a pathway for systemic treatment with patches and lipid-based agent carriers. *Advanced Drug Delivery Reviews*, 18(3), p. 349-378.
- Chien, Y.W., 1978. Transdermal therapeutic systems. *Controlled Drug Delivery: Fundamentals and Applications*. New York: Informa Health Care. p. 157-176.
- Chizmadzhev, Y.A., Zarnitsin, V.G., Weaver, J.C. and Potts, R.O., 1995. Mechanism of Electroinduced Ionic Species Transport through a Multilamellar Lipid System. *Biophysical Journal*, 68(3), p. 749-765.
- Chow, A.H.L., Chow, P.K.K., Zhongshan, W. and Grant, D.J.W., 1985. Modification of acetaminophen crystals: influence of growth in aqueous solutions containing p-acetoxyacetanilide on crystal properties. *International Journal of Pharmaceutics*, 24(2-3), p. 239-258.
- Cilurzo, F., Minghetti, P., Casiraghi, A., Tosi, L., Pagani, S. and Montanari, L., 2005. Polymethacrylates as crystallization inhibitors in monolayer transdermal patches containing ibuprofen. *European Journal of Pharmaceutics and Biopharmaceutics*, 60(1), p. 61-66.
- Clancy, M.J., Corish, J. and Corrigan, O.I., 1994. A comparison of the effects of electrical current and penetration enhancers on the properties of human skin using spectroscopic (FTIR) and calorimetric (DSC) methods. *International Journal of Pharmaceutics*, 105(1), p. 47-56.
- Coldman, M.F., Poulsen, B.J. and Higuchi, T., 1969. Enhancement of Percutaneous Absorption by Use of Volatile - Nonvolatile Systems as Vehicles. *Journal of Pharmaceutical Sciences*, 58(9), p. 1098-1103.
- Delago-Charro, B. and Guy, R.H., 2001. Transdermal Drug Delivery. *Drug delivery and targeting*. London: Taylor and Francis. p. 208-236.
- Denet, A.-R., Vanbever, R. and Pr eat, V., 2004. Skin electroporation for transdermal and topical delivery. *Advanced Drug Delivery Reviews*, 56(5), p. 659-674.
- Diebold, U., 2003. The surface science of titanium dioxide. *Surface Science Reports*, 48(5-8), p. 53-229.
- Dimas, D., Dallas, P., Rekkas, D. and Choulis, N., 2000. Effect of several factors on the mechanical properties of pressure-sensitive adhesives used in transdermal therapeutic systems. *AAPS PharmSciTech*, 1(2), p. 80-87.
- Doherty, C. and York, P., 1987. Evidence for Solid-State and Liquid-State Interactions in a Furosemide Polyvinylpyrrolidone Solid Dispersion. *Journal of Pharmaceutical Sciences*, 76(9), p. 731-737.
- Dover, J.S., Hruza, G.J. and Arndt, K.A., 2000. Lasers in skin resurfacing. *Seminars in Cutaneous Medicine and Surgery*, 19(4), p. 207-220.
- Draize, J., Woodard, G. and Calvery, H., 1944. Methods for the study of irritation and toxicity of substances topically applied to skin and mucous membranes. *J. Pharmacol. Exp. Ther.*, 82 p. 377-390.
- Eckert, R.L., 1989. Structure, Function, and Differentiation of the Keratinocyte. *Physiological Reviews*, 69(4), p. 1316-1346.
- El Maghraby, G.M., Barry, B.W. and Williams, A.C., 2008. Liposomes and skin: From drug delivery to model membranes. *European Journal of Pharmaceutical Sciences*, 34(4-5), p. 203-222.
- Elias, P.M., Brown, B.E., Fritsch, P., Goerke, J., Gray, G.M. and White, R.J., 1979. Localization and Composition of Lipids in Neonatal Mouse Stratum Granulosum and Stratum-Corneum. *Journal of Investigative Dermatology*, 73(5), p. 339-348.

- Elias, P.M., Tsai, J., Menon, G.K., Holleran, W.M. and Feingold, K.R., 2002. The potential of metabolic interventions to enhance transdermal drug delivery. *Journal of Investigative Dermatology Symposium Proceedings*, 7(1), p. 79-85.
- Erienne, J.A. and Winter, L., 1997. Comparison of the local tolerability and adhesion of a new matrix system (Menorest(R)) for estradiol delivery with an established transdermal membrane system (Estraderm TTS(R)). *Maturitas*, 26(2), p. 95-101.
- Finnin, B.C. and Morgan, T.M., 1999. Transdermal penetration enhancers: Applications, limitations, and potential. *Journal of Pharmaceutical Sciences*, 88(10), p. 955-958.
- Flynn, G.L. and Yalkowsk.Sh, 1972. Correlation and Prediction of Mass-Transport across Membranes .1. Influence of Alkyl Chain-Length on Flux-Determining Properties of Barrier and Diffusant. *Journal of Pharmaceutical Sciences*, 61(6), p. 838-843.
- Foldvari, M., 2000. Non-invasive administration of drugs through the skin: challenges in delivery system design. *Pharmaceutical Science & Technology Today*, 3(12), p. 417-425.
- Friedland, J.A. and Buchel, E.W., 2000. Skin care and the topical treatment of aging skin. *Clinics in Plastic Surgery*, 27(4), p. 501-504.
- Friedrich, H., Fussnegger, B., Kolter, K. and Bodmeier, R., 2006. Dissolution rate improvement of poorly water-soluble drugs obtained by adsorbing solutions of drugs in hydrophilic solvents onto high surface area carriers. *European Journal of Pharmaceutics and Biopharmaceutics*, 62(2), p. 171-177.
- Fujii, M., Okada, H., Shibata, Y., Teramachi, H., Kondoh, M. and Watanabe, Y., 2005. Preparation, characterization, and tableting of a solid dispersion of indomethacin with crospovidone. *International Journal of Pharmaceutics*, 293(1-2), p. 145-153.
- Fujimura, A., Ebihara, A., Ohashi, K., Shiga, T., Kumagai, Y., Nakashima, H. and Kotegawa, T., 1994. Comparison of the Pharmacokinetics, Pharmacodynamics, and Safety of Oral (Catapres) and Transdermal (M-5041t) Clonidine in Healthy-Subjects. *Journal of Clinical Pharmacology*, 34(3), p. 260-265.
- Funke, A.P., Gunther, C., Muller, R.H. and Lipp, R., 2002a. In-vitro release and transdermal fluxes of a highly lipophilic drug and of enhancers from matrix TDS. *Journal of Controlled Release*, 82(1), p. 63-70.
- Funke, A.P., Schiller, R., Motzkus, H.W., Gunther, C., Muller, R.H. and Lipp, R., 2002b. Transdermal delivery of highly lipophilic drugs: In vitro fluxes of antiestrogens, permeation enhancers, and solvents from liquid formulations. *Pharmaceutical Research*, 19(5), p. 661-668.
- Gambichler, T., Matip, R., Moussa, G., Altmeyer, P. and Hoffmann, K., 2006. In vivo data of epidermal thickness evaluated by optical coherence tomography: Effects of age, gender, skin type, and anatomic site. *Journal of Dermatological Science*, 44(3), p. 145-152.
- Ghosh, T.K. and Pfister, W.R., 1997. Transdermal and topical delivery systems: An overview and future trends. *Transdermal and topical drug delivery systems*. Buffalo Grove: Interpharm Press. p. 1-32.
- Ginn, M.E., Noyes, C.M. and Jungerma.E, 1968. Contact Angle of Water on Viable Human Skin. *Journal of Colloid and Interface Science*, 26(2), p. 146-149.
- Goodman, M. and Barry, B.W., 1989. Lipid-protein-partitioning (LPP) theory of skin enhancer activity: finite dose technique. *International Journal of Pharmaceutics*, 57(1), p. 29-40.
- Gordon, R.D. and Peterson, T.A., 2003. 4 Myths About Transdermal Drug Delivery. *Drug Delivery Technology*, 3(4), p. 15-20.
- Gorsline, J., Okerholm, R.A., Rolf, C.N., Moos, C.D. and Hwang, S.S., 1992. Comparison of Plasma Nicotine Concentrations after Application of Nicoderm (Nicotine

- Transdermal System) to Different Skin Sites. *Journal of Clinical Pharmacology*, 32(6), p. 576-581.
- Grzesiak, A.L., Lang, M.D., Kim, K. and Matzger, A.J., 2003. Comparison of the four anhydrous polymorphs of carbamazepine and the crystal structure of form I. *Journal of Pharmaceutical Sciences*, 92(11), p. 2260-2271.
- Haaf, F., Sanner, A. and Straub, F., 1985. Polymers of N-Vinylpyrrolidone - Synthesis, Characterization and Uses. *Polymer Journal*, 17(1), p. 143-152.
- Hadgraft, J., 1999. Passive enhancement strategies in topical and transdermal drug delivery. *International Journal of Pharmaceutics*, 184(1), p. 1-6.
- Hadgraft, J., 2001. Skin, the final frontier. *International Journal of Pharmaceutics*, 224(1-2), p. 1-18.
- Hadgraft, J. and Lane, M.E., 2005. Skin permeation: The years of enlightenment. *International Journal of Pharmaceutics*, 305(1-2), p. 2-12.
- Halprin, K.M., 1972. Epidermal Turnover Time - Re-Examination. *British Journal of Dermatology*, 86(1), p. 14-19.
- Hammell, D.C., Hamad, M., Vaddi, H.K., Crooks, P.A. and Stinchcomb, A.L., 2004. A duplex "Gemini" prodrug of naltrexone for transdermal delivery. *Journal of Controlled Release*, 97(2), p. 283-290.
- Higgins, J.J., Jagisch, F.C. and Strucker, N.E., 1989. Butyl rubber and polyisobutylene. *Handbook of pressure sensitive adhesive technology*. New York: Van Nostrand Reinhold. p. 374-395.
- Higuchi, T., 1960. Physical chemical analysis of percutaneous absorption process from creams and ointments. *J. Soc. Cosmet. Chem.*, 11 p. 85-97.
- Hipasawa, N., Ishise, S., Miyata, H. and Danjo, K., 2004. Application of nilvadipine solid dispersion to tablet formulation and manufacturing using crospovidone and methylcellulose as dispersion carriers. *Chemical & Pharmaceutical Bulletin*, 52(2), p. 244-247.
- Hirvonen, J., Sutinen, R., Paronen, P. and Urtti, A., 1993. Transdermal Penetration Enhancers in Rabbit Pinna Skin - Duration of Action, Skin Irritation, and in-Vivo in-Vitro Comparison. *International Journal of Pharmaceutics*, 99(2-3), p. 253-261.
- Hoegberg, L.C.G., Angelo, H.R., Christophersen, A.B. and Christensen, H.R., 2002. Effect of ethanol and pH on the adsorption of acetaminophen (paracetamol) to high surface activated charcoal, in vitro studies. *Journal of Toxicology-Clinical Toxicology*, 40(1), p. 59-67.
- Horita, A. and Weber, L.J., 1964. Skin penetrating property of drugs dissolved in dimethylsulfoxide (DMSO) and other vehicles. *Life Sciences*, 3(12), p. 1389-1395.
- Horn, D. and Ditter, W., 1982. Chromatographic Study of Interactions between Polyvinylpyrrolidone and Drugs. *Journal of Pharmaceutical Sciences*, 71(9), p. 1021-1026.
- Hougham, A.J., Hawkinson, R.W., Crowley, J.K., Wilson, R.R., Glode, J.E., Hilty, R.W., Hughes, S.O., Koepl, C.G., Kovaric, T.R. and Wyskoarko, N.P., 1989. Improved Skin Adherence and Patient Acceptance in a New Transdermal Nitroglycerin Delivery System. *Clinical Therapeutics*, 11(1), p. 23-31.
- Hurkmans, J., Bodde, H.E., Vandriel, L.M.J., Vandoorne, H. and Junginger, H.E., 1985. Skin Irritation Caused by Transdermal Drug Delivery Systems During Long-Term (5 Days) Application. *British Journal of Dermatology*, 112(4), p. 461-467.
- Iervolino, M., Raghavan, S.L. and Hadgraft, J., 2000. Membrane penetration enhancement of ibuprofen using supersaturation. *International Journal of Pharmaceutics*, 198(2), p. 229-238.

- Ishida, T., Doi, M., Shimamoto, M., Minamino, N., Nonaka, K. and Inoue, M., 1989. Physicochemical Properties of Crystalline Forms of Ethynylestradiol Solvates - Comparison of Thermal-Behavior with X-Ray Crystal-Structure. *Journal of Pharmaceutical Sciences*, 78(4), p. 274-280.
- Johansen, H. and Moller, N., 1978. Solvent Deposition Method for Enhancement of Dissolution Rate - Importance of Drug-to-Excipient Ratio. *Journal of Pharmaceutical Sciences*, 67(1), p. 134-136.
- Jong, L., 2007. Viscoelastic properties of natural rubber composites reinforced by defatted soy flour and carbon black co-filler. *Journal of Applied Polymer Science*, 106(5), p. 3444-3453.
- Jungbauer, F.H., Coenraads, P.J. and Kardaun, S.H., 2001. Toxic hygroscopic contact reaction to N-methyl-2-pyrrolidone. *Contact Dermatitis*, 45(5), p. 303-304.
- Kaestli, L.Z., Wasilewski-Rasca, A.F., Bonnabry, P. and Vogt-Ferrier, N., 2008. Use of transdermal drug formulations in the elderly. *Drugs & Aging*, 25(4), p. 269-280.
- Kalia, Y.N., Naik, A., Garrison, J. and Guy, R.H., 2004. Iontophoretic drug delivery. *Advanced Drug Delivery Reviews*, 56(5), p. 619-658.
- Karande, P., Jain, A. and Mitragotri, S., 2004. Discovery of transdermal penetration enhancers by high-throughput screening. *Nat Biotech*, 22(2), p. 192-197.
- Karande, P., Jain, A. and Mitragotri, S., 2006. Insights into synergistic interactions in binary mixtures of chemical permeation enhancers for transdermal drug delivery. *Journal of Controlled Release*, 115(1), p. 85-93.
- Kaushik, S., Hord, A.H., Denson, D.D., McAllister, D.V., Smitra, S., Allen, M.G. and Prausnitz, M.R., 2001. Lack of pain associated with microfabricated microneedles. *Anesthesia and Analgesia*, 92(2), p. 502-504.
- Kelly, H.M., Deasy, P.B., Busquet, M. and Torrance, A.A., 2004. Bioadhesive, rheological, lubricant and other aspects of an oral gel formulation intended for the treatment of xerostomia. *International Journal of Pharmaceutics*, 278(2), p. 391-406.
- Kemken, J., Ziegler, A. and Muller, B.W., 1992. Influence of Supersaturation on the Pharmacodynamic Effect of Bupranolol after Dermal Administration Using Microemulsions as Vehicle. *Pharmaceutical Research*, 9(4), p. 554-558.
- Kim, J.-H. and Choi, H.-K., 2002. Effect of additives on the crystallization and the permeation of ketoprofen from adhesive matrix. *International Journal of Pharmaceutics*, 236(1-2), p. 81-85.
- Kleiner, L. and Gale, R., US 6375978, 2002
- Kligman, A.M., 1965. Topical Pharmacology and Toxicology of Dimethyl Sulfoxide. 1. *Jama*, 193 p. 796-804.
- Kogan, A. and Garti, N., 2006. Microemulsions as transdermal drug delivery vehicles. *Advances in Colloid and Interface Science*, 123-126 p. 369-385.
- Konno, Y., Kawata, H., Aruga, M., Sonobe, T. and Mitomi, M., US 4685911, 1985
- Kotiyani, P.N. and Vavia, P.R., 2001. Eudragits: Role as crystallization inhibitors in drug-in-adhesive transdermal systems of estradiol. *European Journal of Pharmaceutics and Biopharmaceutics*, 52(2), p. 173-180.
- Lademann, J., Richter, H., Teichmann, A., Otberg, N., Blume-Peytavi, U., Luengo, J., Weiß, B., Schaefer, U.F., Lehr, C.-M., Wepf, R. and Sterry, W., 2007. Nanoparticles - An efficient carrier for drug delivery into the hair follicles. *European Journal of Pharmaceutics and Biopharmaceutics*, 66(2), p. 159-164.
- Lake, Y. and Pinnock, S., 2000. Improved patient acceptability with a transdermal drug-in-adhesive oestradiol patch. *Australian & New Zealand Journal of Obstetrics & Gynaecology*, 40(3), p. 313-316.

- Latsch, S., Selzer, T., Fink, L., Horstmann, M. and Kreuter, J., 2004. Use of isothermal heat conduction microcalorimetry, X-ray diffraction, and optical microscopy for characterisation of crystals grown in steroid combination-containing transdermal drug delivery systems. *European Journal of Pharmaceutics and Biopharmaceutics*, 57(2), p. 397-410.
- Lee, W.R., Shen, S.C., Wang, K.H., Hu, C.H. and Fang, J.Y., 2003. Lasers and microdermabrasion enhance and control topical delivery of vitamin C. *Journal of Investigative Dermatology*, 121(5), p. 1118-1125.
- Leuner, C. and Dressman, J., 2000. Improving drug solubility for oral delivery using solid dispersions. *European Journal of Pharmaceutics and Biopharmaceutics*, 50(1), p. 47-60.
- Liebig, M., Egeler, P., Oehlmann, J. and Knacker, T., 2005. Bioaccumulation of 14C-17[alpha]-ethinylestradiol by the aquatic oligochaete *Lumbriculus variegatus* in spiked artificial sediment. *Chemosphere*, 59(2), p. 271-280.
- Lin, S. and Chien, Y.W., 2006. Transdermal contraceptive patches: Development, clinical performance, and future prospects. *American journal of drug delivery*, 4(4), p. 201-213.
- Lipp, R., 1998. Selection and use of crystallization inhibitors for matrix-type transdermal drug-delivery systems containing sex steroids. *Journal of Pharmacy and Pharmacology*, 50(12), p. 1343-1349.
- Lipp, R., Laurent, H., Gunther, C., Riedl, J., Esperling, P. and Tauber, U., 1998. Prodrugs of gestodene for matrix-type transdermal drug delivery systems. *Pharmaceutical Research*, 15(9), p. 1419-1424.
- Lippold, B.C. and Schneemann, H., 1984. The influence of vehicles on the local bioavailability of betamethasone-17-benzoate from solution- and suspension-type ointments. *International Journal of Pharmaceutics*, 22(1), p. 31-43.
- LoBrutto, R. and Kazakevich, Y., 2007. HPLC for pharmaceutical scientists. Hoboken, New Jersey: John Wiley & Sons, Inc. p. 139-241.
- Lombry, C., Dujardin, N. and Preat, V., 2000. Transdermal delivery of macromolecules using skin electroporation. *Pharmaceutical Research*, 17(1), p. 32-37.
- Ma, X., Taw, J. and Chiang, C.-M., 1996. Control of drug crystallization in transdermal matrix system. *International Journal of Pharmaceutics*, 142(1), p. 115-119.
- Man, M.Q., Brown, B.E., Wupong, S., Feingold, K.R. and Elias, P.M., 1995. Exogenous Nonphysiologic Vs Physiological Lipids - Divergent Mechanisms for Correction of Permeability Barrier Dysfunction. *Archives of Dermatology*, 131(7), p. 809-816.
- Martin, A., 1993a. Interfacial Phenomena. *Physical Pharmacy*. Philadelphia: Lea and Febiger. p. 379-386.
- Martin, A., 1993b. Solubility and Distribution Phenomena. *Physical Pharmacy*. Philadelphia: Lea and Febiger. p. 212-250.
- Martin, A., 1993c. States of matter. *Physical Pharmacy*. Philadelphia: Lea and Febiger. p. 22-52.
- Martini, A., Torricelli, C. and De Ponti, R., 1991. Physico-pharmaceutical characteristics of steroid/crosslinked polyvinylpyrrolidone coground systems. *International Journal of Pharmaceutics*, 75(2-3), p. 141-146.
- Marty, J.-P., 1996. Menorest®: Technical development and pharmacokinetic profile. *European Journal of Obstetrics & Gynecology and Reproductive Biology*, 64(Supplement 1), p. 29-33.
- Mattsson, L., Bohnet, Gredmark, Torhorst, Hornig and Hüls, 1999. Continuous, combined hormone replacement: randomized comparison of transdermal and oral preparations. *Obstetrics and gynecology*, (94), p. 61-65.

- McAllister, D.V., Wang, P.M., Davis, S.P., Park, J.H., Canatella, P.J., Allen, M.G. and Prausnitz, M.R., 2003. Microfabricated needles for transdermal delivery of macromolecules and nanoparticles: Fabrication methods and transport studies. *Proceedings of the National Academy of Sciences of the United States of America*, 100(24), p. 13755-13760.
- McGinity, J.W. and Harris, M.R., 1980. Increasing Dissolution Rates of Poorly Soluble Drugs by Adsorption to Montmorillonite. *Drug Development and Industrial Pharmacy*, 6(1), p. 35-48.
- Megrab, N.A., Williams, A.C. and Barry, B.W., 1995. Estradiol Permeation through Human Skin and Silastic Membrane - Effects of Propylene-Glycol and Supersaturation. *Journal of Controlled Release*, 36(3), p. 277-294.
- Menon, G.K., 2002. New insights into skin structure: scratching the surface. *Advanced Drug Delivery Reviews*, 54 (Supplement 1), p. 3-17.
- Merk, H.F. and Jugert, F.K., 1993. Metabolic activation and detoxification of drugs and xenobiotics by the skin. *Dermal and transdermal drug delivery*. Stuttgart: Wissenschaftliche Verlagsgesellschaft mbH. p. 33-58.
- Michaels, A.S., Chandrasekaran, S.K. and Shaw, J.E., 1975. Drug Permeation through Human Skin - Theory and In Vitro Experimental Measurement. *Aiche Journal*, 21(5), p. 985-996.
- Mikszta, J.A., Alarcon, J.B., Brittingham, J.M., Sutter, D.E., Pettis, R.J. and Harvey, N.G., 2002. Improved genetic immunization via micromechanical disruption of skin-barrier function and targeted epidermal delivery. *Nature Medicine*, 8(4), p. 415-419.
- Minghetti, P., Cilurzo, F. and Casiraghi, A., 2004. Measuring adhesive performance in transdermal delivery systems. *American journal of drug delivery*, 2(3), p. 194-206.
- Mitchell, A.E., Hong, Y.J., May, J.C., Wright, C.A. and Bamforth, C.W., 2005. A comparison of polyvinylpyrrolidone (PVPP), silica xerogel and a polyvinyl pyrrolidone (PVP)-silica co-product for their ability to remove polyphenols from beer. *Journal of the Institute of Brewing*, 111(1), p. 20-25.
- Mitragotri, S., Blankschtein, D. and Langer, R., 1995. Ultrasound-Mediated Transdermal Protein Delivery. *Science*, 269(5225), p. 850-853.
- Mitragotri, S. and Kost, J., 2004. Low-frequency sonophoresis: A review. *Advanced Drug Delivery Reviews*, 56(5), p. 589-601.
- Monkhouse, D.C. and Lach, J.L., 1972a. Use of Adsorbents in Enhancement of Drug Dissolution 1. *Journal of Pharmaceutical Sciences*, 61(9), p. 1430-1435.
- Monkhouse, D.C. and Lach, J.L., 1972b. Use of Adsorbents in Enhancement of Drug Dissolution 2. *Journal of Pharmaceutical Sciences*, 61(9), p. 1435-1441.
- Moser, K., Kriwet, K., Froehlich, C., Kalia, Y.N. and Guy, R.H., 2001a. Supersaturation: Enhancement of skin penetration and permeation of a lipophilic drug. *Pharmaceutical Research*, 18(7), p. 1006-1011.
- Moser, K., Kriwet, K., Naik, A., Kalia, Y.N. and Guy, R.H., 2001b. Passive skin penetration enhancement and its quantification in vitro. *European Journal of Pharmaceutics and Biopharmaceutics*, 52(2), p. 103-112.
- Myatt, R., Oladiran, G. and Batchelor, H., 2008. Measuring the solubility of a model drug in drug-in-adhesive transdermal patches to validate a theoretical solubility calculator. *Drug Delivery Technology*, 8(3), p. 56-59.
- Neugebauer, M., 1992. Chromatographische Analysemethoden. *Instrumentelle pharmazeutische Analytik*. Stuttgart: Wissenschaftliche Verlagsgesellschaft mbH. p. 242-296.

- O'Connor, A.E. and Willenbacher, N., 2004. The effect of molecular weight and temperature on tack properties of model polyisobutylenes. *International Journal of Adhesion and Adhesives*, 24(4), p. 335-346.
- Oertel, R.P., 1977. Protein Conformational-Changes Induced in Human Stratum-Corneum by Organic Sulfoxides - Ir Spectroscopic Investigation. *Biopolymers*, 16(10), p. 2329-2345.
- Oguchi, T., Matsumoto, K., Yonemochi, E., Nakai, Y. and Yamamoto, K., 1995. Dissolution studies in organic solvents for evaluating hydrogen-bond matrix of cellulose in the ground mixture. *International Journal of Pharmaceutics*, 113(1), p. 97-102.
- Ogura, M., Paliwal, S. and Mitragotri, S., 2008. Low-frequency sonophoresis: Current status and future prospects. *Advanced Drug Delivery Reviews*, 60(10), p. 1218-1223.
- Otberg, N., Patzelt, A., Rasulev, U., Hagemester, T., Linscheid, M., Sinkgraven, R., Sterry, W. and Lademann, J., 2008. The role of hair follicles in the percutaneous absorption of caffeine. *British Journal of Clinical Pharmacology*, 65(4), p. 488-492.
- Panchagnula, R., Pillai, O., Nair, V.B. and Ramarao, P., 2000. Transdermal iontophoresis revisited. *Current Opinion in Chemical Biology*, 4(4), p. 468-473.
- Patzelt, A., Antoniou, C., Sterry, W. and Lademann, J., 2008. Skin penetration from the inside to the outside: A review. *Drug Discovery Today: Disease Mechanisms*, 5(2), p. 229-235.
- Payne, R., Mathias, S.D., Pasta, D.J., Wanke, L.A., Williams, R. and Mahmoud, R., 1998. Quality of life and cancer pain: Satisfaction and side effects with transdermal fentanyl versus oral morphine. *Journal of Clinical Oncology*, 16(4), p. 1588-1593.
- Pellett, M.A., Castellano, S., Hadgraft, J. and Davis, A.F., 1997. The penetration of supersaturated solutions of piroxicam across silicone membranes and human skin in vitro. *Journal of Controlled Release*, 46(3), p. 205-214.
- Percival, F.W., 1986. Isolation of Indole-3-Acetyl Amino-Acids Using Polyvinylpyrrolidone Chromatography. *Plant Physiology*, 80(1), p. 259-263.
- Pershing, L.K., Lambert, L.D. and Knutson, K., 1990. Mechanism of Ethanol-Enhanced Estradiol Permeation across Human Skin In vivo. *Pharmaceutical Research*, 7(2), p. 170-175.
- Peterson, T.A., Wick, S.M. and Ko, C., 1997. Design, development, manufacturing, and testing of transdermal drug delivery systems. *Transdermal and topical drug delivery systems*. Buffalo Grove: Interpharm Press. p. 249-298.
- Pflegel, P. and Dittgen, M., 1987. Drugs and Organism .6. Transdermal Therapeutic System. *Pharmazie*, 42(12), p. 799-809.
- Prausnitz, M., Allen, M., McCallister, D. and Henry, S., US 6503231, 2002
- Prausnitz, M.R., Mitragotri, S. and Langer, R., 2004. Current status and future potential of transdermal drug delivery. *Nature Reviews Drug Discovery*, 3(2), p. 115-124.
- Queuille, A. and Larde, R., US 3725541, 1973
- Raghavan, S.L., Kiepfer, B., Davis, A.F., Kazarian, S.G. and Hadgraft, J., 2001a. Membrane transport of hydrocortisone acetate from supersaturated solutions; the role of polymers. *International Journal of Pharmaceutics*, 221(1-2), p. 95-105.
- Raghavan, S.L., Trividic, A., Davis, A.F. and Hadgraft, J., 2000. Effect of cellulose polymers on supersaturation and in vitro membrane transport of hydrocortisone acetate. *International Journal of Pharmaceutics*, 193(2), p. 231-237.
- Raghavan, S.L., Trividic, A., Davis, A.F. and Hadgraft, J., 2001b. Crystallization of hydrocortisone acetate: influence of polymers. *International Journal of Pharmaceutics*, 212(2), p. 213-221.

- Rautio, J., Kumpulainen, H., Heimbach, T., Oliyai, R., Oh, D., Jarvinen, T. and Savolainen, J., 2008. Prodrugs: design and clinical applications. *Nat Rev Drug Discov*, 7(3), p. 255-270.
- Rivera, S.L. and Ghodbane, S., 1994. In-Vitro Adsorption-Desorption of Famotidine on Microcrystalline Cellulose. *International Journal of Pharmaceutics*, 108(1), p. 31-38.
- Robert M. Franz, G.E.P., 1982. In vitro adsorption-desorption of fluphenazine dihydrochloride and promethazine hydrochloride by microcrystalline cellulose. *Journal of Pharmaceutical Sciences*, 71(11), p. 1193-1199.
- Robinson, D.S. and Amsterdam, J.D., 2008. The selegiline transdermal system in major depressive disorder: A systematic review of safety and tolerability. *Journal of Affective Disorders*, 105(1-3), p. 15-23.
- Rothberg, S., Crouse, R.G. and Lee, J.L., 1961. Glycine-C-14 Incorporation into the Proteins of Normal Stratum Corneum and the Abnormal Stratum Corneum of Psoriasis. *Journal of Investigative Dermatology*, 37(6), p. 497-505.
- Roy, S.D., 1997. Preformulation aspects of transdermal drug delivery. *Transdermal and topical drug delivery systems*. Buffalo Grove: Interpharm Press. p. 139-166.
- Roy, S.D. and Manoukian, E., 1995. Transdermal Delivery of Ketorolac Tromethamine - Permeation Enhancement, Device Design, and Pharmacokinetics in Healthy Humans. *Journal of Pharmaceutical Sciences*, 84(10), p. 1190-1196.
- Rupprecht, H., 1972. Influence of Solvents on Adsorption of Ionic Surfactants on Highly Dispersed Silicas. *Journal of Pharmaceutical Sciences*, 61(5), p. 700-702.
- Santoro, A. and Rovati, L.C., US 6440454, 2002
- Santoyo, S., Arellano, A., Ygartua, P. and Martin, C., 1995. Penetration enhancer effects on the in vitro percutaneous absorption of piroxicam through rat skin. *International Journal of Pharmaceutics*, 117(2), p. 219-224.
- Satas, D., 1989a. Peel. *Handbook of pressure sensitive adhesive technology*. Warwick: Satas and Associates. p. 62-86.
- Satas, D., 1989b. Tack. *Handbook of pressure sensitive adhesive technology*. Warwick: Satas and Associates. p. 36-61.
- Scheuplein, R., 1965. Mechanism of Percutaneous Adsorption .I. Routes of Penetration and Influence of Solubility. *Journal of Investigative Dermatology*, 45(5), p. 334-346.
- Schulz, M., Fussnegger, B. and Bodmeier, R., 2008. Adsorption properties of crospovidone and recrystallization inhibition of carbamazepine in adsorbates onto crospovidone. *in preparation*.
- Schurad, B., Tack, J. and Lipp, R., 2005. Evaluation of the transdermal permeation behavior of proterguride from drug in adhesive matrix patches through hairless mouse skin. *Drug Development and Industrial Pharmacy*, 31(6), p. 505-513.
- Scifinder, 2008. Calculated using Advanced Chemistry Development (ACD/Labs) Software V8.14 for Solaris.
- Seidel-Morgenstern, A., 2004. Experimental determination of single solute and competitive adsorption isotherms. *Journal of Chromatography A*, 1037(1-2), p. 255-272.
- Sekizaki, H., Danjo, K., Eguchi, H., Yonezawa, Y., Sunada, H. and Otsuka, A., 1995. Solid-State Interaction of Ibuprofen with Polyvinylpyrrolidone. *Chemical & Pharmaceutical Bulletin*, 43(6), p. 988-993.
- Shah, V.P., Behl, C.R., Flynn, G.L., Higuchi, W.I., Schaefer, H., Barry, B.W., Behl, C.R., Conners, D.P., Evans, C.C., Flynn, G.L., Franz, T.J., Gans, E.H., Higuchi, W.I., Kail, N., Krueger, G.G., Leyden, J., Maibach, H.I., Malick, A.W., Nacht, S., Ng, S., Peck, C.C., Pershing, L.K., Potts, R.O., Poulsen, B.J., Schaefer, H., Scott, R.C., Sequeira, J.A., Shah, V.P., Sharma, D., Skelly, J.P. and Wu, M.-S., 1992. Principles and criteria in the development and optimization of topical therapeutic products : Sponsored by

- the American Association of Pharmaceutical Scientists (AAPS) and U.S. Food and Drug Administration (FDA). *International Journal of Pharmaceutics*, 82(1-2), p. 21-28.
- Shibata, Y., Fujii, M., Kokudai, M., Noda, S., Okada, H., Kondoh, M. and Watanabe, Y., 2007. Effect of characteristics of compounds on maintenance of an amorphous state in solid dispersion with crospovidone. *Journal of Pharmaceutical Sciences*, 96(6), p. 1537-1547.
- Shibata, Y., Fujii, M., Noda, S., Kokudai, M., Okada, H., Kondoh, M. and Watanabe, Y., 2006. Fluidity and tableting characteristics of a powder solid dispersion of the low melting drugs ketoprofen and ibuprofen with crospovidone. *Drug Development and Industrial Pharmacy*, 32(4), p. 449-456.
- Small, G. and Dubois, B., 2007. A review of compliance to treatment in Alzheimer's disease: potential benefits of a transdermal patch. *Current Medical Research and Opinion*, 23(11), p. 2705-2713.
- Smirnova, I., Suttiruengwong, S., Seiler, M. and Arlt, W., 2004. Dissolution rate enhancement by adsorption of poorly soluble drugs on hydrophilic silica aerogels. *Pharmaceutical Development and Technology*, 9(4), p. 443-452.
- Sobue, S., Sekiguchi, K., Kikkawa, H. and Irie, S., 2005. Effect of application sites and multiple doses on nicotine pharmacokinetics in healthy male Japanese smokers following application of the transdermal nicotine patch. *Journal of Clinical Pharmacology*, 45(12), p. 1391-1399.
- Southwell, D. and Barry, B.W., 1983. Penetration enhancers for human skin: mode of action of 2-pyrrolidone and dimethylformamide on partition and diffusion of model compounds water, n-alcohols, and caffeine. *J Invest Dermatol*, 80(6), p. 507-514.
- Spencer, T.S., 1997. Preclinical assessment of transdermal drug delivery systems. *Transdermal and topical drug delivery systems*. Buffalo Grove: Interpharm Press. p. 167-190.
- Stott, P.W., Williams, A.C. and Barry, B.W., 1998. Transdermal delivery from eutectic systems: enhanced permeation of a model drug, ibuprofen. *Journal of Controlled Release*, 50(1-3), p. 297-308.
- Sun, Y., 1997. Skin absorption enhancement by physical means: Heat, ultrasound and electricity. *Transdermal and topical drug delivery systems*. Buffalo Grove: Interpharm Press. p. 327-356.
- Tachibana, K. and Tachibana, S., 1991. Transdermal Delivery of Insulin by Ultrasonic Vibration. *Journal of Pharmacy and Pharmacology*, 43(4), p. 270-271.
- Tan, H.S. and Pfister, W.R., 1999. Pressure-sensitive adhesives for transdermal drug delivery systems. *Pharmaceutical Science & Technology Today*, 2(2), p. 60-69.
- Taylor, L.S. and Zografí, G., 1997. Spectroscopic characterization of interactions between PVP and indomethacin in amorphous molecular dispersions. *Pharmaceutical Research*, 14(12), p. 1691-1698.
- Toole, J., Silagy, S., Maric, A., Fath, B., Quebe-Fehling, E., Ibarra de Palacios, P., Laurin, L. and Giguere, M., 2002. Evaluation of irritation and sensitisation of two 50 $\mu\text{g}/\text{day}$ oestrogen patches. *Maturitas*, 43(4), p. 257-263.
- Tordjeman, P., Papon, E. and Villenave, J.J., 2000. Tack properties of pressure-sensitive adhesives. *Journal of Polymer Science Part B-Polymer Physics*, 38(9), p. 1201-1208.
- Torreslabandeira, J.J., Davignon, P. and Pitha, J., 1991. Oversaturated Solutions of Drug in Hydroxypropylcyclodextrins - Parenteral Preparation of Pancreatistatin. *Journal of Pharmaceutical Sciences*, 80(4), p. 384-386.

- Tsai, J.C., Guy, R.H., Thornfeldt, C.R., Gao, W.N., Feingold, K.R. and Elias, P.M., 1996. Metabolic approaches to enhance transdermal drug delivery .1. Effect of lipid synthesis inhibitors. *Journal of Pharmaceutical Sciences*, 85(6), p. 643-648.
- Twist, J.N. and Zatz, J.L., 1986. Influence of Solvents on Paraben Permeation through Idealized Skin Model Membranes. *Journal of the Society of Cosmetic Chemists*, 37(6), p. 429-444.
- Uekama, K., Oh, K., Irie, T., Otagiri, M., Nishimiya, Y. and Nara, T., 1985. Stabilization of isosorbide 5-mononitrate in solid state by [beta]-cyclodextrin complexation. *International Journal of Pharmaceutics*, 25(3), p. 339-346.
- Valenta, C., Siman, U., Kratzel, M. and Hadgraft, J., 2000. The dermal delivery of lignocaine: influence of ion pairing. *International Journal of Pharmaceutics*, 197(1-2), p. 77-85.
- Van Hal, D.A., Jeremiasse, E., Junginger, H.E., Spies, F. and Bouwstra, J.A., 1996. Structure of fully hydrated human stratum corneum: a freeze-fracture electron microscopy study. *J Invest Dermatol*, 106(1), p. 89-95.
- Venkatraman, S. and Gale, R., 1998. Skin adhesives and skin adhesion 1. Transdermal drug delivery systems. *Biomaterials*, 19(13), p. 1119-1136.
- Wagner, H., Kostka, K.-H., Lehr, C.-M. and Schaefer, U.F., 2003. pH profiles in human skin: influence of two in vitro test systems for drug delivery testing. *European Journal of Pharmaceutics and Biopharmaceutics*, 55(1), p. 57-65.
- Warner, R.R., Stone, K.J. and Boissy, Y.L., 2003. Hydration disrupts human stratum corneum ultrastructure. *J Invest Dermatol*, 120(2), p. 275-284.
- Watanabe, T., Isobe, T. and Senna, M., 1996. Mechanisms of incipient chemical reaction between Ca(OH)(2) and SiO₂ under moderate mechanical stressing .1. A solid state acid-base reaction and charge transfer due to complex formation. *Journal of Solid State Chemistry*, 122(1), p. 74-80.
- Watanabe, T., Liao, J.F. and Senna, M., 1995. Changes in the Basicity and Species on the Surface of Me(OH)(2)-SiO₂ (Me=Ca, Mg, Sr) Mixtures Due to Mechanical Activation. *Journal of Solid State Chemistry*, 115(2), p. 390-394.
- Watanabe, T., Ohno, I., Wakiyama, N., Kusai, A. and Senna, M., 2002. Stabilization of amorphous indomethacin by co-grinding in a ternary mixture. *International Journal of Pharmaceutics*, 241(1), p. 103-111.
- Watanabe, T., Wakiyama, N., Usui, F., Ikeda, M., Isobe, T. and Senna, M., 2001. Stability of amorphous indomethacin compounded with silica. *International Journal of Pharmaceutics*, 226(1-2), p. 81-91.
- Wexler, A. and Hasegawa, S., 1954. Relative Humidity-Temperature Relationships of Some Saturated Salt Solutions in the Temperature Range 0-Degree to 50-Degrees-C. *Journal of Research of the National Bureau of Standards*, 53(1), p. 19-26.
- White, S.H., Mirejovsky, D. and King, G.I., 1988. Structure of Lamellar Lipid Domains and Corneocyte Envelopes of Murine Stratum-Corneum - an X-Ray-Diffraction Study. *Biochemistry*, 27(10), p. 3725-3732.
- Williams, A.C. and Barry, B.W., 2004. Penetration enhancers. *Advanced Drug Delivery Reviews*, 56(5), p. 603-618.
- Williams, A.C., Timmins, P., Lu, M. and Forbes, R.T., 2005. Disorder and dissolution enhancement: Deposition of ibuprofen on to insoluble polymers. *European Journal of Pharmaceutical Sciences*, 26(3-4), p. 288-294.
- Wokovich, A.M., Prodduturi, S., Doub, W.H., Hussain, A.S. and Buhse, L.F., 2006. Transdermal drug delivery system (TDDS) adhesion as a critical safety, efficacy and quality attribute. *European Journal of Pharmaceutics and Biopharmaceutics*, 64(1), p. 1-8.

- Wolf, R., Tuzun, B. and Tuzun, Y., 1998. Adverse skin reactions to the nicotine transdermal system. *Clinics in Dermatology*, 16(5), p. 617-623.
- Yu, L., 2001. Amorphous pharmaceutical solids: preparation, characterization and stabilization. *Advanced Drug Delivery Reviews*, 48(1), p. 27-42.
- Zernikow, B., Michel, E. and Anderson, B., 2007. Transdermal fentanyl in childhood and adolescence: A comprehensive literature review. *Journal of Pain*, 8(3), p. 187-207.
- Zhai, L.L., Ling, G. and Wang, Y.W., 2008. Effect of nano-Al₂O₃ on adhesion strength of epoxy adhesive and steel. *International Journal of Adhesion and Adhesives*, 28(1-2), p. 23-28.
- Zosel, A., 1998. The effect of fibrillation on the tack of pressure sensitive adhesives. *International Journal of Adhesion and Adhesives*, 18(4), p. 265-271.

7 PUBLICATIONS & PRESENTATIONS RESULTING FROM THIS WORK

Journal publications

M. Schulz, B. Fussnegger and R. Bodmeier, Adsorption properties of crospovidone and recrystallization inhibition of carbamazepine in adsorbates onto crospovidone. (in preparation)

M. Schulz, B. Fussnegger and R. Bodmeier, Influence of adsorbents in transdermal matrix patches on the release and the physical state of ethinyl estradiol and levonorgestrel. (in preparation)

M. Schulz, B. Fussnegger and R. Bodmeier, Adsorption properties of crospovidone and recrystallization inhibition of carbamazepine in adsorbates onto crospovidone. (in preparation)

Conference publications

M. Schulz, B. Fussnegger and R. Bodmeier, Optimisation of drug - carrier ratio to molecularly disperse the poorly water soluble model drug carbamazepine onto crospovidone in order to enhance its dissolution, Annual Meeting of the American Association of Pharmaceutical Scientists, AAPS, San Antonio, USA, (2006)

M. Schulz, B. Fussnegger and R. Bodmeier, Investigation of solvent effects on the adsorption of carbamazepine onto crospovidone by determination of adsorption isotherms and ATR FT-IR spectroscopy, Annual Meeting of the American Association of Pharmaceutical Scientists, AAPS, San Antonio, USA, (2006)

M. Schulz, B. Fussnegger and R. Bodmeier, Influence of crospovidone particle size and concentration of low molecular weight polyisobutene on the in-vitro drug release of ethinyl estradiol and levonorgestrel from a transdermal matrix patch, Annual Meeting of the American Association of Pharmaceutical Scientists, AAPS, San Diego, USA, (2007)

M. Schulz, B. Fussnegger and R. Bodmeier, Influence of micronized crospovidone on the adhesive properties of transdermal polyisobutene matrix patches, Annual Meeting of the American Association of Pharmaceutical Scientists, AAPS, Georgia, USA, (2008)

7 CURRICULUM VITAE

Martin Schulz

Date of birth aus Datenschutzgründen in der Online-Publikation entfernt

Place of birth aus Datenschutzgründen in der Online-Publikation entfernt

Education and Qualifications

06/2004 - 01/2009 *Freie Universität Berlin*, College of Pharmacy, supervisor: Prof. Dr. Roland Bodmeier, Ph.D. student

03/2004 Third state examination and registration as pharmacist

05/1998 - 11/2002 *Bayerische Julius-Maximilians-Universität*, Würzburg
Second state examination in Pharmacy

11/1995 - 03/1997 *Bayerische Julius-Maximilians-Universität*, Würzburg
Studies of business administration

06/1995 *Matthias-Grünwald-Gymnasium*, Würzburg
Abitur

Professional Experience and Internships

02/2009 - to date *Pfizer GmbH - Arzneimittelwerk Gödeke*, Freiburg, Management
Trainee Pharmazie

01/2007 - 04/2008 *KOS Pharmaceuticals/Abbott Laboratories*, Hollywood, FL, USA,
Department Solid Dose Research and Development, intern

06/2003 - 11/2003 *Nordring Apotheke*, Berlin, pre-registration trainee

03/2003 - 05/2003 *Schering AG*, Berlin, Department Oral Dosage Forms Research and
Development, pre-registration trainee

11/2002 - 02/2003 *Repatriation General Hospital*, Adelaide, AU, pre-registration trainee

Further Work Experience

04/1997 - 04/1998 *Arbeiter-Samariter-Bund*, Würzburg, alternative civilian service